TECHNIQUES FOR SUPERHETERODYNE RECEIVERS ABOVE 100 GIGACYCLES

Final Report
Contract NASw-662

ELECTRONIC COMMUNICATIONS, INC.

RESEARCH DIVISION
1830 YORK ROAD
TIMONIUM, MARYLAND

TECHNIQUES FOR SUPERHETERODYNE RECEIVERS ABOVE 100 GIGACYCLES

Final Report

Contract NASw-662

Electronic Communications, Inc.
Research Division
1830 York Road
Timonium, Maryland

April 14, 1964

Contributing Authors

M. Cohn
J.W. Dozier
A.F. Eikenberg
R.F. Packard
J.D. Rodgers

ABSTRACT

3320e

The development of techniques and components applicable to superheterodyne receivers operating above 100 Gc is reported. The principle of operation, methods of fabrication, and experimental results are presented for a ferroelectric device capable of measuring absolute power at millimeter and submillimeter wavelengths. The results of a statistically designed diode evaluation program are given. A description is given of an improved technique for the fabrication of millimeter waveguide and movable shorting plungers. A report is made on the performance data obtained for point-contact semiconductor devices such as conventional mixers, harmonic mixers, and harmonic generators. Improvements in the design and performance of a 2mm ferrite modulator employing the principle of Faraday rotation are reported.

TABLE OF CONTENTS

LIST OF ILLUSTRATIONS

LIST OF ILLUSTRATIONS (Cont'd)

LIST OF ILLUSTRATIONS (Cont'd)

I. INTRODUCTION

The research program undertaken under Contract NASw-662 is a continuation of some of the studies performed under a previous NASA program (Contract NASw-259). The purpose of this program was to conduct research and develop techniques and components applicable to superheterodyne receivers operating at frequencies above 100 Gc. An eventual goal of this research effort on superheterodyne receiver techniques and components was their application to space borne radiometers operating at millimeter and sub-millimeter wavelengths.

One of the tasks of this program (Task II) was the development and evaluation of such semi-conductor diode devices as conventional mixers, harmonic mixers, and harmonic generators. The fabrication, assembly and measurement techniques which have resulted in improved repeatability and performance of these diode devices are described. Within this task, extensive efforts have been devoted to developing improved millimeter wave harmonic generators. These harmonic generators can be used in conjunction with lower frequency solid state RF power sources to extend the frequency range in which superheterodyne receivers employing solid state local oscillator sources are feasible.

Many measurements such as harmonic generation efficiency and mixer conversion loss are either very inaccurate or impossible to perform at millimeter and sub-millimeter wavelengths due to the lack of instruments with which to make low level absolute power measurements. Task I of this contract was a program to establish the feasibility of a ferroelectric bolometer and develop it into a working model. The principle of operation, fabrication procedure, and performance characteristics of such a bolometer are described.

Task III of this contract was to improve the performance of a 2mm ferrite modulator employing the principle of Faraday Rotation. The objective of this task was to achieve a broadband ferrite modulator

suitable for use with a broadband Dicke type, harmonic mixing superheterodyne radiometer of the type developed at this laboratory, which employs a microwave intermediate frequency.

II. FERROELECTRIC BOLOMETER (TASK I)

A. Introduction

Many measurements at millimeter and submillimeter wavelengths are either very inaccurate or impossible to perform due to the lack of instruments with which to make low level absolute power measurements. As a result, it is difficult to measure such semiconductor device parameters as harmonic generation efficiency and mixer crystal conversion loss. The above cited measurement deficiencies in turn make it difficult to either predict or measure the sensitivity of superheterodyne receivers at mm or sub-mm wavelengths.

Due to the need for accurate, low level power measurements, a program to demonstrate the feasibility and develop a working model of a ferroelectric bolometer has been performed both within the scope of this contract and a preceding one (Contract NASw-259).

B. Principle of Operation

An experimental program has established the feasibility of utilizing the properties of ferroelectric materials in the vicinity of their Curie temperature as the basis for fabricating sensitive, frequency independent power measuring devices. The principle of operation is that a large change in the permittivity of the ferroelectric material is produced by a small temperature change, which in turn results from the absorption of millimeter wavelength energy. Ferroelectric materials have high dissipation factors at mm wavelengths; but since they have relatively high Q's (10^2 to 10^3) at audio frequencies, the permittivity change can be measured at these low frequencies with a negligible amount of the audio frequency power absorbed. The ceramic ferroelectric element is suitably shaped and mounted in a millimeter waveguide to efficiently absorb RF power. Electrodes are baked onto two parallel surfaces of the ferroelectric element to form a capacitor connected by thin wires to the audio frequency measuring terminals located outside of the waveguide.

The observed capacity change as a function of incident RF power level will be frequency independent provided that (1) the dissipation factor of the ferroelectric material remains sufficiently high, and (2) the element is suitably shaped to provide a good impedance match over the required frequency interval. When the above conditions are satisfied over a large frequency range, the capacity change (ΔC) versus RF power change (ΔP) relation can be determined by measurements made at the lower end of the frequency range where alternate absolute power measuring devices are available. The ferroelectric bolometer, so calibrated, can then be used to measure power levels at other frequencies within the applicable interval.

The dielectric constant of a ferroelectric material is very temperature sensitive near its Curie Temperature. Ambient temperature fluctuations as well as RF power absorption can therefore produce a capacity change. In order to minimize the effects of ambient temperature fluctuations, which determine the threshold power measuring capability, two identical ferroelectric bolometers can be used in a temperature compensating bridge circuit. A bridge circuit of this type has been constructed and will be described.

A related device, which also utilizes the unique temperature dependent properties of ferroelectric materials, has been proposed as a sensitive detector of modulated infrared radiation.[1] It should be noted that the objective of the program described in this report is the development of an accurate, absolute power measuring device.

C. Material Properties

Initial measurements were made on a ferroelectric element consisting of a ceramic mixture of 35% lead titanate ($PbTiO_3$) and 65%

---

1. R.A. Hanel, "Dielectric bolometer: a new type of thermal radiation detector," J. Opt. Soc. Amer, Vol. 51, pp. 220-224; February 1961.

strontium titanate ($SrTiO_3$). The mixture is referred to in mole percent. A typical capacitance versus temperature characteristic of this material is shown in Figure 1. The Curie Temperature of this material is in the vicinity of room temperature ($T_c = 28^oC$). As is the case with many ferroelectric materials, the slope of the capacitance versus temperature curve ($\Delta C/\Delta T$) is greater for $T < T_c$. In order to maintain the material in the region of constant slope below the Curie Temperature, refrigeration equipment rather than a simple heating coil would be required. In addition it was found that the ceramic ferroelectric materials absorbed moisture from the air which caused the audio frequency dissipation factor to increase. It was necessary to bake the ferroelectric element prior to performing measurements in order to drive out the absorbed moisture.

A higher Curie Temperature ferroelectric material was investigated. This allows convenient operation below the Curie temperature, but at a sufficiently high temperature to preclude the absorption of moisture. The material was a ceramic mixture of 45% $PbTiO_3$ and 55% $SrTiO_3$. A capacitance versus temperature curve for this material is shown in Figure 2.

The specific heat (C_p) and density(ρ) of each of these ferroelectric materials were measured. The results are shown in Table I. Included in the table are the results for two different batches of 45% $PbTiO_3$ purchased from Gulton Industries, Inc. of Metuchen, N.J. (UR 5324 and UR 5359). These two batches had identical constituents but were fired at different temperatures.

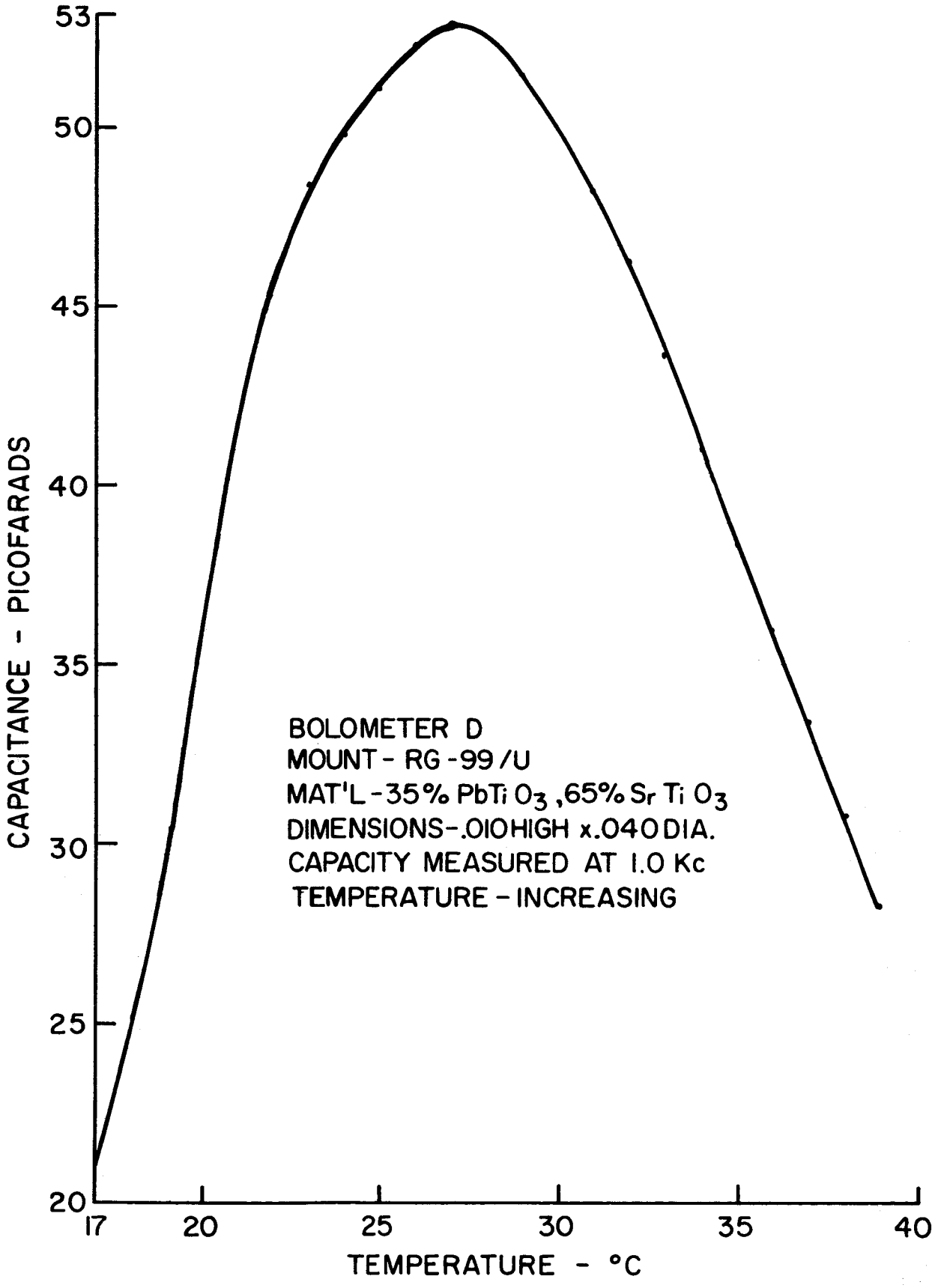

CAPACITANCE VS MOUNT TEMPERATURE FOR THE FERROELECTRIC BOLOMETER

FIGURE 1

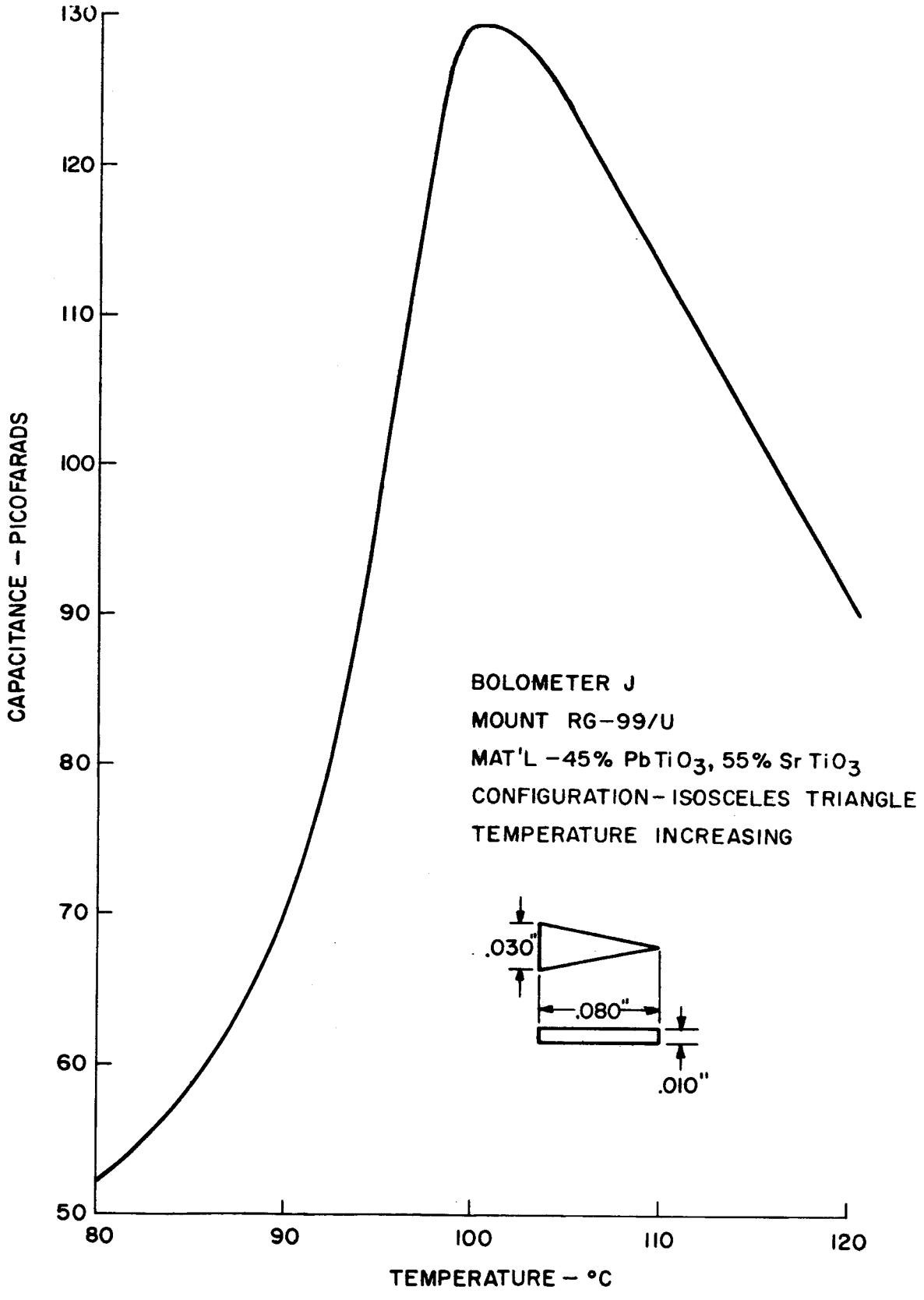

FIG. 2 – CAPACITANCE vs MOUNT TEMPERATURE FOR FERROELECTRIC BOLOMETER

Ferroelectric Material	Gulton UR 5324	Gulton UR 5359	Gulton -
Constituents	45% $PbTiO_3$ 55% $SrTiO_3$	45% $PbTiO_3$ 55% $SrTiO_3$	35% $PbTiO_3$ 65% $SrTiO_3$
Firing Temperature	2325°F	2250°F	-
Curie Temperature (T_c)	98°C	98°C	28°C
Specific Heat (C_p) - $\frac{\text{calories}}{\text{gm-}^\circ\text{C}}$	0.15 ±.02	0.11 ±.02	0.15 ±.03
Density (ρ) - $\frac{\text{gm}}{\text{cm}^3}$	5.54 ±.01	5.53 ±.01	5.8 ±.3

TABLE I

D. Theoretical Analysis

An idealized analysis has been performed to determine the dependence of the bolometer performance on the electrical, thermal, and geometric parameters of the device.

The analysis of the thermal system assumes that initially the ferroelectric pellet is at the same temperature (T) as the waveguide assembly. The only source for differential heating of the element is the continuously applied RF power (P) which is assumed to uniformly heat the pellet. Heat can be transferred from the ferroelectric pellet to the waveguide walls only via conduction through the small diameter wires used to both support the pellet and provide terminals to measure the capacitance change. The pertinent parameters of these wires are their thermal conductivity (k), cross-sectional area (A), and their length from the edge of the pellet to the waveguide wall(S).

The heat energy introduced (q_{in}) and extracted (q_{out}) from the ferroelectric pellet are

$$q_{in} = Pt \tag{1}$$

and

$$q_{out} = \frac{kA}{S}\,\delta T\, t, \tag{2}$$

where δT is the temperature rise of the pellet and t is the time measured from the instant when the RF power is applied. The energy stored in the pellet (q_{stored}) is

$$q_{stored} = m C_p \delta T, \tag{3}$$

where m and C_p are respectively the mass and specific heat of the ferroelectric pellet. The heat balance equation requires that

$$q_{in} - q_{out} = q_{stored} \tag{4}$$

Substituting Equations 1, 2, and 3 into 4, one obtains the following equation for the temperature rise of the pellet as a function of time.

$$\delta T = \frac{Pt}{m C_p + \frac{kA}{S} t} \tag{5}$$

If, after equilibrium has been reached ($t \to \infty$), one considers the additional incremental temperature rise of the pellet from $T + \delta T$ to $T + \delta T + \Delta T$ due to a change of RF power level from P to $P + \Delta P$, it is readily shown that

$$\Delta T = \frac{\Delta P t}{m C_p + \frac{kA}{S} t} \tag{6}$$

The equilibrium temperature rise is given by

$$\lim_{t \to \infty} \Delta T = \frac{S \Delta P}{kA} \tag{7}$$

Let

$$\Delta T(t) = r \lim_{t \to \infty} \Delta T = r \frac{S \Delta P}{kA}, \tag{8}$$

where $0 \leq r \leq 1$, and is the ratio of the instantaneous temperature rise to the equilibrium temperature rise. From Equations 6 and 8 an expression for the time required for the pellet to reach any fraction of its final equilibrium temperature rise is obtained.

$$t_r = \frac{SmC_p}{kA} \cdot \frac{r}{1-r} \tag{9}$$

The time required for the ferroelectric pellet to reach half of its equilibrium temperature rise is

$$t_{0.5} = \frac{SmC_p}{kA} . \tag{10}$$

A graph of r as a function of $t/t_{0.5}$ is shown in Figure 3. If the ferroelectric bolometer is operated at a temperature such that $\Delta C/\Delta T$ is constant (for example $91^{\circ}C < T < 98^{\circ}C$ in Figure 2) then curves of the measured capacitance change as a function of time should have a shape like that of Figure 3.

For an actual ferroelectric bolometer element some of the parameters such as S and m are difficult to specify. When the pellet size is large, the RF power is not dissipated uniformly throughout the ferroelectric element. The path through which heat is conducted away from the pellet includes not only the wire leads but also portions of the electrodes baked onto the pellet. The analysis does however indicate the manner in which the performance of the ferroelectric bolometer depends upon the various electrical, thermal and geometric parameters of the ferroelectric element and waveguide mount. It serves as a guide in the design of the bolometer and indicates the basic compromise which must be made between sensitivity and response time.

E. Preliminary Measurements

Most of the preliminary measurements were made on ferroelectric pellets fabricated in the shape of a small circular cylinder (.010" high x .040" diameter). Gold electrodes were formed by brushing DuPont No. 6976 gold paste on the plane circular faces and

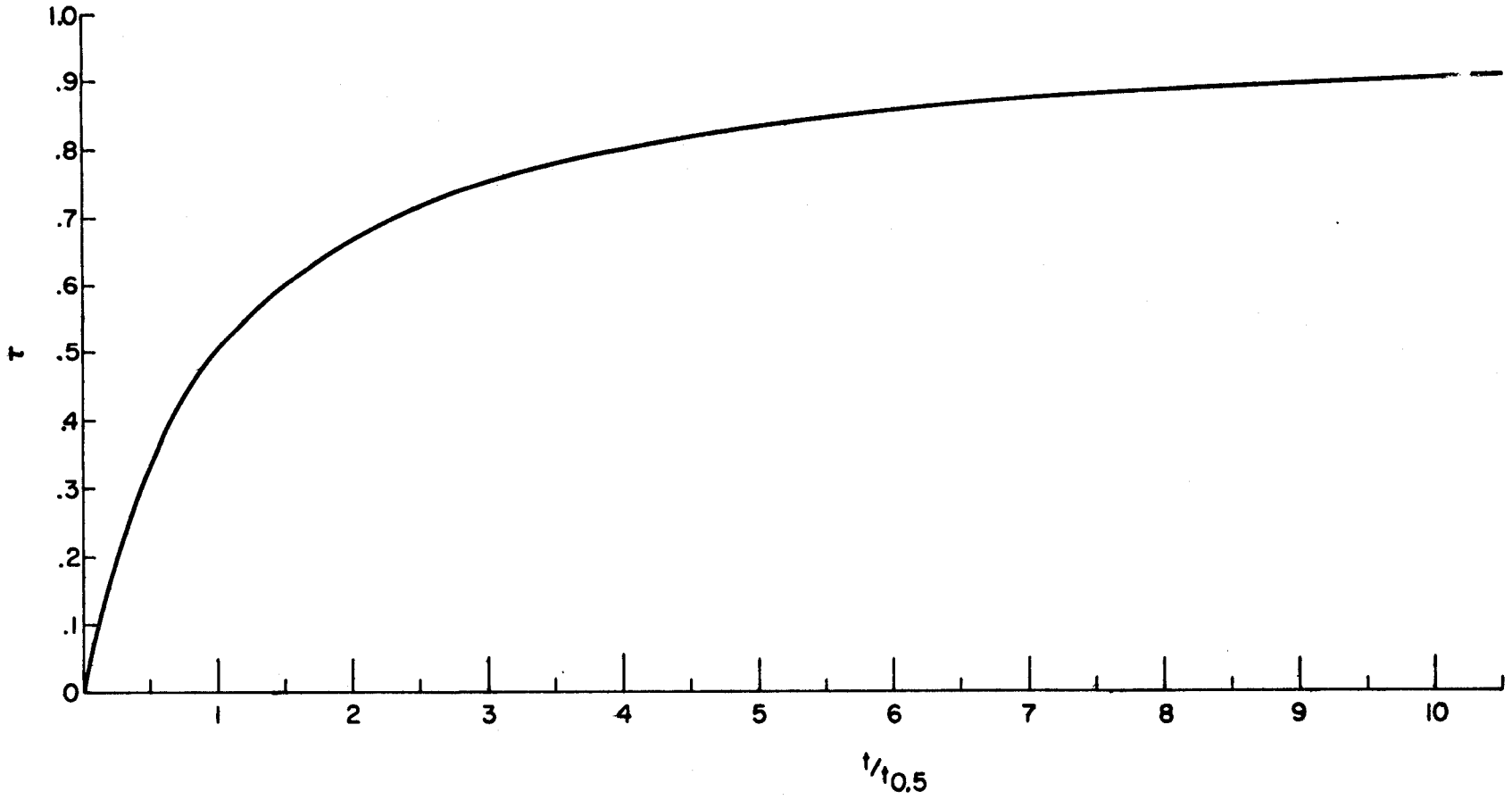

FIG. 3 - NORMALIZED CURVE OF TEMPERATURE RISE vs TIME FOR A FERROELECTRIC BOLOMETER

then baking for one hour at 760°C. Wire leads were used to both support the pellet in RG-99/U waveguide and provide a connection to the audio frequency capacitance measuring equipment outside of the waveguide. These wires had a diameter of 3 mils and consisted of an alloy of 90% platinum and 10% ruthenium. Gold paste was used to attach these wires to the gilded ferroelectric pellet. Microphotographs of the bolometer element with its attached wire leads prior to and after mounting in the waveguide are shown in Figures 4 and 5.

A thermocouple was attached to the waveguide to measure the mount temperature. A heater coil, used to maintain the mount at a specified temperature, was wrapped around the waveguide. Curves of the type shown in Figures 1 and 2 were obtained by varying the mount temperature with the heater coil.

With the mount held at a constant temperature, known amounts of millimeter wavelength power were applied to the ferroelectric bolometer. The RF power level was measured with both a barreter and a water calorimeter. The capacitance change was measured at a frequency of 1.0 kc with a precision capacitance bridge. The results of such a measurement on a ferroelectric bolometer consisting of 35% $PbTiO_3$ - 65% $SrTiO_3$ are shown in Figure 6.

Although the preliminary measurements had verified the principle of operation and established the basic feasibility of a ferroelectric bolometer, they also indicated many deficiencies in the original design. These measurements showed that the threshold power measuring capability was limited by ambient temperature fluctuations rather than the minimum capacitance change which could be measured. The mount design was such that this threshold was at much too high a power level. In essence the ferroelectric bolometer was an excellent thermometer. Frequently, with no RF power applied, temperature changes too small to be measured with the thermocouple were readily observed as capacitance changes of the ferroelectric bolometer. These measurements pointed out the need for better thermal isolation of the

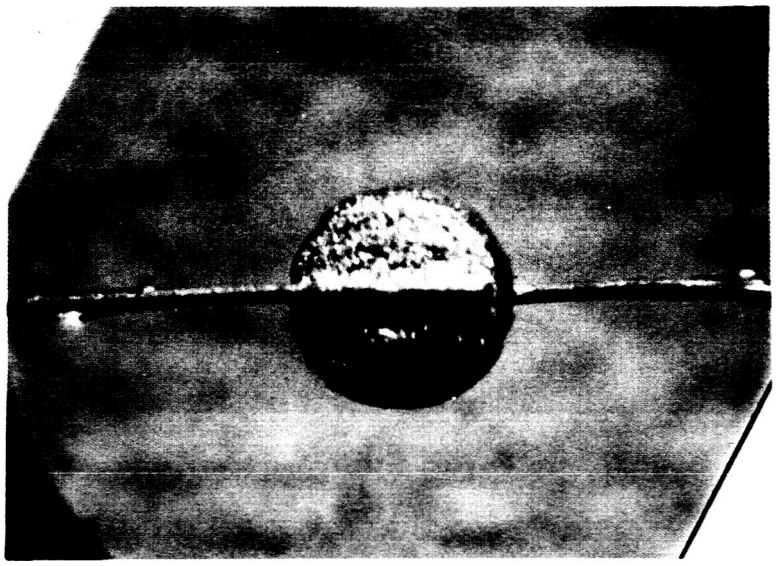

Figure 4 - Ferroelectric Bolometer with Radial Wire Leads

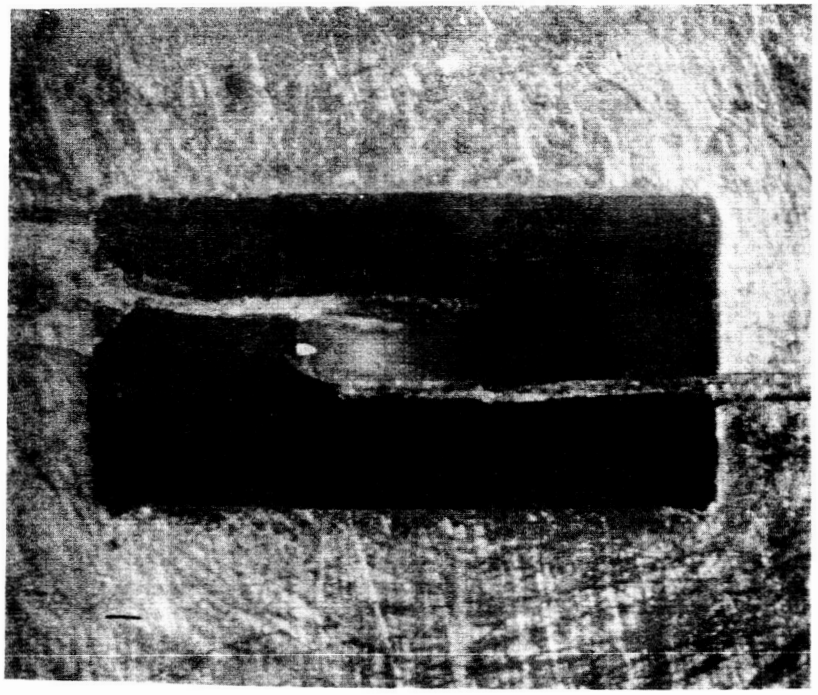

Figure 5 - Ferroelectric Bolometer Across Waveguide
.122" x .061" I.D.

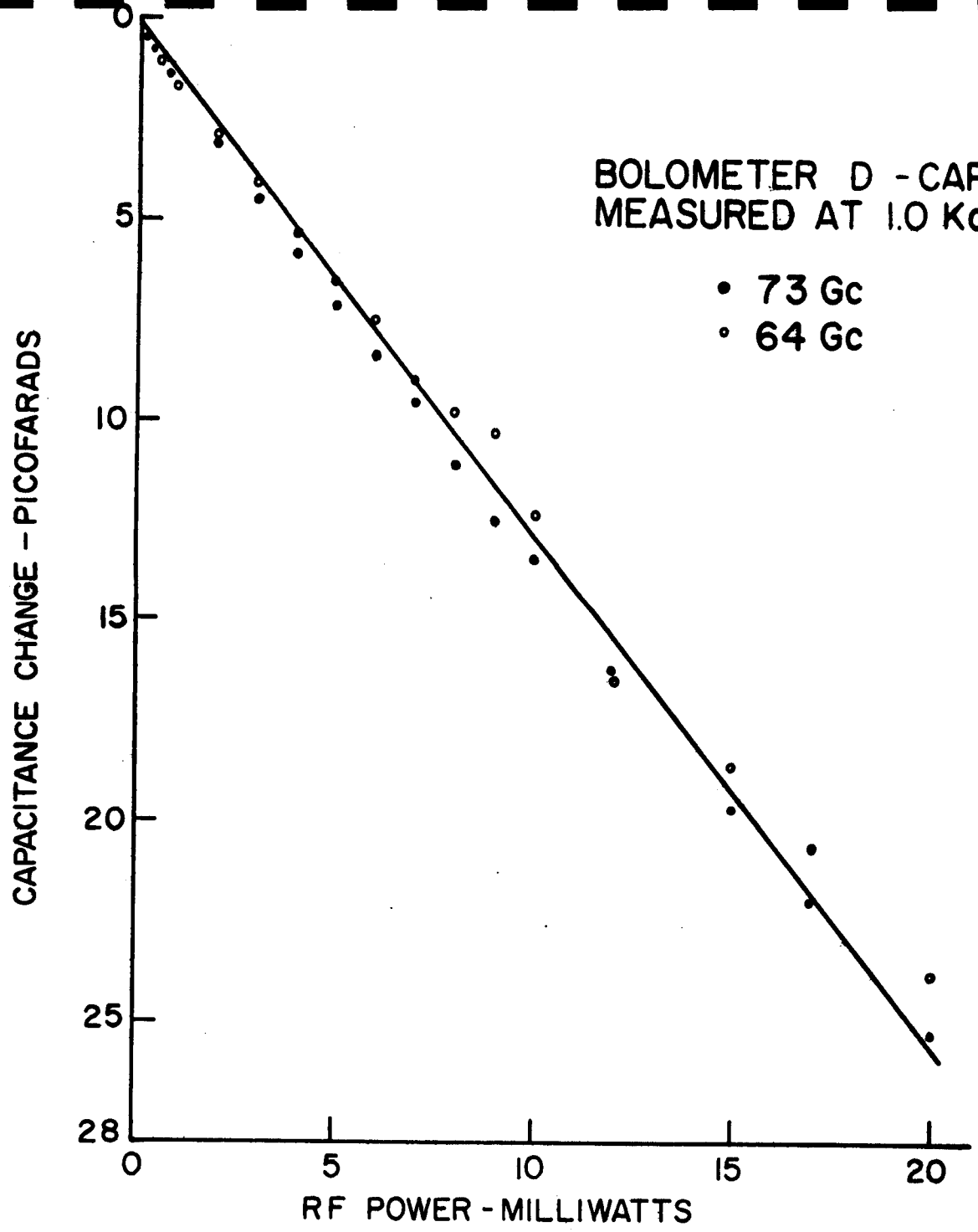

CAPACITANCE VS RF POWER LEVEL FOR THE FERROELECTRIC BOLOMETER

FIGURE 6

bolometer mount and in addition a method of compensating for ambient temperature fluctuations. The effect of a slow temperature drift is illustrated in the measured capacitance change versus time curves shown in Figures 7 and 8. This curve asymptotically approaches a straight line corresponding to the drifting mount temperature rather than a constant value like the curve of Figure 3. As would be expected the effect is more severe for small power changes (Figure 6) where the capacitance change due to thermal drifts is a larger percentage of the total change.

It was observed that the change of capacity due to a change of RF power level ($\Delta C/\Delta P$) was not frequency independent. It was furthermore observed that some bolometers which yielded a large capacitance change per unit temperature change ($\Delta C/\Delta T$) and whose geometry and mounting configuration should yield a large $\Delta T/\Delta P$ did not yield a large $\Delta C/\Delta P$. RF impedance measurements were made to determine if an impedance mismatch was responsible for the discrepancy. It should be noted that an E-H tuner was used to provide a good impedance match to the ferroelectric bolometer mount for all of the measurements of ΔC versus P previously performed. It was observed that the measured ΔC versus P data was not always repeatable, and on occasion the maximum $\Delta C/\Delta P$ was not obtained when the tuner was adjusted for minimum input VSWR.

In order to make the impedance measurements, a matched termination was placed on the load side of the ferroelectric pellet. The normalized admittance (Y') of the parallel combination of matched load and ferroelectric bolometer was determined by the customary method of measuring the VSWR and position of the voltage minimum in the slotted line. The normalized admittance of the ferroelectric bolometer alone was then determined from the following relationship:

$$Y = Y' - 1 \tag{11}$$

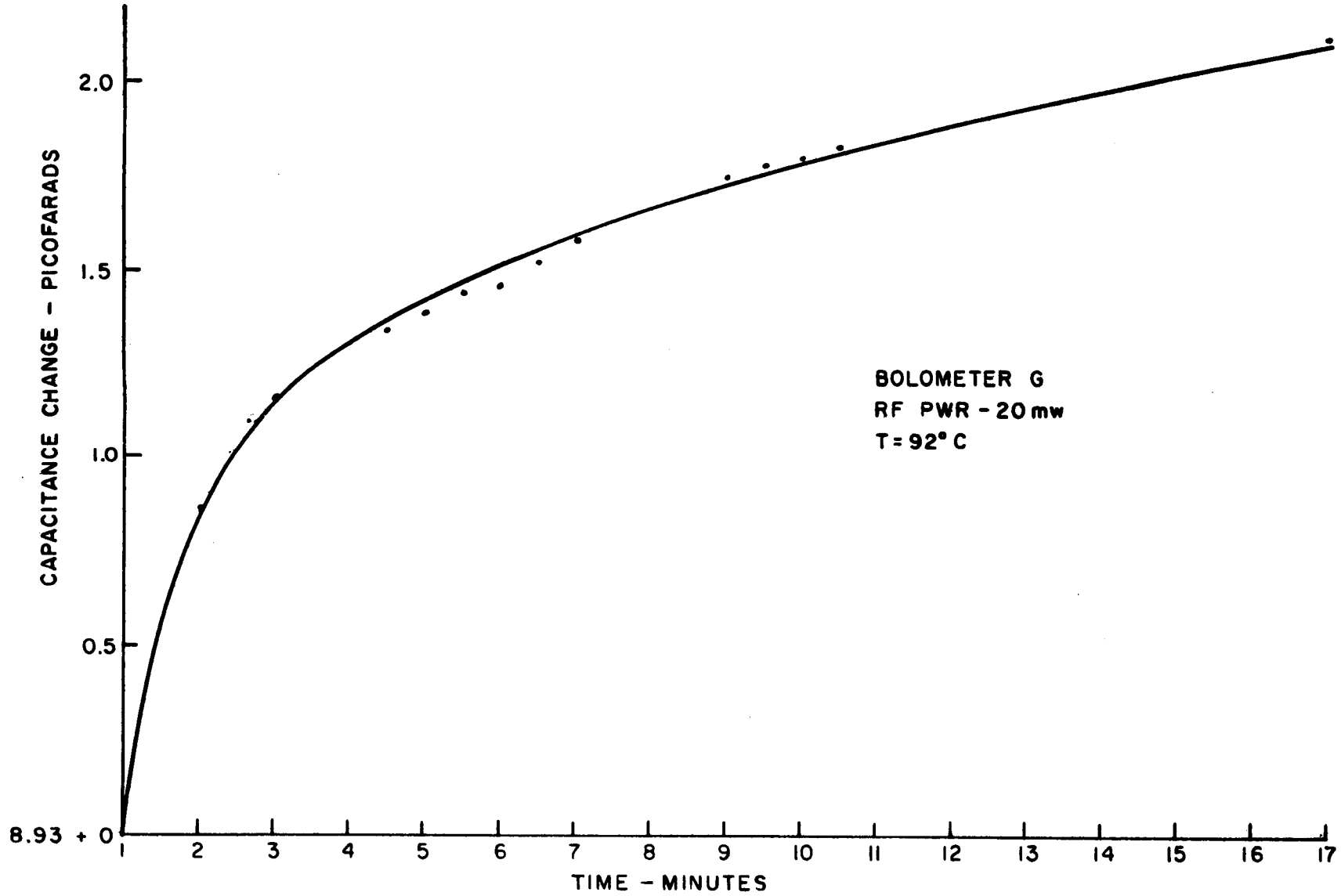

FIG. 7 – CAPACITANCE CHANGE VS TIME FOR FERROELECTRIC BOLOMETER

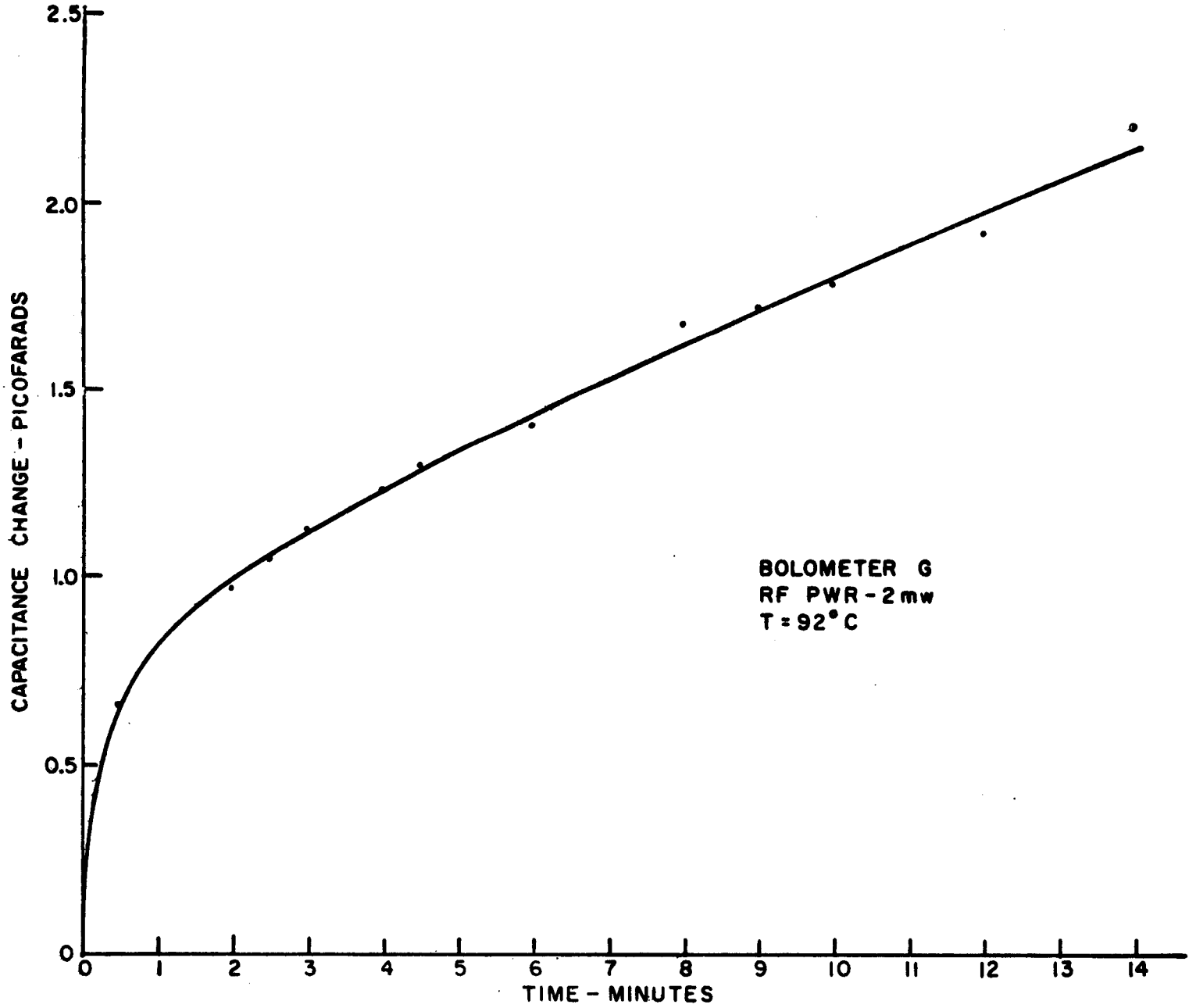

FIG. 8 - CAPACITANCE CHANGE VS TIME FOR FERROELECTRIC BOLOMETER

A Smith Chart plot of the admittance as a function of frequency for one of the circular cylindrical ferroelectric bolometers is shown in Figure 9. Similar admittance characteristics were obtained with other circular ferroelectric pellets.

The admittance locus of Figure 9 is both very frequency dependent and located near the periphery of the Smith Chart. These admittance characteristics indicate that these bolometers have a large reflection coefficient, either by virtue of their geometry or their electrical properties at millimeter wavelengths. At some frequencies reflection coefficients in excess of 0.96 have been observed. Impedance matching devices such as E-H tuners have been used to obtain a low input VSWR. If the ferroelectric bolometer element was the only dissipative element in the structure and the E-H tuner was lossless, one would be assured that all of the available millimeter wave power was absorbed in the ferroelectric pellet. Unfortunately the tuner is not lossless, and the movable short circuit located behind the ferroelectric bolometer has losses due primarily to leakage around it. An additional, though probably small, loss is contributed by the small slots which the bolometer leads go through. If the ferroelectric pellet presented a better match, the other slightly dissipative elements would absorb only a small percentage of the available power. Since the ferroelectric bolometer element has such a large reflection coefficient, it is likely that the power absorbed by the other dissipative elements is comparable to or much larger than that absorbed by the bolometer. The above cited impedance mismatch is believed to be responsible for the previously observed lack of sensitivity and repeatability.

Impedance measurements performed on the disk shaped bolometers showed that they presented a very poor match and were absorbing only a small percentage of the RF power. It was evident from these measurements that a different configuration should be tried

1- 67.8 Gc
2- 68.8 Gc
3- 70.0 Gc
4- 71.0 Gc
5- 72.0 Gc
6- 73.2 Gc

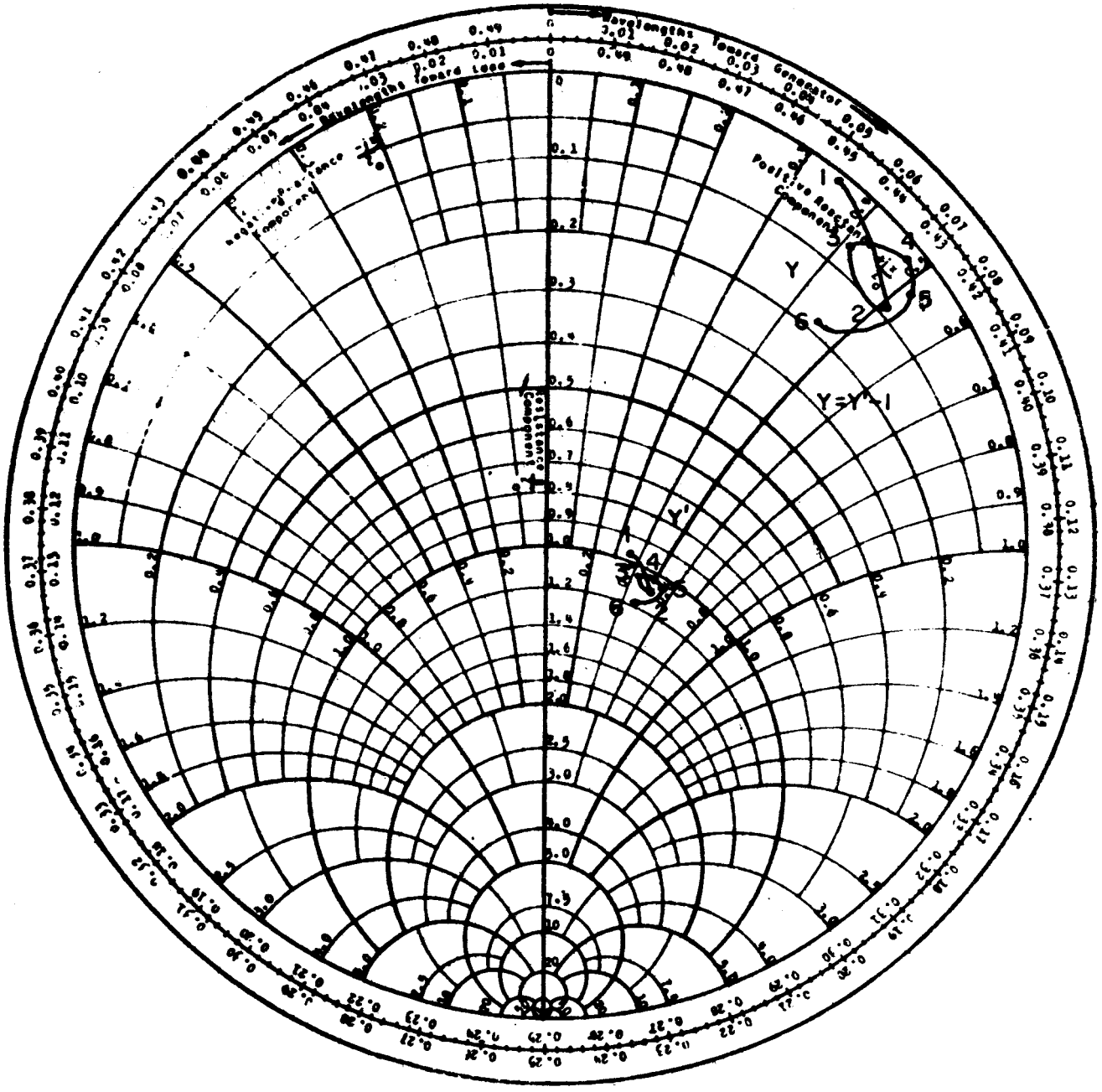

FIG. 9 -ADMITTANCE OF BOLOMETER "G" AS A FUNCTION OF FREQUENCY.

in an attempt to improve the match. For this reason two bolometers, designated "J" and "K", were constructed and tested.

Bolometer J, constructed from a ferroelectric ceramic mixture of 45% $PbTiO_3$ and 55% $SrTiO_3$, was in the shape of an isosceles triangle of dimensions .030" base, .080" altitude, and .010" thick. Platinum leads were attached to the planes of the triangle using the same gold paste technique employed with previous bolometers. This unit was then mounted in a section of RG-99/U waveguide for testing.

Temperature sensitivity ($\frac{\Delta C}{\Delta T}$) measurements were performed first. In a region from 93°C to 98°C, the capacitance change of bolometer J was 7.4 pf/°C and the change was linear in that temperature region. The Curie point occurred at 100°C.

Impedance measurements were made with the plane of the ferroelectric triangle parallel to the broad wall and then repeated with the plane parallel to the narrow wall of the waveguide. Due to the greater insertion loss of these triangular pellets, their RF impedance could not be measured by the previously described technique which employed a matched termination on the load side of the bolometer. The input VSWR and insertion loss were measured by a technique described by Tomiyasu.[2] These measurements showed that, with the plane parallel to the broad wall, the VSWR of the bolometer was 1.5 and the insertion loss was 1 db. With the plane of the triangle parallel to the narrow wall, the VSWR was 2.4 and the insertion loss was 2 db. The latter orientation is preferred since a high insertion loss minimizes the effect of power dissipated in other parts of the bolometer mount.

Power sensitivity measurements were made on bolometer J at several frequencies. The number of frequencies at which the tests could be made was limited by the availability of RF sources and

---

2. Kiyo Tomiyasu, "Intrinsic Insertion Loss of a Mismatched Microwave Network," IRE Transaction, Vol. MTT-3, pp. 40-44; January, 1955.

equipment to measure a reference power. At 70 Gc, the tests performed with the plane of the ferroelectric triangle parallel to the broad wall of the waveguide showed a power sensitivity ($\frac{\Delta C}{\Delta P}$) of 2.2 pf/mw and, with the plane parallel to the narrow wall, 2.5 pf/mw. The same measurements were then made at 66, 73, and 93 Gc with the plane parallel to the narrow wall and at each frequency, the $\frac{\Delta C}{\Delta P}$ was 2.5 pf/mw. All of the measurements were made with the bolometer mount temperature between 93° and 95°C.

Additional power sensitivity measurements were attempted at 310 Gc but the results were inconclusive. At this frequency, there is no equipment available for making precise reference power measurements. The 310 Gc power measurements were made with a water calorimeter built in RG-98/U waveguide. Since both the RG-98/U waveguide and the RG-99/U waveguide containing the ferroelectric bolometer are capable of supporting many modes, the efficiency of both mounts is questionable. The results of this test indicated a $\frac{\Delta C}{\Delta P}$ of 1 pf/mw; but because of the many uncertainties connected with measurements at this frequency, the principal information gained was that the ferroelectric bolometer did absorb energy at 310 Gc.

The next bolometer constructed was designated K. It was fabricated from the same material and in the same manner as J, but is diamond shaped. The dimensions of bolometer K are given in Figure 10. This configuration was chosen to increase the length of the taper and therefore improve the RF match, and, at the same time keep the plate area-thickness ratio the same as that of bolometer J. This ratio is such that the capacitance can be read on a single range of the bridge without switching to a less sensitive range. The initial test of temperature sensitivity ($\frac{\Delta C}{\Delta T}$) indicated a capacitance change of 9.5 pf/°C from 93° to 98°C with the Curie point occurring at approximately 102°C. A plot of the data is shown in Figure 10.

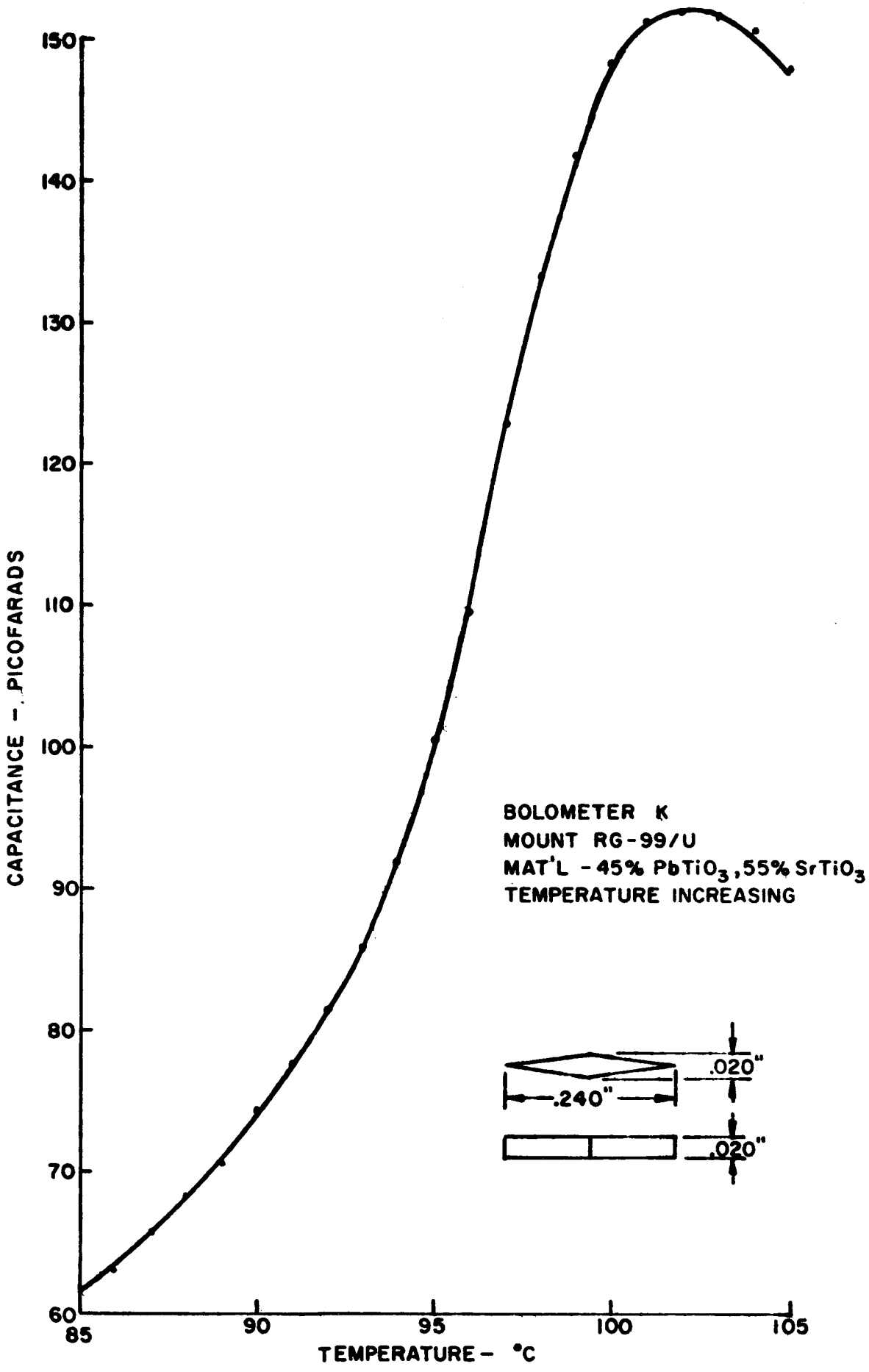

FIG. 10-CAPACITANCE vs MOUNT TEMPERATURE FOR FERROELECTRIC BOLOMETER

Impedance measurements on bolometer K, using the same method[2] as on J, showed that the bolometer had a VSWR of 2.3 and an insertion loss of approximately 4.5 db at a frequency of 70 Gc. The plane of the diamond was parallel to the narrow wall of the waveguide. Figure 11 shows the results of power sensitivity measurements performed on bolometer K. The linear region of the curve, from 4 to 10 mw, indicates $\frac{\Delta C}{\Delta P}$ of 3.1 pf/mw.

A measurement was made on bolometer K to note the thermal time response of the unit. The results of this test are shown in Figure 12. These response time curves are similar to those obtained with many of the prior ferroelectric bolometers and their shape is as predicted by the prior analysis.

The improved performance obtained with bolometer K was due not only to the improved impedance match, but also to improved temperature stability of the bolometer mount. As can be seen from Figure 10, an ambient mount temperature variation of $\pm 0.1^{\circ}C$ will cause a capacitance change of approximately 1 picofarad which is equal to the capacitance change produced by the absorption of 0.3 milliwatts of RF power. The improvements on the mount to reduce temperature fluctuations were: (1) the waveguide mount and heater coil were insulated from air currents by a polystyrene foam box, and (2) a special thin walled waveguide section was inserted between the bolometer mount and the RF source to reduce the conduction of heat to the remainder of the waveguide assembly. The special thin walled section was 1.5" long with a wall thickness of approximately .001". This unit was electroformed.

F. Final Bolometer Measurements

A final ferroelectric bolometer was designed and built to take advantage of the information acquired during the preliminary measurements. This new design entailed changes in both the shape of the ferroelectric and the method of mounting it in the waveguide.

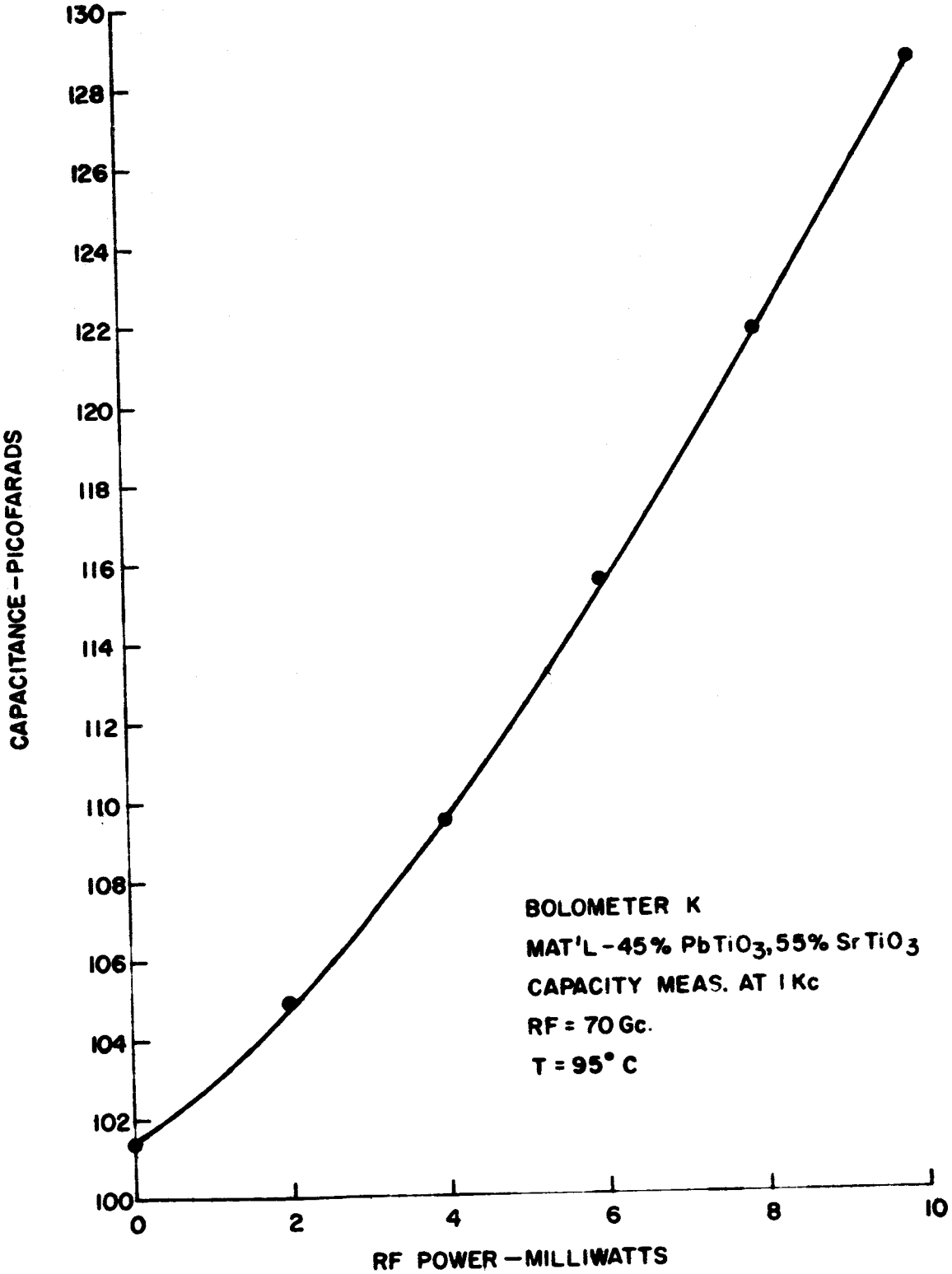

FIG. 11 - CAPACITANCE vs RF POWER FOR FERROELECTRIC BOLOMETER

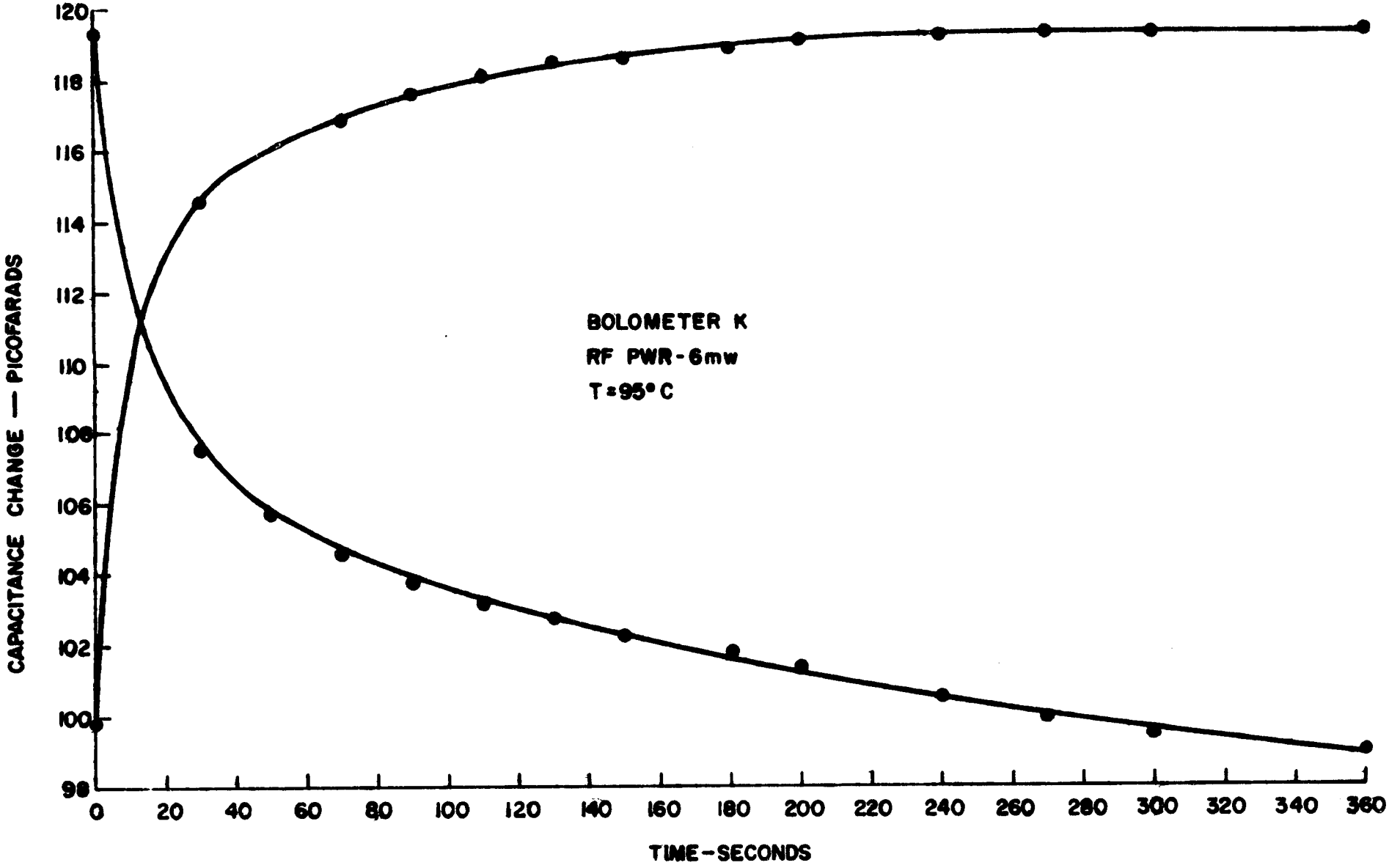

FIG.12 -CAPACITANCE CHANGE vs TIME FOR FERROELECTRIC BOLOMETER

Figure 13 shows the dimensions of the ferroelectric and Figure 14 is the mount. Figure 15 is a photograph of the ferroelectric with the platinum leads attached by gold paste to the plane sides. Figure 16 is the mounted ferroelectric. The small end of the phenolic mount is a press fit in RG-99/U waveguide and aligns the wedge end of the ferroelectric in the center of the guide.

This design is the result of efforts to improve the impedance match of the bolometer and, at the same time, simplify construction. By eliminating the movable short, the bolometer leads can be brought out through the end of the guide rather than through the flanges as had been done with previous bolometers; and the heating coil can be wound directly on the waveguide since the shorting plunger drive has been removed.

Tests performed on bolometer L indicated a temperature sensitivity ($\frac{\Delta C}{\Delta T}$) of 50 pf/^{o}C in the most active region below the Curie temperature. The results of this test are plotted in Figure 17. It should be noted that the apparent Curie temperature for bolometer L is approximately 7^{o}C lower than previous bolometers of the same material. This may be due to the fact that the monitoring thermocouple is in a new location in this mount.

The next test on bolometer L was the power sensitivity ($\frac{\Delta C}{\Delta P}$) and the results are shown in Figures 18 and 19. This data was taken at a frequency of 70 Gc. At an operating temperature of 88^{o}C, the $\frac{\Delta C}{\Delta P}$ was 4.6 pf/mw in the region from 6 to 20 milliwatts (see Figure 18). Figure 19 is a plot of data taken at lower power levels; the first point being 0.2 milliwatts. This test was performed to see how accurately lower power levels could be read.

Although much progress has been made in reducing temperature fluctuations, better temperature stability was needed to measure power levels of less than 100 microwatts. To obtain this stability two ferroelectric bolometers and mounts were constructed similar to

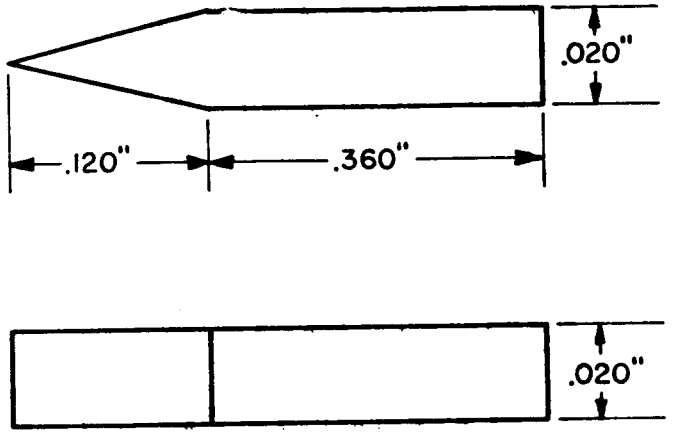

MATERIAL : 45% $PbTiO_3$, 55% $SrTiO_3$

FIG. 13 – BOLOMETER L CONFIGURATION

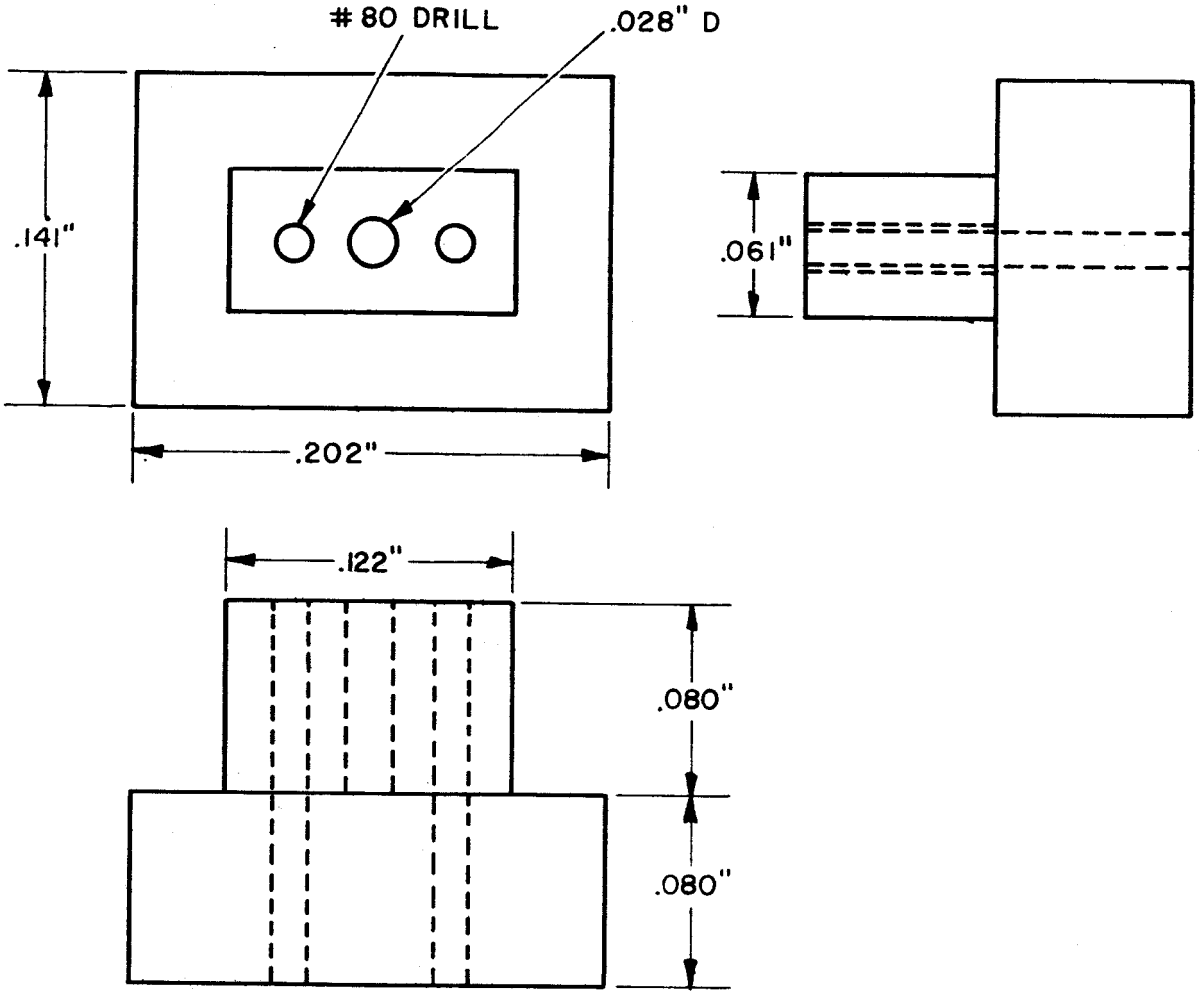

MATERIAL : PHENOLIC

FIG. 14 – MOUNT FOR BOLOMETER L

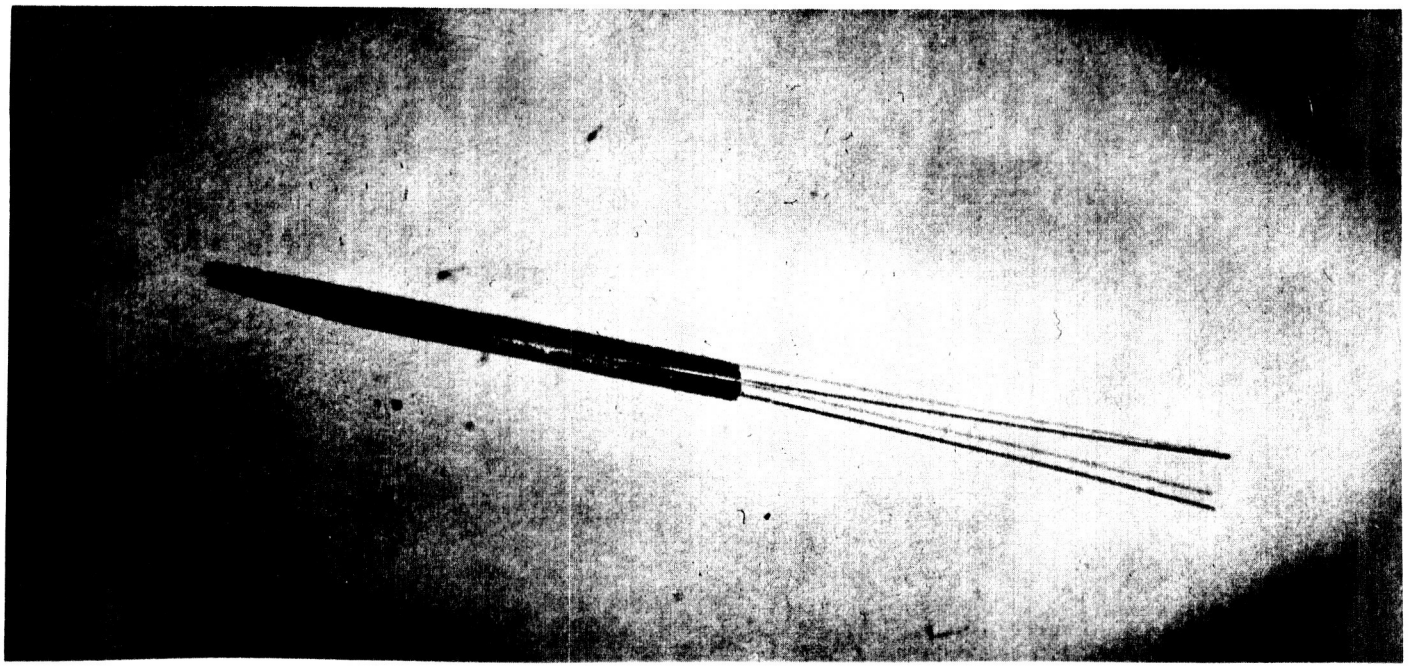

Figure 15 - Ferroelectric Bolometer L

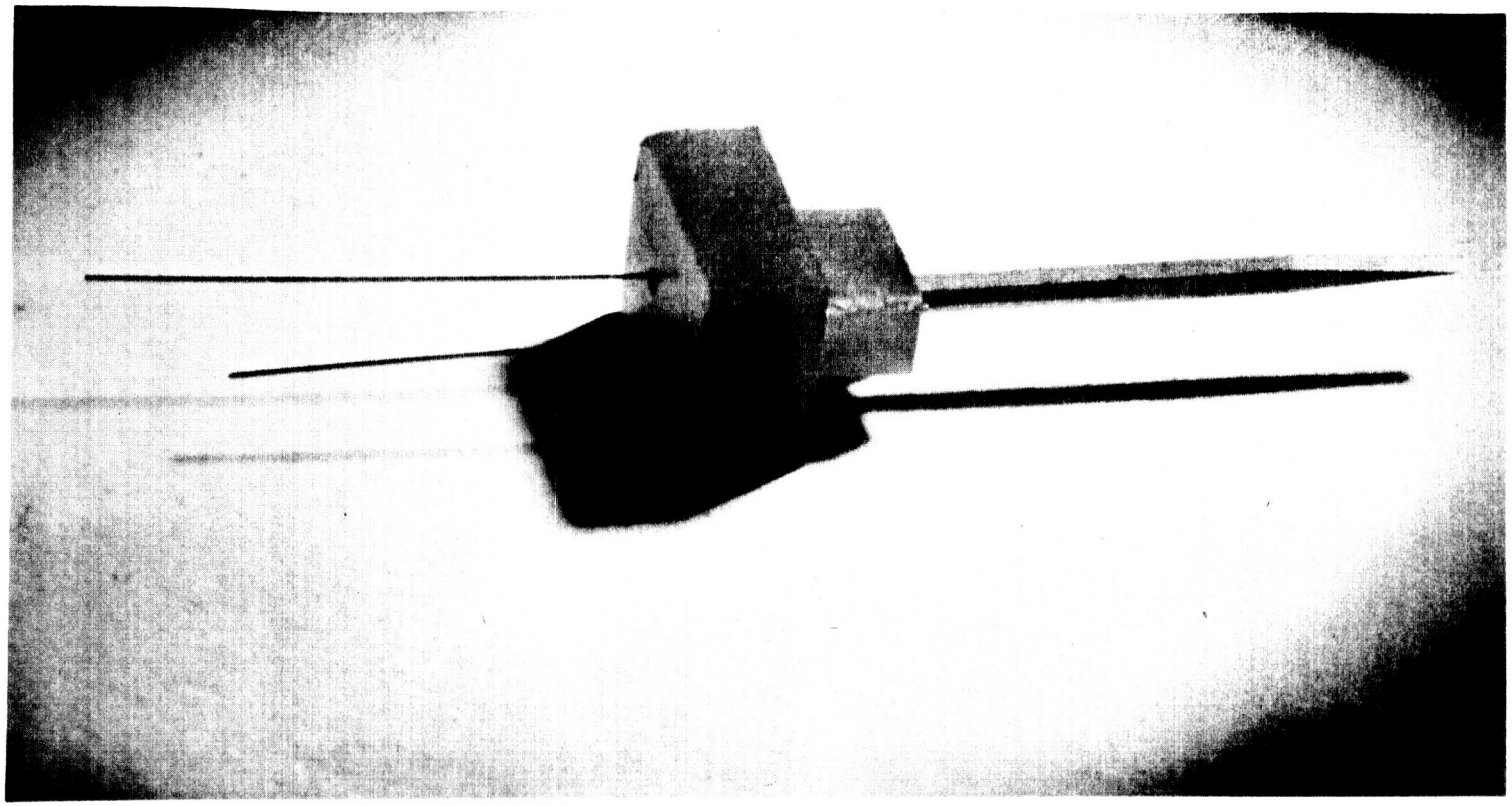

Figure 16 - Ferroelectric Bolometer L in Phenolic Mount

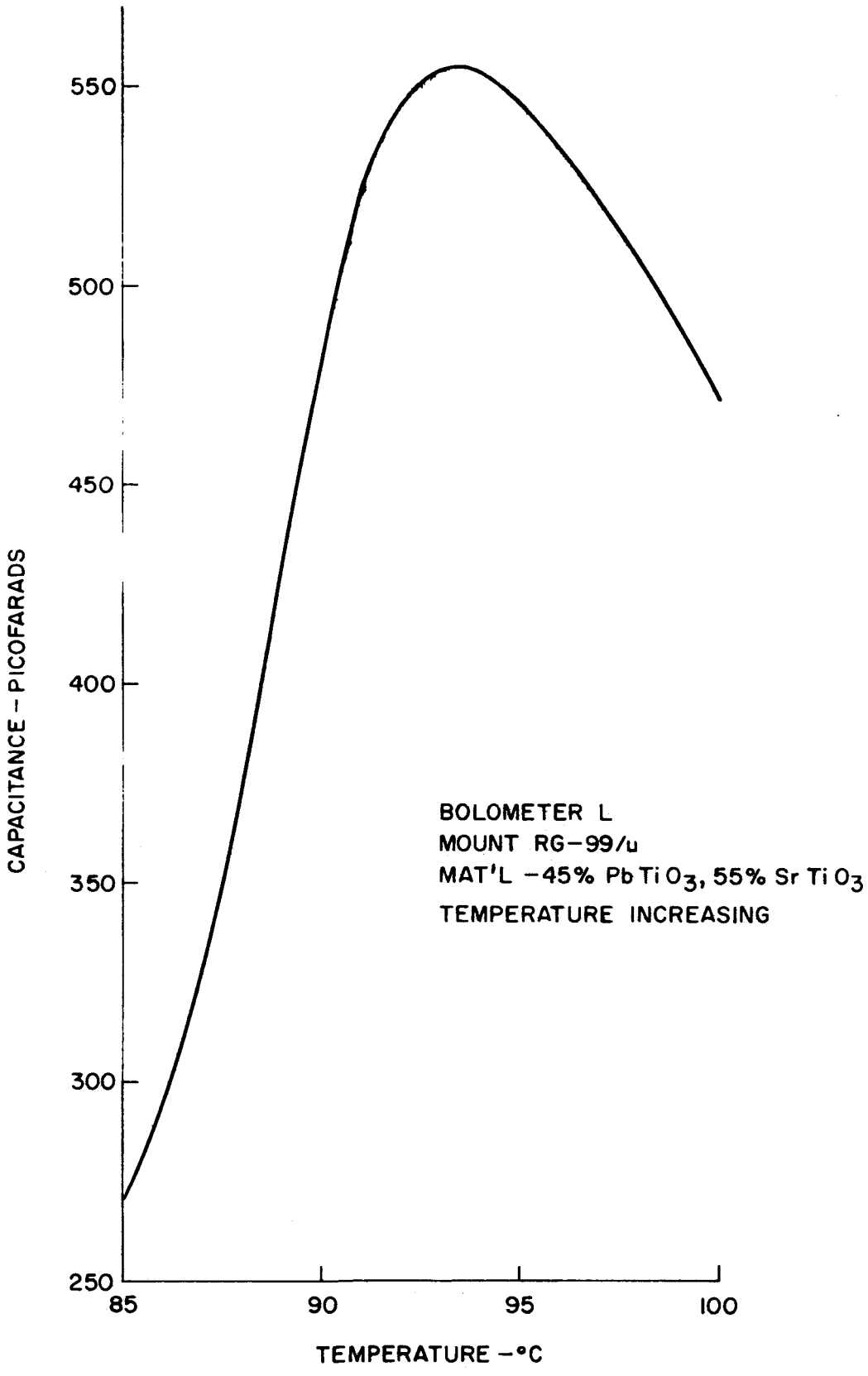

FIG. 17 - CAPACITANCE vs MOUNT TEMPERATURE FOR FERROELECTRIC BOLOMETER

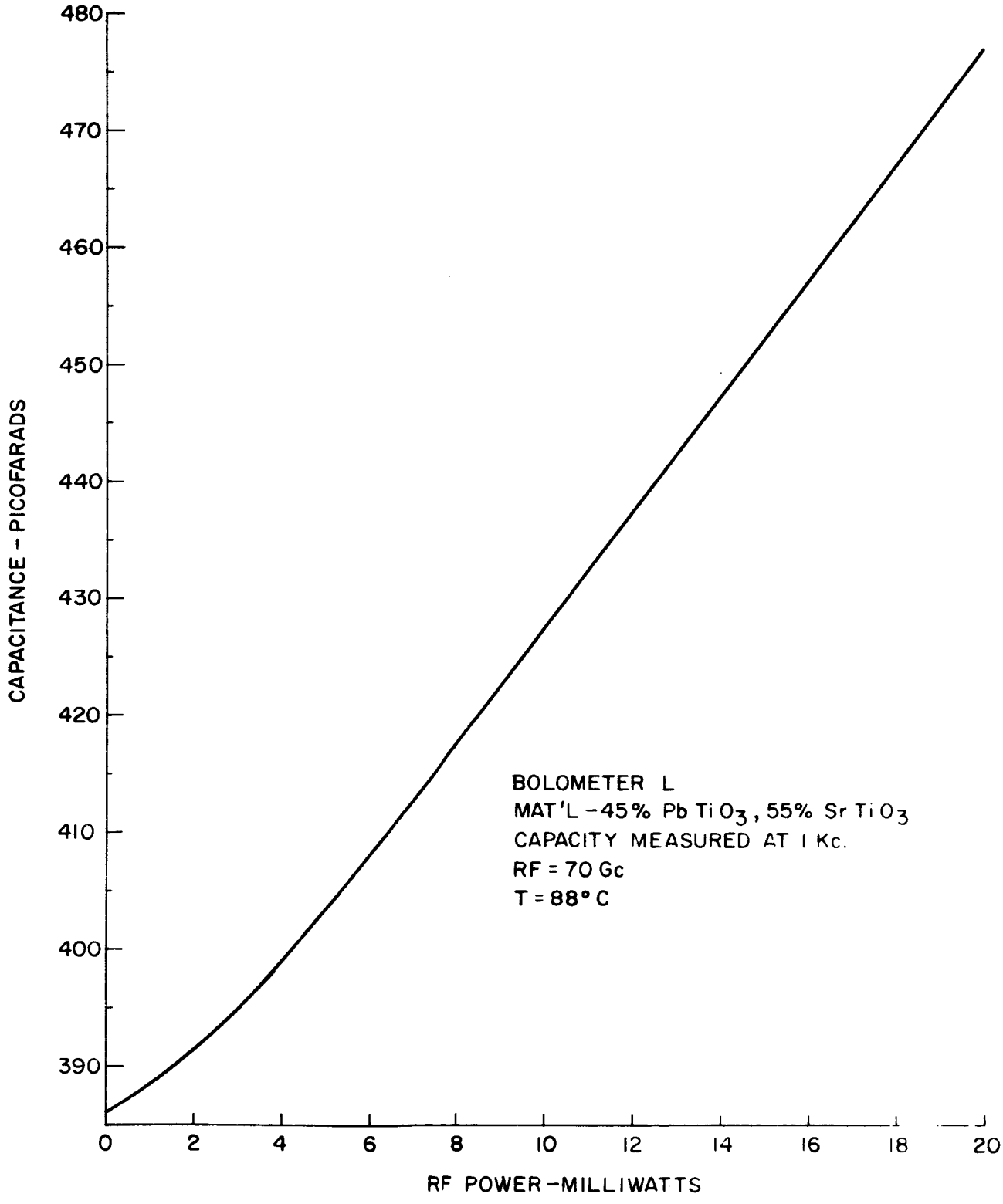

FIG. 18 — CAPACITANCE vs RF POWER FOR FERROELECTRIC BOLOMETER.

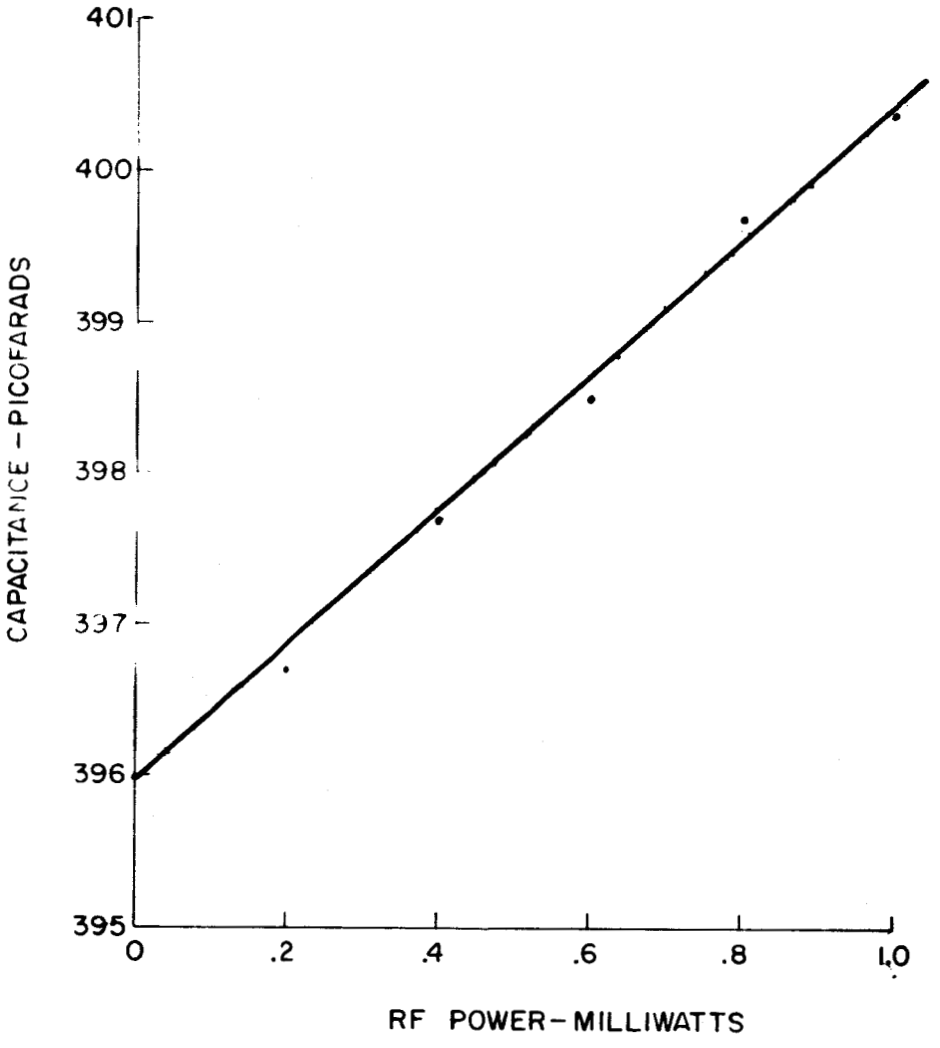

FIG. 19 -CAPACITANCE vs RF POWER FOR FERROELECTRIC BOLOMETER L.

L and as identical to each other as machining techniques would permit. These two bolometers were then mounted in sections of waveguide as shown in Figure 20. One of the sections of guide is connected to the RF system while the other is in physical contact with the guide but is not illuminated with RF power. The leads of the bolometers are brought out through the rear of the phenolic mount and one side of each bolometer is connected together. The heating coil is wound directly around the two guides and then wrapped with insulating material.

The two ferroelectric bolometers are connected in a bridge circuit as shown in Figure 21 and are noted as C_1 and C_2. The principle is the same as any temperature compensating bridge circuit. If the capacitance of C_1 and C_2 are very nearly the same, then ambient temperature fluctuations producing capacitance changes in C_1 should also occur in C_2 and thereby maintain the bridge balance. RF power applied to C_1 will unbalance the bridge to an extent determined by rebalancing with C_4.

Measurements were made at 70 Gc using this system and some very encouraging results were obtained. A complete temperature sensitivity measurement was not made but, by observing the Curie temperature to be approximately 105°C, an operating temperature of 94°C was chosen for the power sensitivity measurements. The results of this test are shown in Figure 22. Since the scale of capacitance is entirely different from that used on previous single bolometers, no direct comparison can be made with the $(\Delta C/\Delta P)$ data of Figure 22. The significant results of this test are that capacitance changes were observed for a power change of less than .04 milliwatts, and that the ambient temperature stability of the bolometer system appeared to be greatly improved.

For the final measurements, batteries were used to supply voltage to the heater coil around the ferroelectric. The use of these batteries increased the depth of the null obtained when balancing the

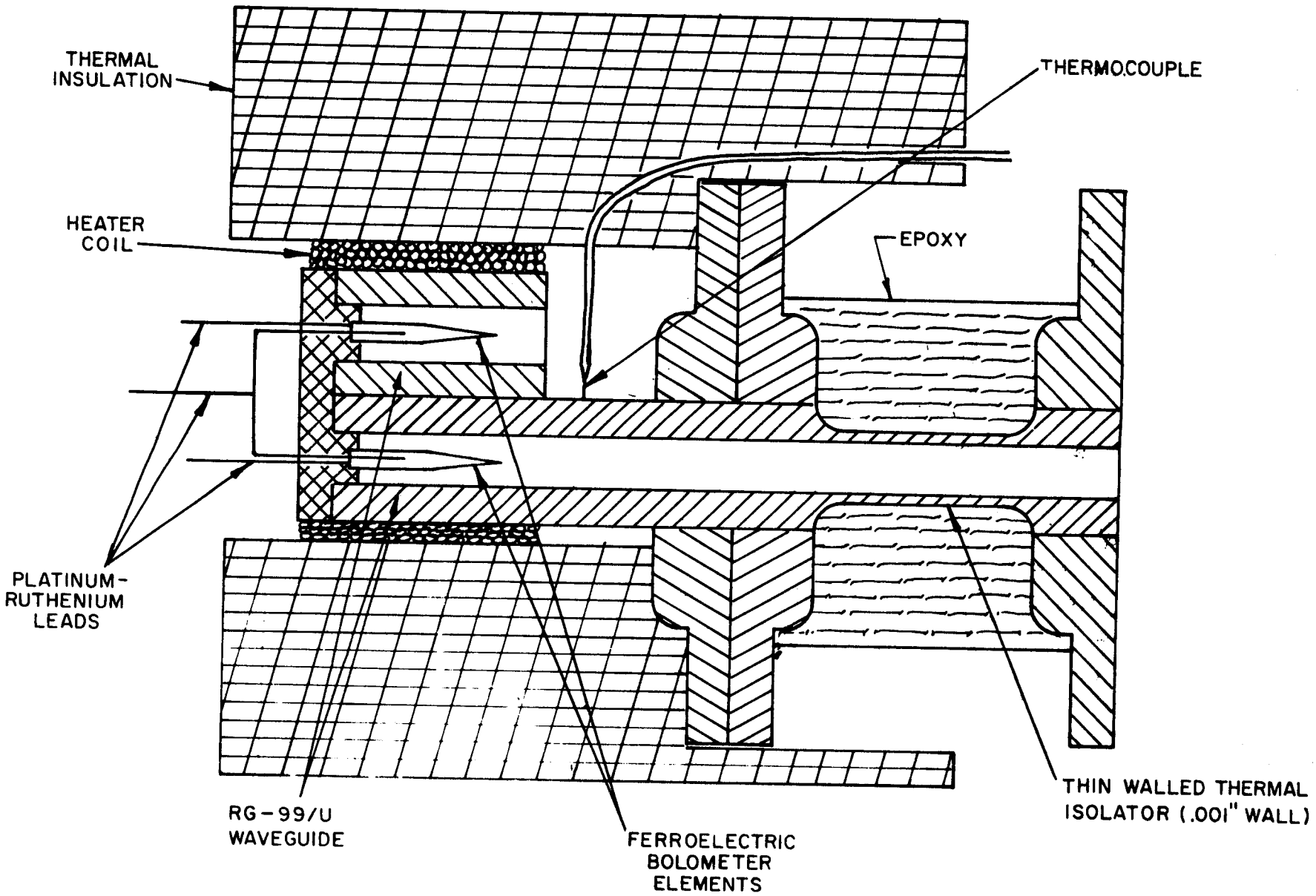

FIG.20- SKETCH OF DOUBLE BOLOMETER MOUNT FOR TEMPERATURE COMPENSATING BRIDGE

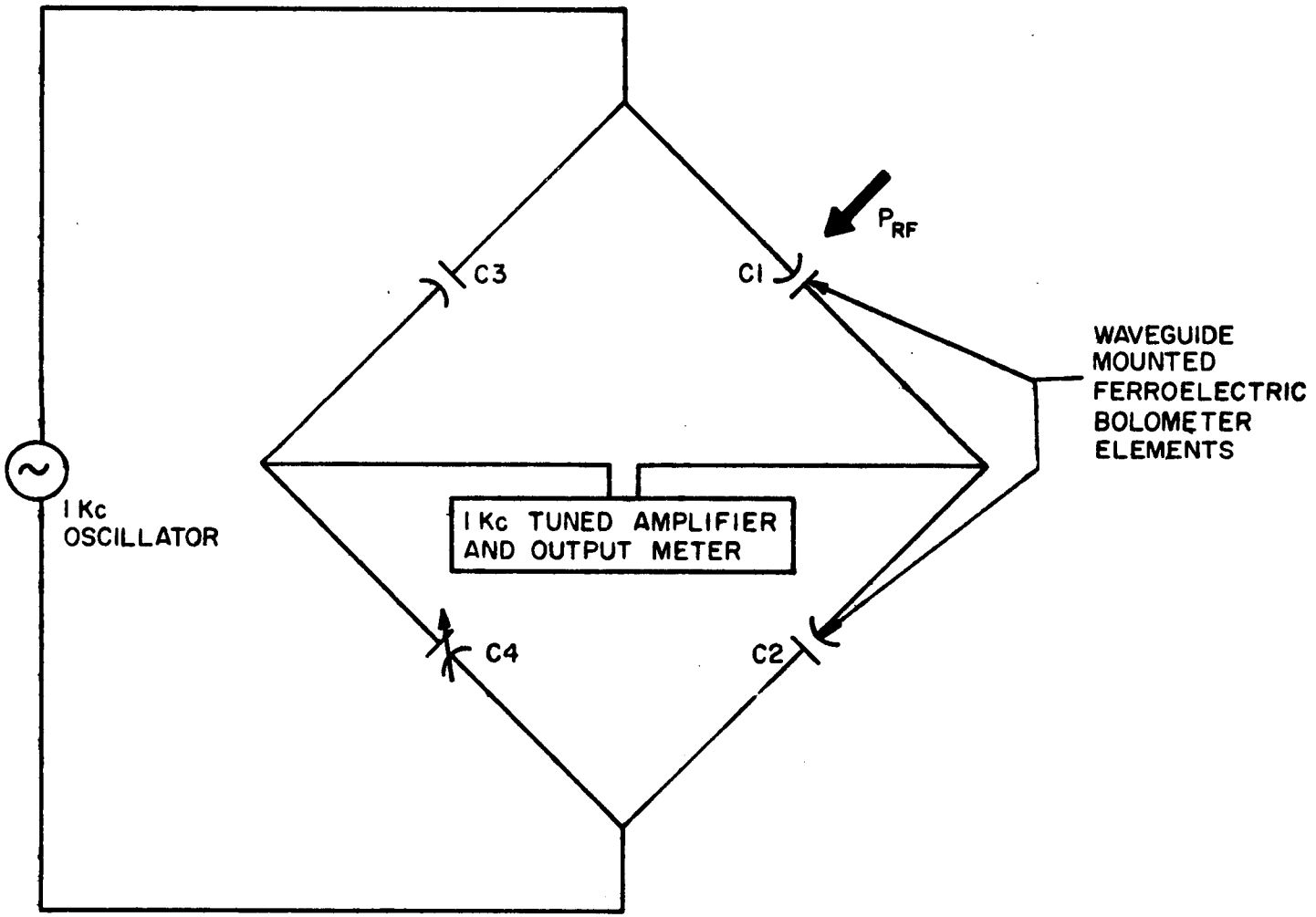

FIG. 21 - TEMPERATURE COMPENSATING POWER BRIDGE EMPLOYING FERROELECTRIC BOLOMETERS.

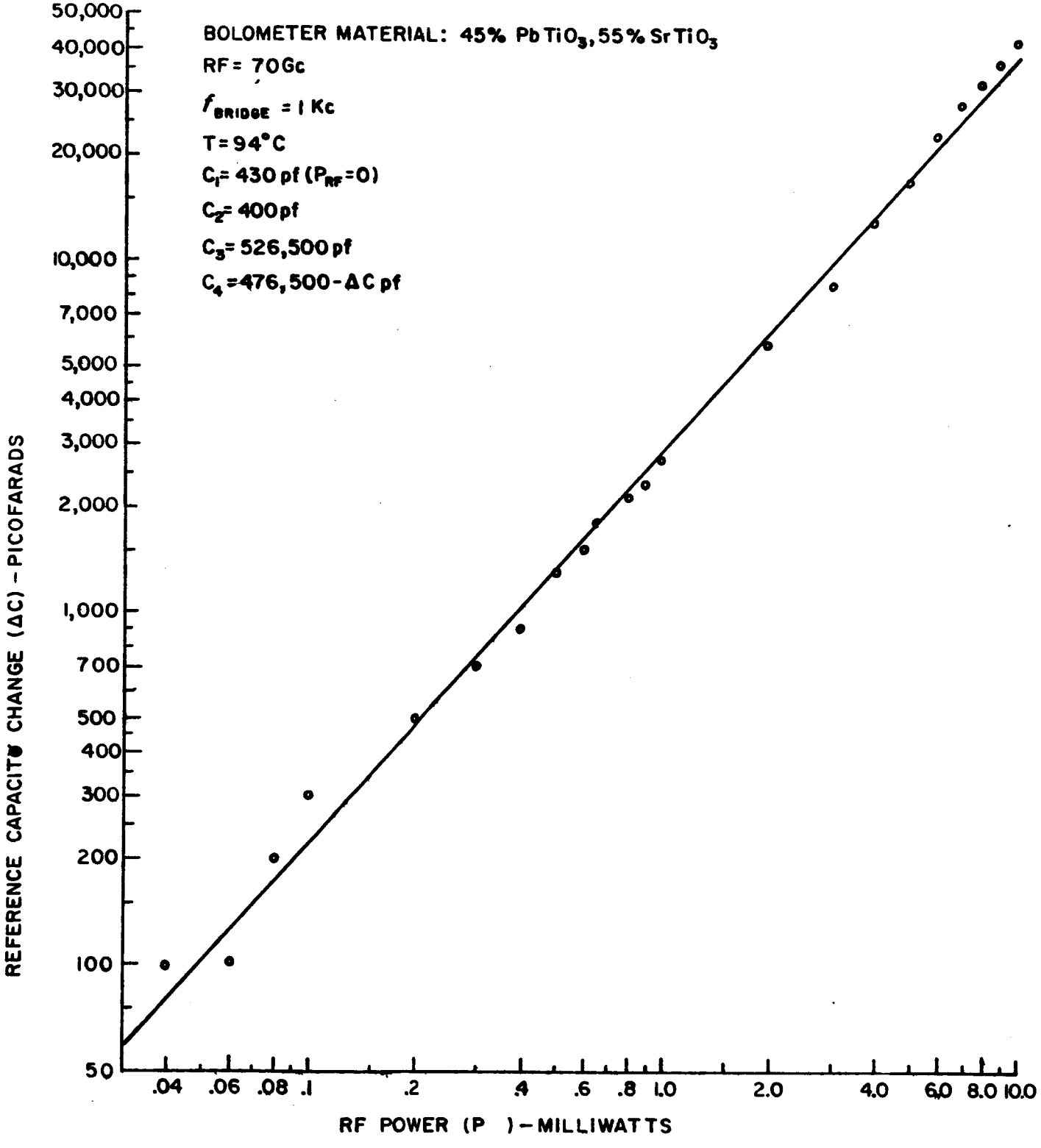

FIG. 22 - REFERENCE CAPACITY CHANGE vs RF POWER FOR THE TEMPERATURE COMPENSATING POWER BRIDGE EMPLOYING FERROELECTRIC BOLOMETERS

bridge through elimination of heater coil power supply ripple. The measurements made included:

(1) capacitance change vs RF power for a number of mount temperatures,

(2) frequency sensitivity measurements,

(3) response time measurements

The first of these measurements was made to determine the temperature range within which the bolometer could be operated before noticeable changes in sensitivity were encountered. The results as shown in Figure 23 indicated that if the ambient mount temperature is held at 94°C, 95°C, or 96°C no substantial difference in sensitivity is observed. At 93°C and 97°C, the sensitivity begins to decrease.

The frequency sensitivity measurements were performed at 70, 94, 140 and 308 Gc. The results of the data obtained is shown in Figure 24. The data taken at 70 and 94 Gc are in excellent agreement with each other. This is to be expected since at these frequencies water calorimeters and precision attenuators are available which are much more reliable than the equipment used at higher frequencies. At 140 and 308 Gc it was necessary to calibrate a precision attenuator and a bolometer in order to set a reference power. At the higher frequencies, multi-mode transmission is possible since the ferroelectric bolometer is mounted in RG-99/U waveguide. Similarly the calorimeter and TRG bolometer mount used to measure the RF power level were also oversize.

The response time of this bolometer is illustrated by the curves of Figure 25. Capacitance change versus time curves are shown for both a half milliwatt increase and decrease of the RF power level. Although the effects of ambient temperature fluctuations are still present, they are much less than were previously observed with single ferroelectric bolometers with an even larger RF power level change. The time required for the bolometer to reach half ($t_{0.5}$) and

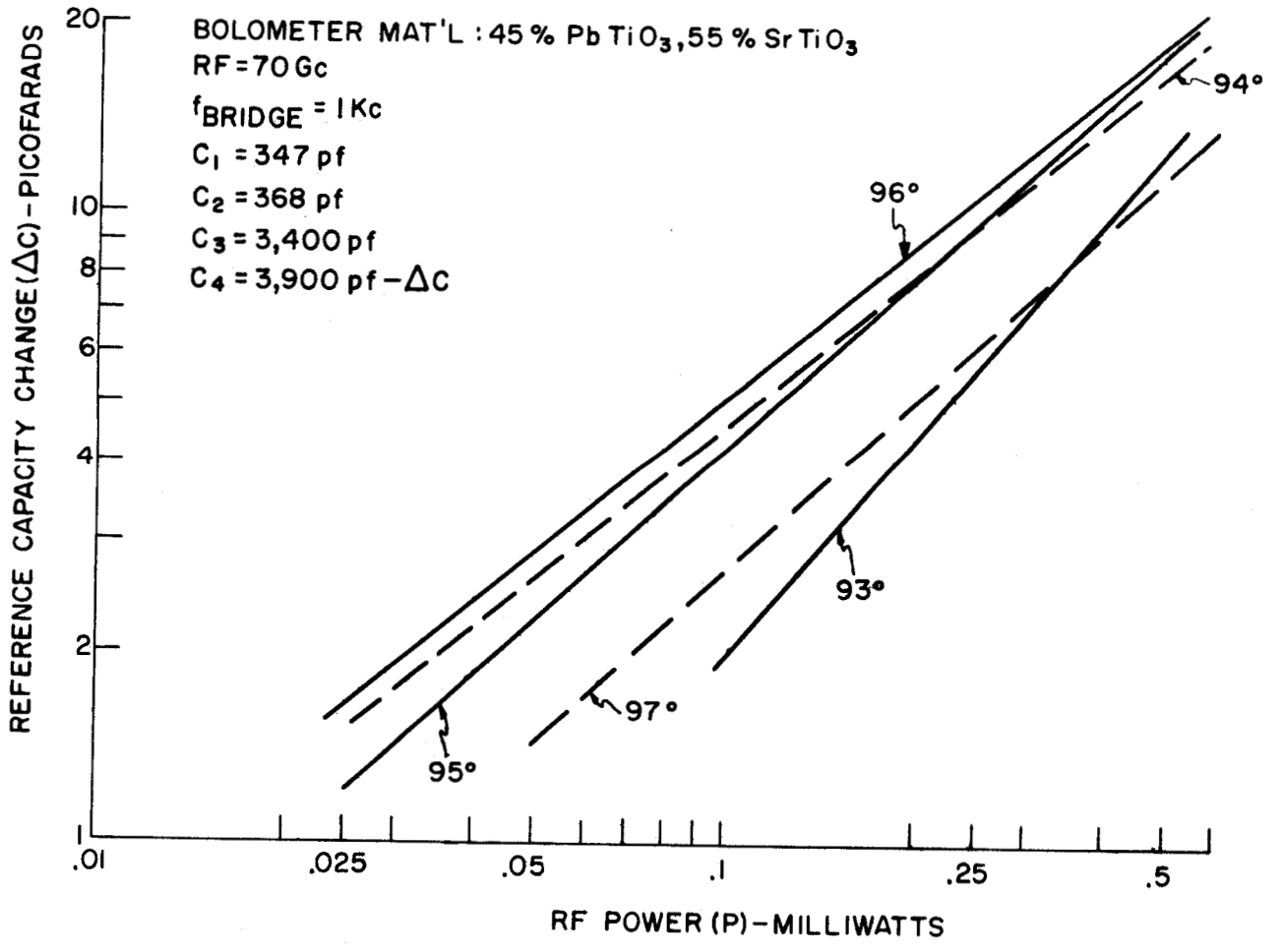

FIG.23 -REFERENCE CAPACITY CHANGE AS A FUNCTION OF MOUNT TEMPERATURE AND RF POWER.

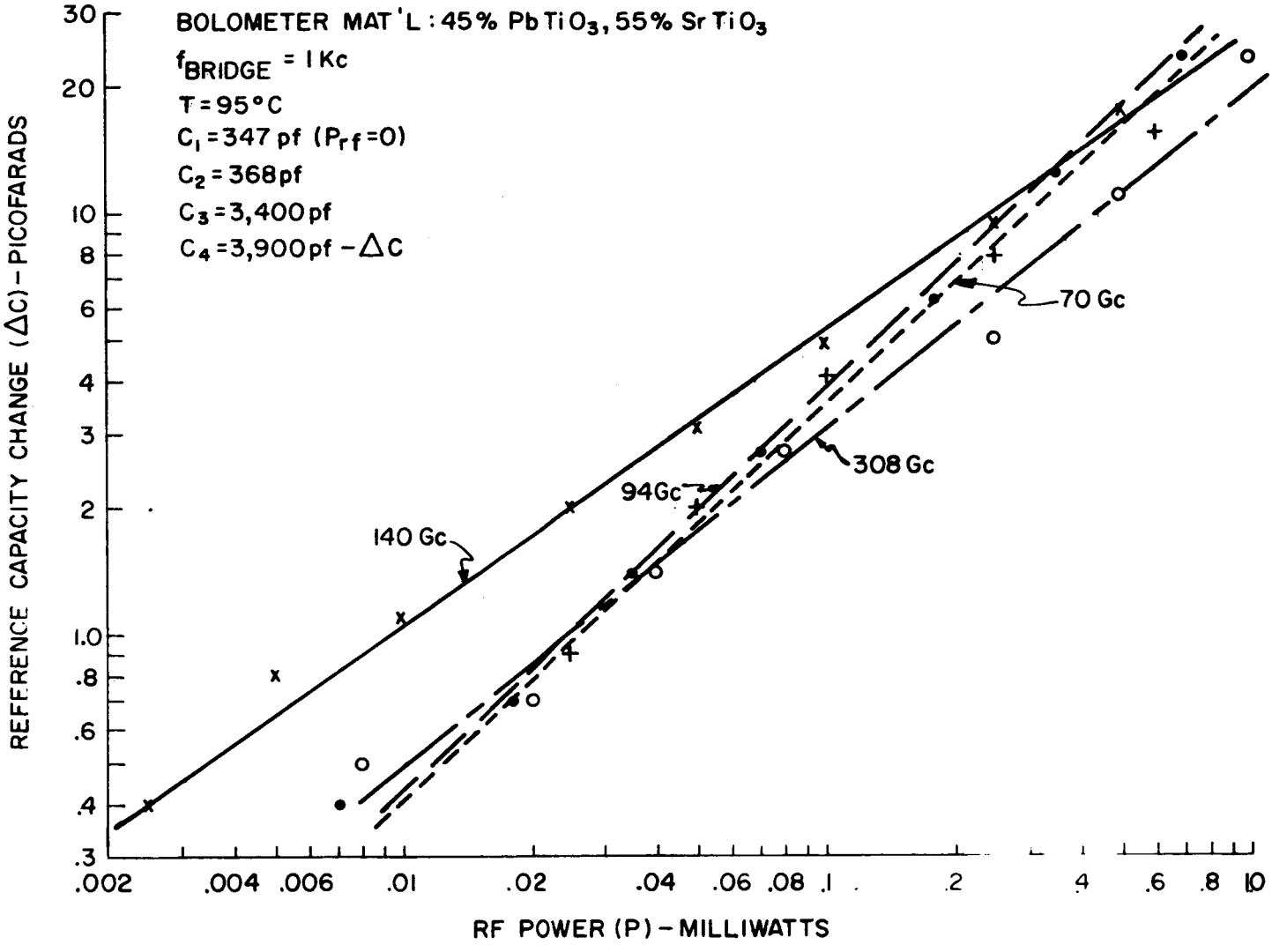

FIG. 24 – REFERENCE CAPACITY CHANGE vs RF POWER FOR THE TEMPERATURE COMPENSATING POWER BRIDGE EMPLOYING FERROELECTRIC BOLOMETERS.

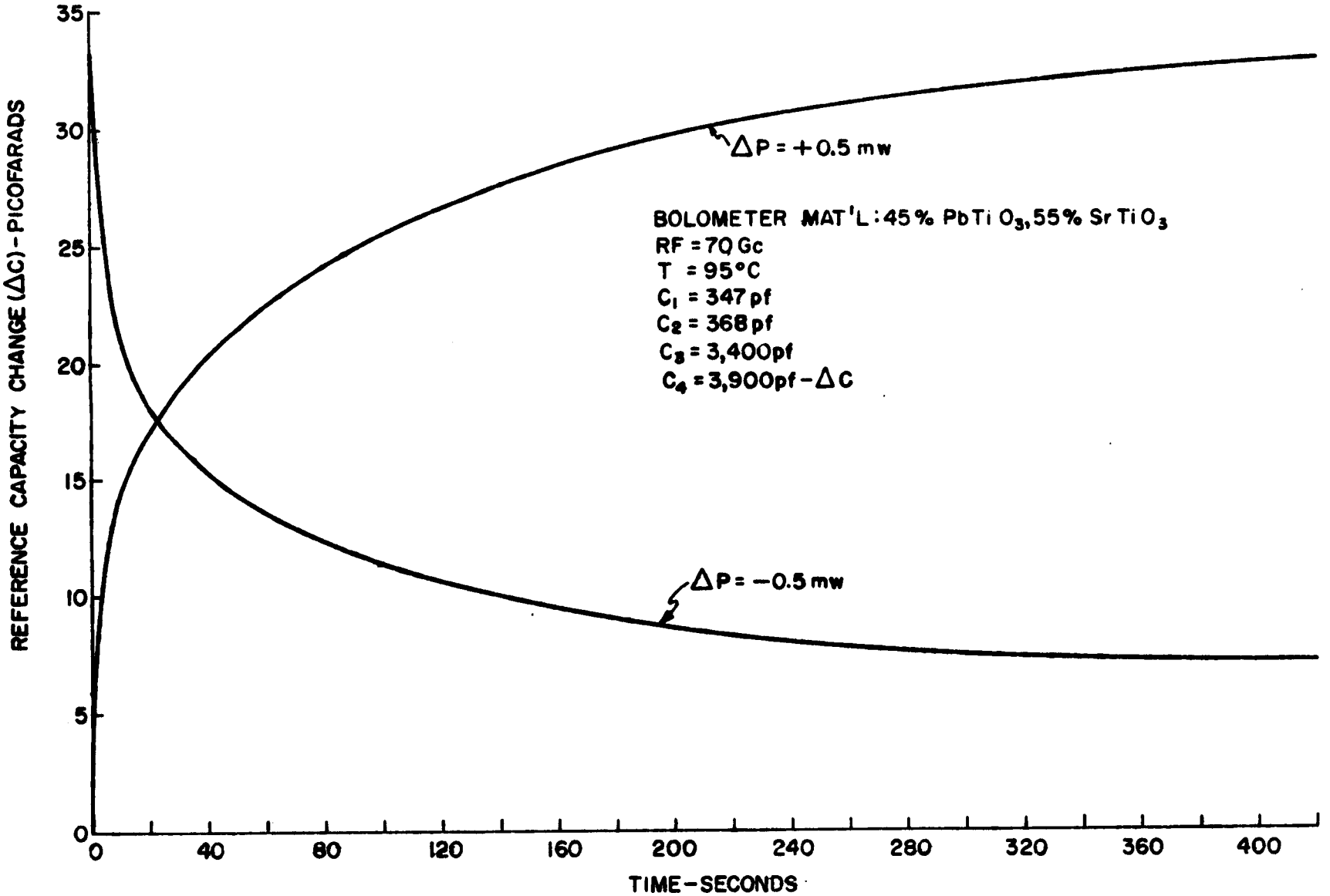

FIG. 25 – REFERENCE CAPACITY CHANGE vs TIME FOR FERROELECTRIC BOLOMETER

90% ($t_{0.9}$) of its final capacitance value are approximately 20 seconds and 180 seconds respectively. Better temperature stabilization and compensation respectively can be achieved by holding the dual mount at a more constant temperature and fabricating the two ferroelectric bolometer elements so that they are more nearly equal.

III. SEMICONDUCTOR DIODE DEVICES (TASK II)

A. Random Balance Experiment

In order to evaluate several different crystal materials, whisker materials, and structural details a simple diode package was designed which could be built economically in quantity and tested in a multipurpose fixture. A diode and the fixture are shown in Figure 26. The combinations of variables were randomized insofar as possible so that the effects of many variables could be ascertained with a minimum number of diodes. The variables were selected by the method of random balance.[3] A random balance experiment is designed to determine the significant variables and the direction of their effects. By its nature it is desirable to include all possible variables.

Five independent variables were included in the experiment. Subsidiary variables were analyzed also although they were not entirely independent and could not be truly randomized. The number of levels of each variable in a random balance experiment is usually low. In fact, two levels of most variables will serve to determine the significance of the variable. Multiple levels of some variables were used in this experiment for reasons to be described. The variables and levels used are given in Table II. The independent variables are underlined.

The experiment was initially designed for 12 crystal samples. A total of 36 diodes were assembled with each level occuring the indicated number of times. Since it was desired to include 15 crystal samples, seven were used only twice and one was used once as no more were available. Fifteen different crystal samples were included because they were all available and comparative data was desired on all of them. Together they represented different levels of several variables. However, the subordinate variables could not be specified independently as the fifteen samples and the combinations they represented were all that were available. Therefore the fifteen samples were combined with the

---

3. T.A. Budne, "Random Balance," Industrial Quality Control, Vol. XV, Nos. 10-11-12; April-May-June, 1959.

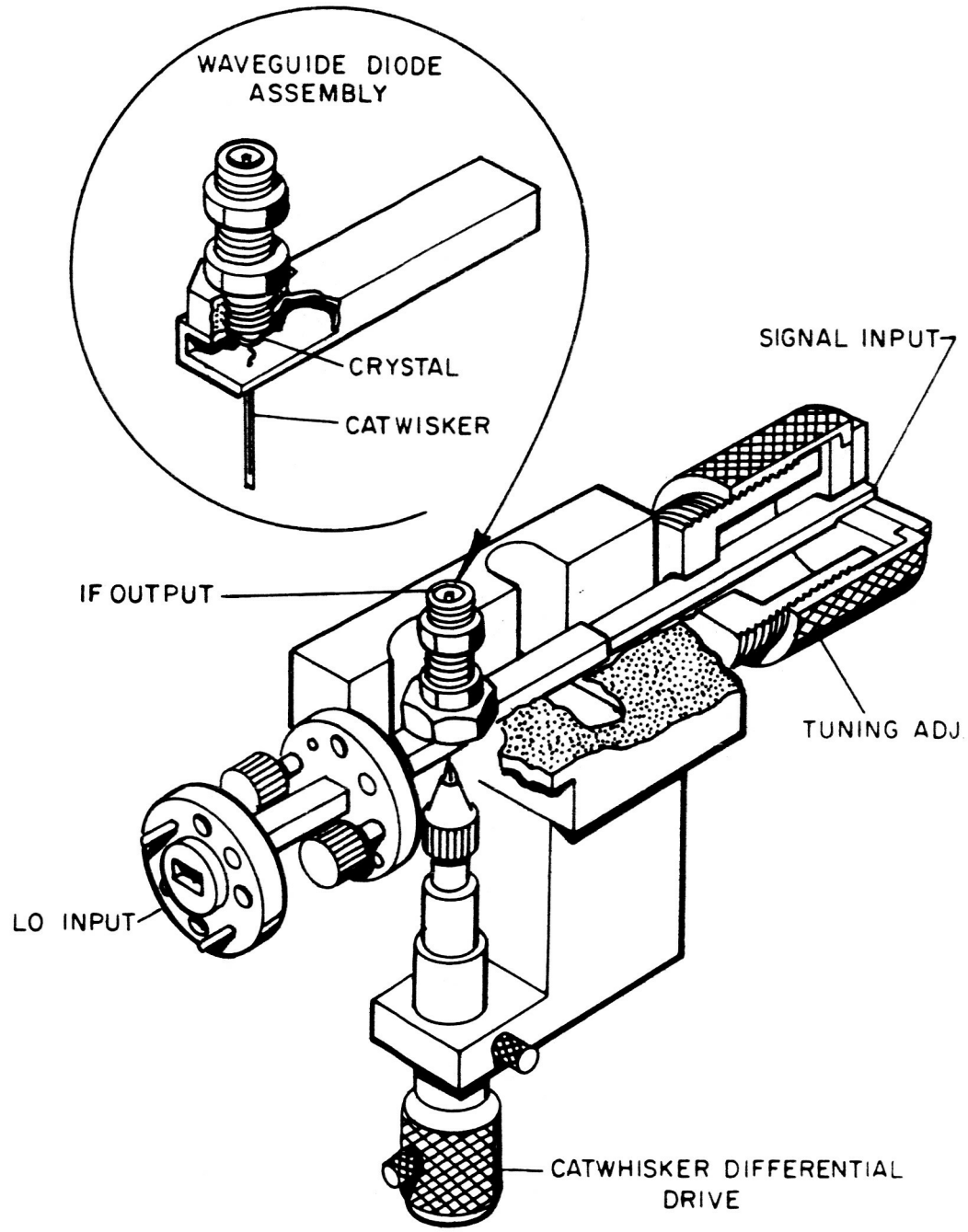

FIG.26- INLINE HARMONIC MIXER FOR DIODE EVALUATION

Variable	Level	Occurrence
Crystal sample	15	2 or 3
Chemical material	4	
Crystalline state	2	
Resistivity	10	
Mobility	9	
Carrier concentration	11	
Figure of merit	11	
Whisker	12	3
Chemical material	7	
Diameter	7	
Form	2	
Orientation if bent	2	
Diameter of hole for coaxial port	2	18
Thickness of crystal die	2	18
Penetration of crystal into waveguide	3	12

TABLE II - Variables in Diode Experiment

other independent variables at random. The test results were analyzed in terms of both independent and subordinate variables. The crystal materials and properties are given in Table III. Values have been rounded off for graphical analysis.

Twelve different whiskers were used representing seven different materials which were of interest. These were only available in certain combinations of sizes as shown in Table IV. Each sample was used in three diodes. Four samples were of too large a diameter to be bent. When installed the whiskers with bends were oriented either with the plane of the bend across or inline to the direction of propagation. These two levels were assigned at random to all 36 diodes but then became inapplicable to the diodes with straight whiskers.

The levels of the other three independent variables were assigned at random an equal number of times. After assigning the variable levels to each diode the occurrence of different combinations of levels of pairs of variables was checked. One or two changes were made but the distribution of combinations was broad, especially for the variables of few levels. Because of the many different crystal samples and whiskers, not all combinations were possible. Gallium arsenide, however, was tested with each different whisker material.

The diodes were tested in the inline mount. One test setup served to give data on detector performance and second harmonic output. A modulated constant power level 70 Gc signal was fed through an attenuator to the inline mount. The diode was formed and the whisker clamped in place. The detected output was taken from the coaxial port and measured as a relative value with a high gain narrow band audio amplifier. The second harmonic propagated through the harmonic output to a 140 Gc detector mount. The detected second harmonic relative level was read on another audio amplifier. A list of the diodes, their combination of variables, and the measured data is given in Table V. This data was taken without external bias.

Sample	Material	Crystalline state	Resistivity (10^{-4} ohm-cm)	Mobility (cm^2/V-S)	Carrier concentration ($10^{17} cm^{-3}$)	Figure of merit (10^9)
A	GaAs	mono	30	3500	5	800
B	"	"	5	2250	55	1500
C	"	"	135	4000	1	400
D	"	"	20	2750	12.5	900
E	"	"	5	2250	60	1600
F	"	"	15	2750	17.5	1100
G	"	"	30	2750	7.5	800
H	"	"	30	3500	7.5	900
I	"	poly	10	1000	70	900
J	"	mono	345	4250	1	300
K	InAs	poly	95	25,500	1	1300
L	InSb	mono	not available	30,000	2 typ	3400 typ
M	Si	"	90 typ	150 typ	50 typ	100 typ
N	"	"	90 typ	150 typ	50 typ	100 typ
O	GaAs	poly	25	3500	10	1000

TABLE III - Crystal Material Properties

Sample	Material	Diameter	Form
AA	Phosphor bronze	1 mil	bent
AE	"	5	straight
BA	Molybdenum	1	bent
BC	"	3	bent
CA	Tungsten	1	bent
CB	"	2	bent
CD	"	4	straight
CF	"	7	straight
DE	Stainless steel	5	straight
EG	Beryllium copper	1.5	bent
FC	Nickel	3	bent
GB	Titanium	2	bent

TABLE IV - Whisker Samples

Diode no.	Crystal sample	Whisker sample	Bend orientation	Hole diameter mils	Die thickness mils	Penetration mils	Output detector	Relative db second-harmonic generator
1	M	CD	---	55	5	10	43	0
2	B	AA	across	55	5	10	38	15
3	C	FC	inline	55	5	5	28	23
4	N	DE	---	55	10	10	42	0
5	G	EG	across	96	5	5	37	12
6	D	EG	"	55	10	0	24	3
7	D	CA	"	55	10	5	13	0
8	E	FC	"	55	5	5	23	0
9	M	GB	"	96	10	10	51	0
10	F	CB	"	55	10	0	32	8
11	E	BC	inline	55	5	10	37	15
12	M	CD	---	96	10	5	45	16
13	I	CF	---	55	10	5	34	0
14	G	CA	across	96	5	5	30	7
15	B	AE	---	96	5	5	20	0
16	K	DE	---	55	5	0	50	0
17	J	CF	---	96	5	5	0	0
18	K	BC	inline	55	10	0	60	24
19	A	EG	"	96	10	10	34	15
20	F	FC	across	96	10	10	12	0
21	J	AE	---	96	10	0	0	0
22	H	DE	---	55	5	0	0	0
23	C	CB	across	96	5	5	25	8
24	O	AE	---	55	10	10	4	0
25	L	AA	inline	96	5	10	55	20
26	F	GB	across	96	10	0	12	10
27	D	CF	---	55	10	0	12	0
28	C	BA	inline	96	5	0	30	24
29	L	CA	across	96	10	0	52	3
30	I	AA	"	96	5	0	38	0
31	H	CD	---	55	5	10	31	21
32	A	BA	across	96	10	5	27	0
33	A	BC	inline	96	5	10	16	14
34	E	BA	"	55	10	10	42	18
35	O	GB	"	55	5	5	19	10
36	B	CB	across	55	10	0	30	0

TABLE V - 36 Diode Random Balance Experiment

The output data of the diodes as detectors were studied first. Scatter diagrams of the output were plotted as a function of each variable. The first scatter diagrams showed the crystal material was the dominant variable. Since this was a discrete variable, the data were replotted as ranked in order of magnitude. Then a regression line was drawn and the effect of crystal material was removed from the data. New scatter diagrams for the other variables were then plotted with the corrected data. The whisker sample then appeared as the principal variable. The effect of the whisker sample was removed in the same manner. The next set of scatter diagrams showed diodes with the smaller output port averaged 8 db more output. The other variables (whisker orientation, crystal thickness, and penetration) showed no correlation with detector output.

The original data was now corrected for whisker sample and output hole diameter and plotted as a function of the subordinate variables: chemical material, resistivity, mobility, carrier concentration, and figure of merit. Figures 27 and 28 are diagrams of the first and last of these. In all cases the points were widely scattered and no meaningful regression lines could be drawn. However some conclusions can be drawn with respect to diodes as 70 Gc detectors:

1. Indium arsenide and indium antimonide shared equally in the best response. (The samples using these materials also had high figures of merit.)
2. Silicon diodes were the next best detectors.
3. Both poly- and monocrystalline gallium arsenide diodes had outputs ranging from 1 to 35 db.
4. Considering the gallium arsenide diodes only, no consistent relations were evident between detector output and resistivity, mobility, carrier concentration, or figure of merit. This was contrary to expectations and may have been caused by:

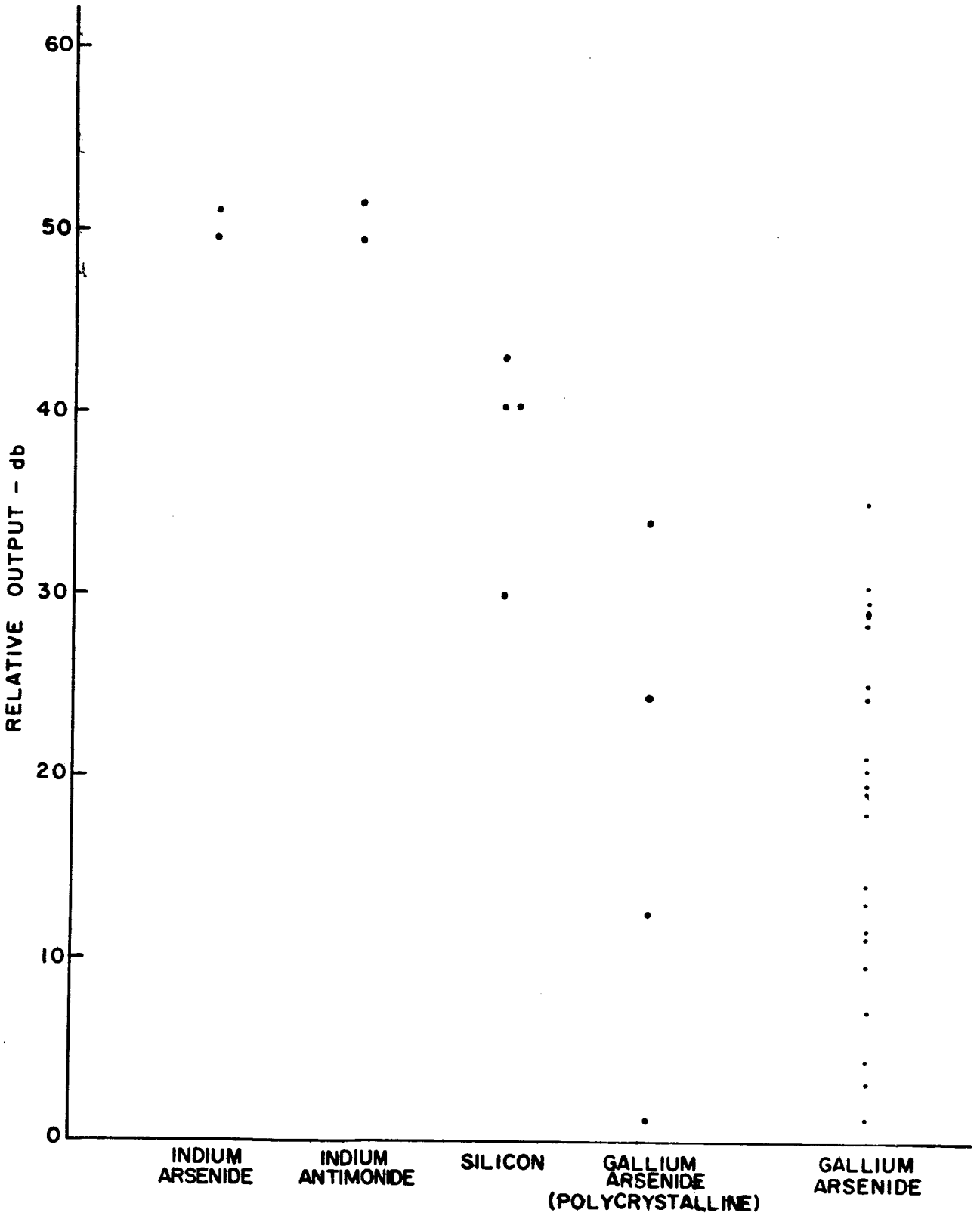

FIG. 27 - 70Gc DETECTOR OUTPUT vs CRYSTAL MATERIAL

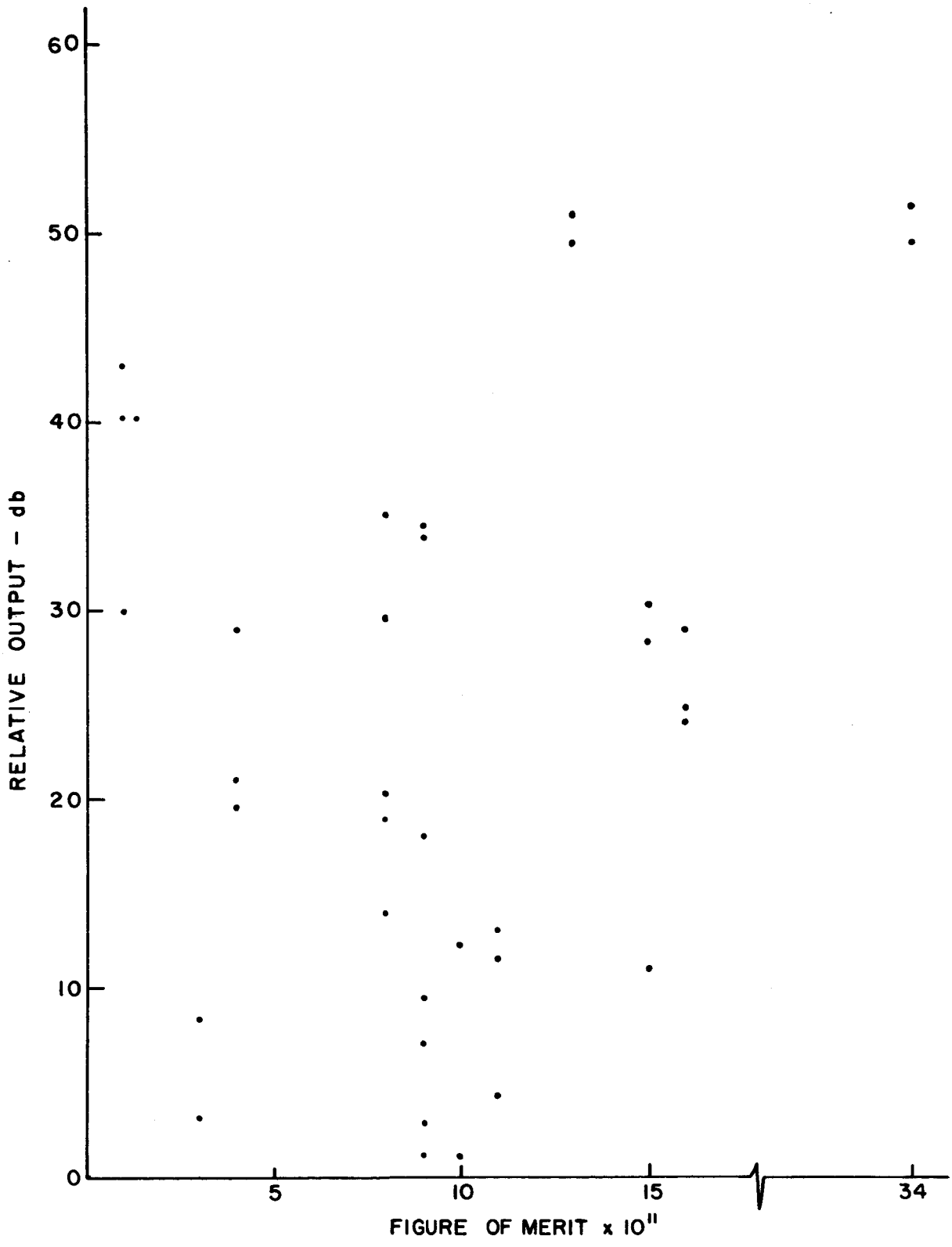

FIG. 28 - 70 Gc DETECTOR OUTPUT vs FIGURE OF MERIT

a. inaccurate knowledge of the properties of individual crystal dice since the values used were averages taken from manufacturer's data for the ingot from which the crystal was cut.

b. unknown, dominant variables either crystal properties, methods of preparation, or test procedures.

The effect of output hole diameter and crystal sample was removed from the original data and the results plotted as a function of whisker diameter. As was expected, the 1 to 2 mil diameter whiskers gave the greater outputs. This effect was also removed and the data plotted versus whisker material as in Figure 29. From this diagram it appears that stainless steel is a poor whisker material for detectors. Tungsten has highly variable performance although it includes the best points. Beryllium copper appears better than most including phosphor bronze. The beryllium copper was silver-plated except in the region of the point. The idea of plotting a scatter diagram for the work function of the whisker material was abandoned because of the wide overlapping ranges of values given in the handbooks for work functions.

The data obtained on second harmonic output included zero output from 17 of the 36 diodes. The data was first analyzed to determine the reason for this. Several scatter diagrams were plotted. That of Figure 30 dramatically shows the dependence upon whisker orientation. All cases of zero output occurred with the whisker bend across the waveguide or with no bend at all. The unbent whiskers were also the large diameter whiskers. With two exceptions it appears it was impossible to obtain a harmonic generating junction with the large, unbent whiskers. These whiskers would be blunted more easily. Pressure of the contact would be less stable. The two exceptions imply that a large, straight whisker will perform well if the junction contact can just be made. These two diodes had 4 mil tungsten whiskers. That diodes with bends across the waveguide should have so many zero outputs and should have non-zero outputs averaging 10 db less than diodes with

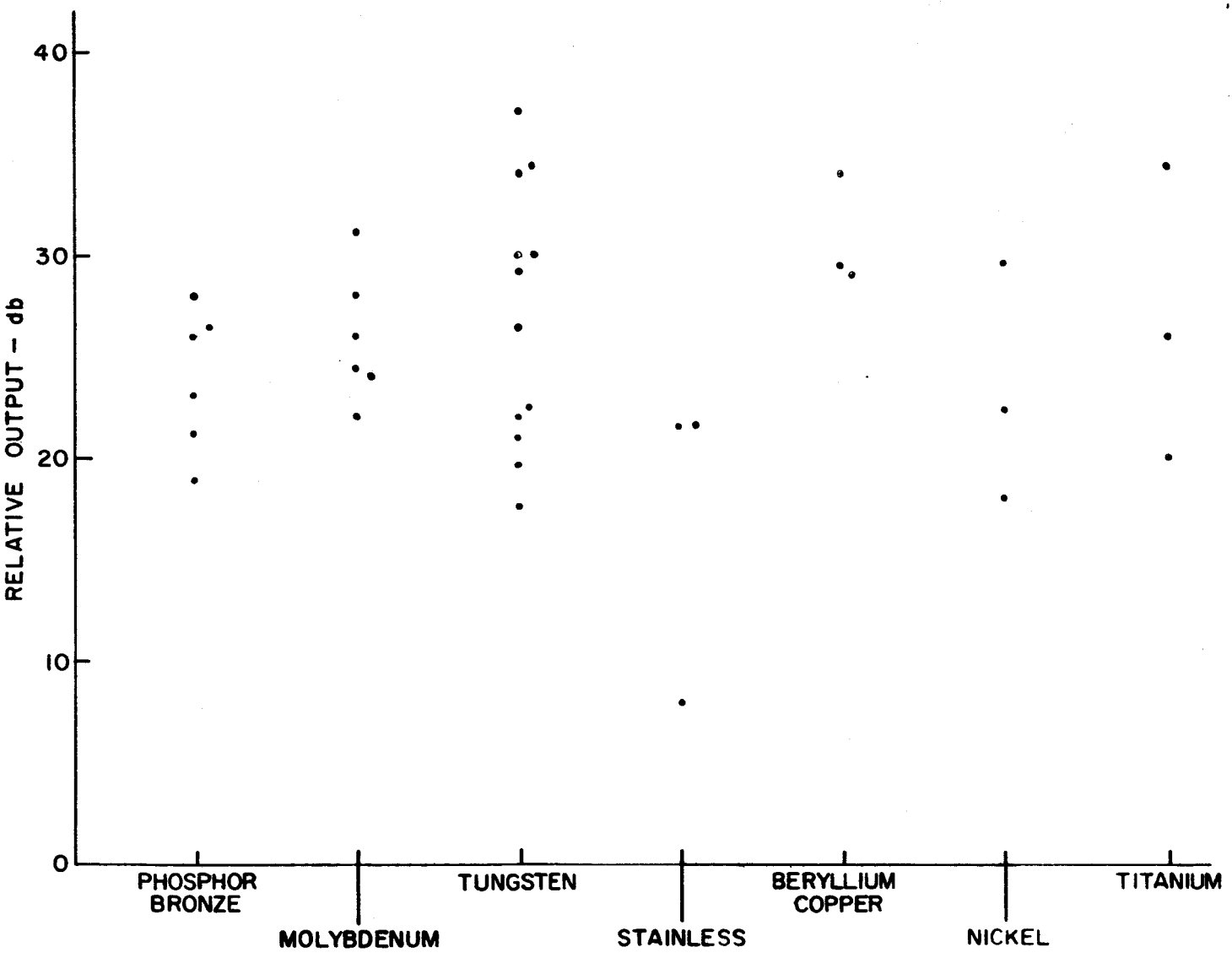

FIG. 29 - 70 Gc DETECTOR OUTPUT vs WHISKER MATERIAL

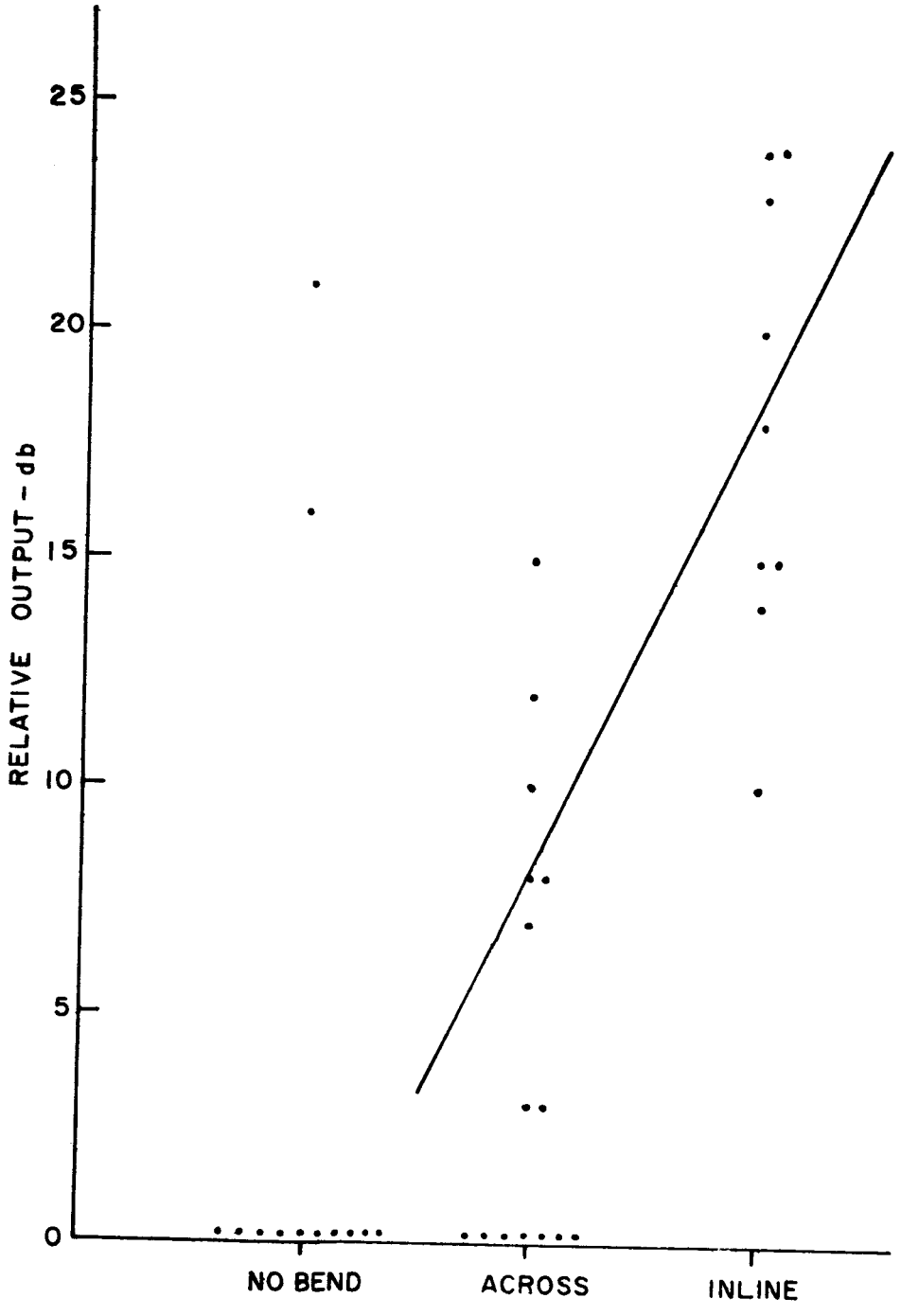

FIG. 30 – SECOND HARMONIC GENERATOR OUTPUT vs WHISKER ORIENTATION

inline bends was unexpected. Further investigation is desirable to determine if this effect depends upon wavelength, bend diameter, the inline structure, or some other factor.

The remainder of the analysis of second harmonic data was done with the diodes of non-zero output only and with the effect of bend orientation removed. As with the detector data, the crystal material was dominant. A scatter diagram was plotted with the outputs ranked in order by crystal sample. Diagrams of the remaining variables were then plotted with the effect of crystal sample also removed. No trend was found in the data for whisker material, coaxial hole diameter crystal thickness, or crystal penetration. The residual scatter for most levels of the variables was 8 db. Any lesser effects would be masked. However, this is low compared to the possible variation between successive contacts of the same crystal and whisker.

Since the effects of no additional variables could be recognized, the data as a function of crystal sample was examined again. The gallium arsenide samples B, C, and G and the indium arsenide had the best performance as second harmonic generators. The one silicon diode remaining in the data set had about 8 db less output. Scatter diagrams were also plotted as a function of crystal resistivity, mobility, carrier concentration, and figure of merit. As with the comparable diagrams for 70 Gc detector outputs, no trends could be identified.

In retrospect, the design of the random balance experiment could be improved in a number of ways. The number of levels of variables should be reduced. This could be done in part if two or three nominal values of crystal properties were chosen, randomly combined with different crystal materials and crystals purchased with these properties. Whisker diameter should be limited to one and three mils and the required wires purchased. Then all whiskers could be bent. It would be desirable to eliminate crystal post penetration as a variable since the coaxial connectors are not secure in the two positions of lesser penetration. This variable did not appear to be significant in the tests

made.

Other variables could be added to the experiment without increasing the number of diodes. Variables it would be useful to include would be: diameter of whisker bend, silver epoxy and plating-soldering bonding techniques for the crystal dice, die surface finish, crystal manufacturer, plane of crystal cut. Also the fundamental frequency of the test could be treated as an independent variable. Two levels such as 70 Gc and 90 Gc could be chosen.

B. Harmonic Generators and Mixers

1. Construction

To obtain quantitative data on point contact diodes as harmonic mixers and generators, two cross-guide units were designed and fabricated. The cross-guide structure has been tested extensively in a number of millimeter wave research programs conducted at this laboratory. The results of these programs have shown that, although more difficult to construct and less versatile than the in-line configuration, the cross-guide units produce considerably better results. It was decided therefore that in order to obtain the maximum performance from a diode the optimum waveguide configuration should be utilized.

The two harmonic generators constructed for this program were identical. Two units were necessary since, for harmonic mixer measurements, one would be used as a harmonic generator producing the signal and the other used as the mixer. They are completely interchangeable and either could be used as the generator or the mixer. In the following text and figures, any reference to harmonic generator or harmonic mixer will infer function only and not separate units. Figure 31 is an exploded drawing of the harmonic generator-mixer showing the location of the various parts. Figure 32 is a photograph of the assembled unit.

Both the fundamental (RG-98/U) and harmonic (RG-138/U) waveguides of the generator-mixers are of electroformed copper. The choice of copper rather than silver was prompted by difficulties in

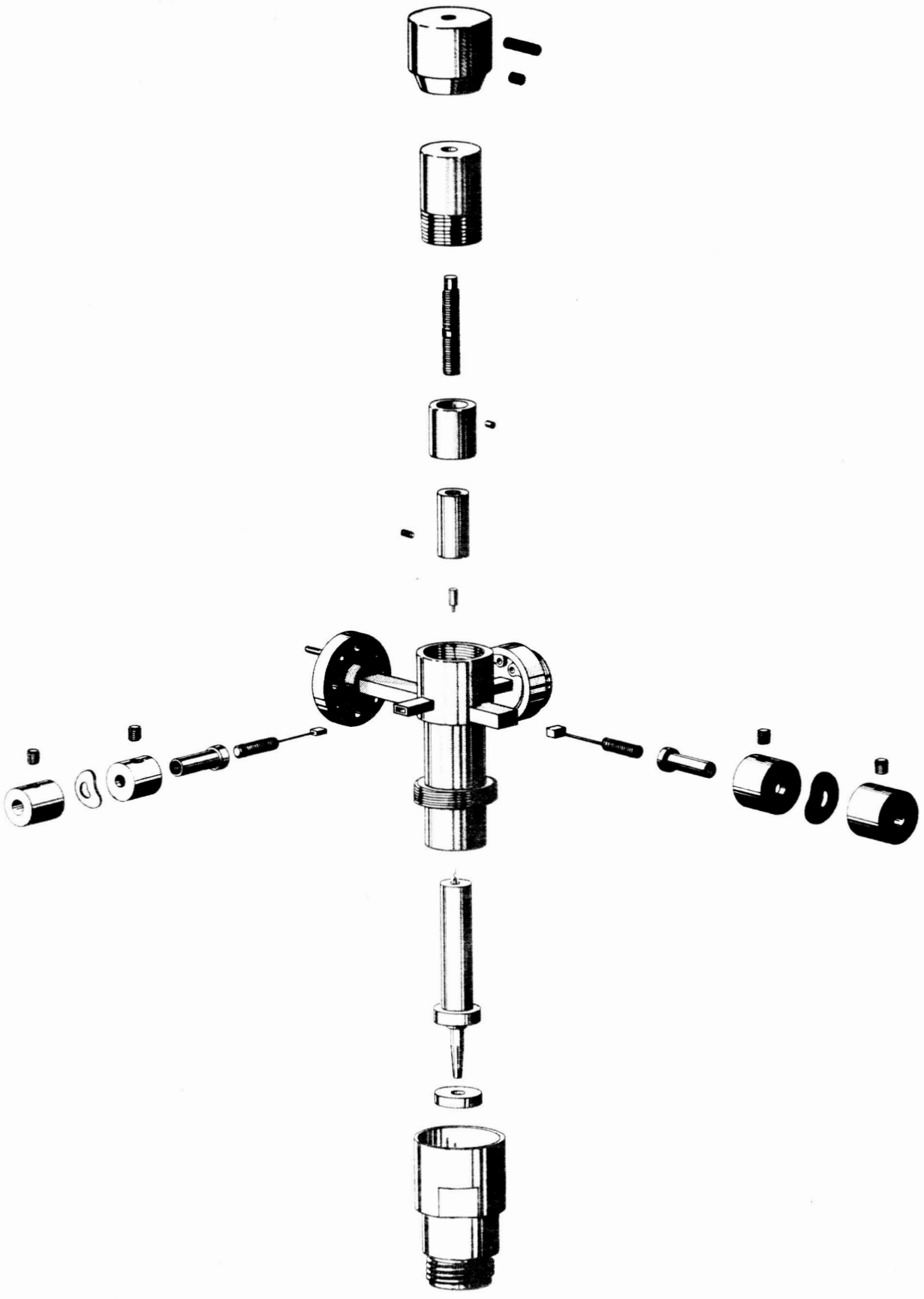

Figure 31 - Exploded View of Harmonic Generator-Mixer

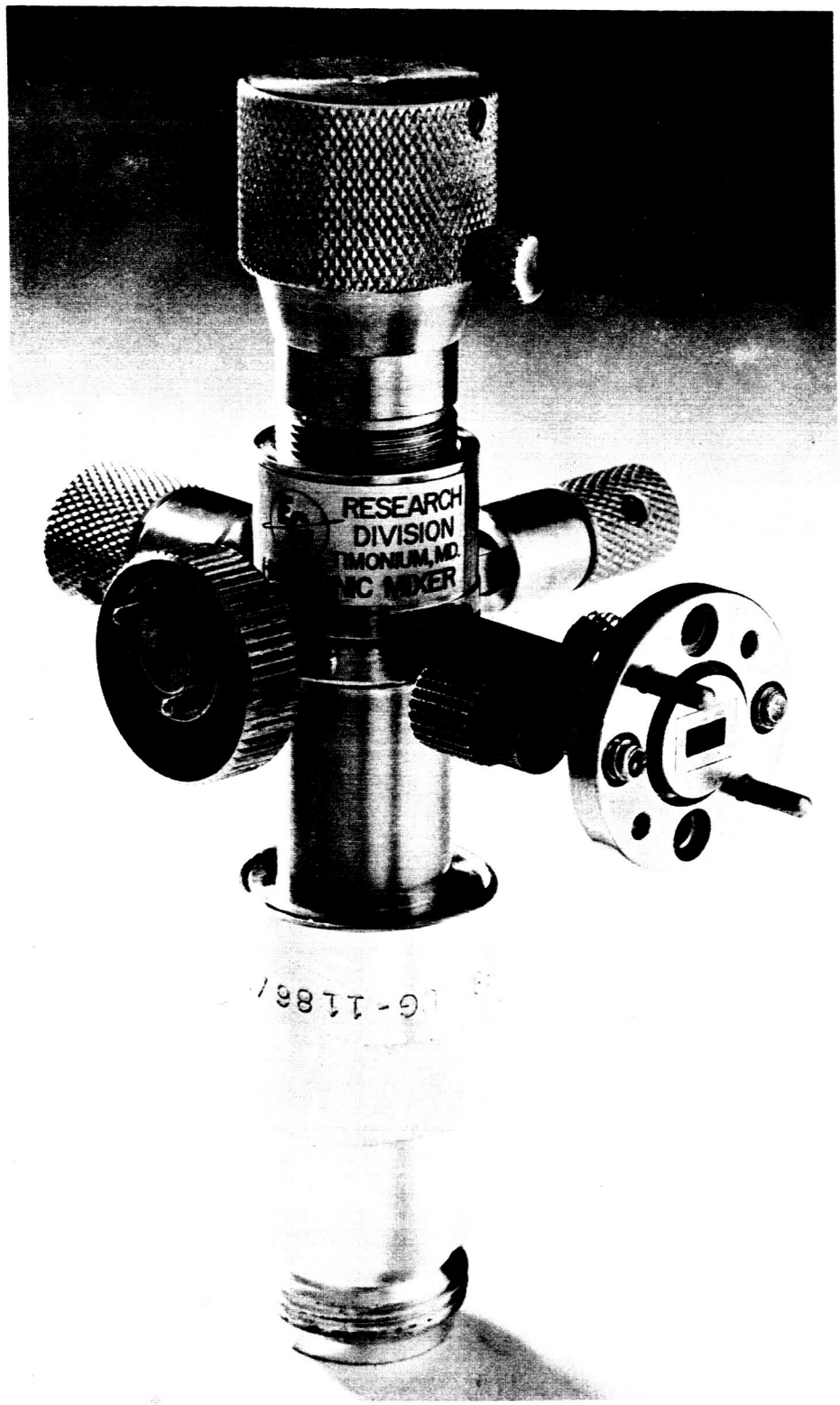

Figure 32 - Photograph of Harmonic Generator-Mixer

obtaining drawn silver waveguide with dimensional tolerances and inner surface finishes suitable for exacting millimeter wave requirements. Considerable improvement in the inner surface and more uniform inside dimensions were realized from the use of the electroformed waveguide.

The complete electroforming procedure is performed in our laboratory. The mandrels are made from polystyrene, machined to the approximate dimensions, and finished to size on a lapidary wheel. The final polishing is done with Linde A (0.3 micron) abrasive. The mandrels are silver plated using a precipitation process and are then placed in a copper fluoborate bath where the walls are plated to a thickness of about .050". They are then removed from the bath machined to the standard .040" wall thickness, and finally, the mandrels are melted out with chloroform.

The uniform inside dimensions of the electroformed guide has resulted in greatly improved performance and repeatability by the movable waveguide short. Our past experience in constructing millimeter waveguide components which require movable shorts has shown that the contacting short is superior to the non-contacting if it can be made close fitting at all points in its travel. This requirement was impossible to achieve with standard drawn silver waveguide but became practical with the electroformed guide.

After many tests, optimum performance was obtained with a solid, fine gold short in the RG-98/U guide and a spring type short in the RG-138/U guide. The fine gold was chosen since it is softer than the copper and would not mar the inner surface. It was found that this material was not suitable for use in the RG-138/U guide where requirements of continuous contact are more severe due to the shorter wavelengths. Therefore, an alloy of 69% gold, 25% silver, and 6% platinum was formed into a loop short .001" thick. This alloy has spring properties so that the loop maintains pressure against the

broad wall of the guide. Figure 33 is a photograph of the loop short. This type short has been used at frequencies up to 420 Gc and, although equipment is not available for conducting reflection coefficient measurements at these frequencies, the results have been quite satisfactory.

2. Semiconductor Materials

Four types of semiconductor material, three gallium arsenide and one silicon, were prepared for use in the harmonic generators. In the preparation the crystals were first lapped and plated, then polished and soldered to a brass post. The gallium arsenide materials were plated in an electroless nickel solution. The silicon first had to be gold plated, heated to alloy the gold into the silicon, then nickel plated and soldered to the brass post. The finished crystal has a .020" diameter and is approximately .005" thick. The brass post, with the crystal attached, fits into the differential drive screw mechanism and can be removed with little difficulty.

3. Whiskers

Tungsten and phosphor bronze whiskers of .001" diameter were used in this program. The finished whisker is .130" long with a half loop bend along its length to provide axial spring action upon making contact with the crystal. The whiskers are first bent to shape then soft soldered into a .185" long beryllium copper tube of .020" diameter. The tungsten whiskers are nickel plated on the mount end so that they may be soldered.

The whiskers are pointed electrolytically in a 7 normal solution of potassium hydroxide (KOH). The end of the whisker is lowered into the solution and withdrawn until contact with the solution is made only through the meniscus. When the current is passed through the contact, the whisker material passes into the electrolyte until the meniscus drops off and the contact is broken. By observing the bubbling action at the contact one can determine when the process is finished.

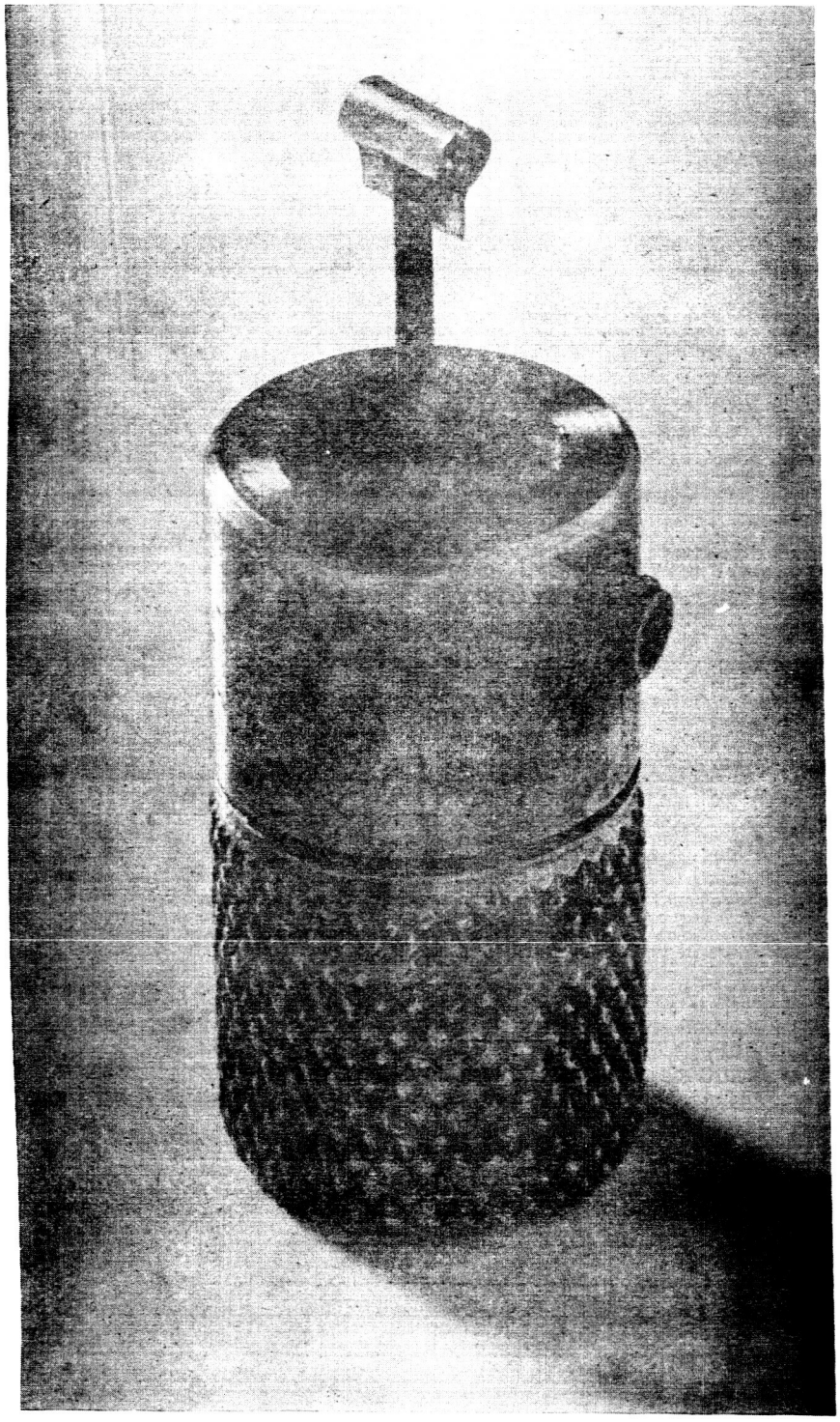

Figure 33 - Gold Loop Variable Waveguide Short

4. Junction Forming

The diodes used in this program are point contact devices and the variation in millimeter wave characteristics from one junction to another is quite apparent. It is imperative therefore that the best contact conditions are realized before any extensive tests are performed. The diode forming method which has proved most successful is that of making the contact in an RF set-up while observing the rectified current on an I-V curve tracer connected to the IF port of the harmonic mixer. Figure 34 is a photograph of the I-V characteristics of a diode formed in this manner. The forward characteristic is to the right and the backward characteristic to the left.

The lower curve of Figure 34 is due to the 60 cycle sweep voltage applied to the diode by the I-V curve tracer. In addition to the 60 cycle voltage, 70 Gc RF power square wave modulated at approximately 1000 cycles is fed to the diode. The upper curve results from simultaneous application of the modulated RF and the 60 cycle voltage to the diode. The discontinuous dual trace shown in Figure 34 is obtained when the square wave modulation frequency is a multiple of 60 cycles. The separation between the curves is a measure of the efficiency of RF detection and as such provides a qualitative measure of the device degradation due to the parasitic elements (spreading resistance and junction or barrier capacity). The degradation of RF performance due to these parasitic elements occurs in semiconductor diodes when they are used as detectors, mixers, or harmonic generators. This dual trace method of observing diode performance, allows one to simultaneously determine if a satisfactory non-linear characteristic has been obtained and if satisfactory RF performance can be expected. Prior to the use of this dual trace technique, many diodes had been formed which yielded excellent 60 cycle I-V characteristics but totally unsatisfactory millimeter wave behavior. That was a frustrating but not an unexpected result since the effect of the parasitics would not be observable at 60 cycles. The new dual trace technique of observing diode formation

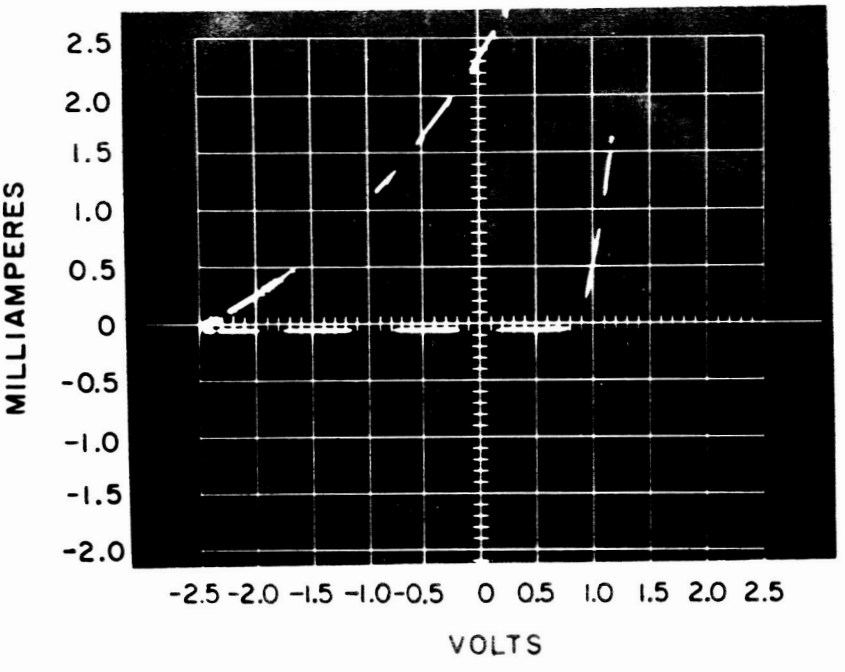

FIG. 34 - DUAL I-V TRACES FOR A MM WAVE SEMICONDUCTOR DIODE

yields a substantially greater correlation between I-V characteristics and observed millimeter wave device performance.

5. Harmonic Generators

Harmonic generation efficiency measurements were performed on the four semiconductor materials. Generation efficiency data was obtained as a function of input power, DC bias, and DC load resistance. The materials tested and their characteristics are given in Table VI.

Material	Resistivity (Ω-cm)	Mobility (cm^2/V-S)	Carrier Concentration (cm^{-3})
n-GaAs(Te)	1.3×10^{-3}	2800	1.8×10^{18}
n-GaAs	13.4×10^{-3}	4100	1.14×10^{17}
n-GaAs	2.6×10^{-3}	3540	6.77×10^{17}
p-Si(B)	1×10^{-2}	---	----

TABLE VI - Crystal Material Properties

The 70 Gc fundamental power for these measurements was supplied by a klystron and was measured by a water calorimeter. The generated harmonic power was measured with a TRG F990 bolometer which had been calibrated with a 140 Gc Carcinatron, precision attenuator, and a water calorimeter. Connection of a DC bias voltage or DC load resistance is made thru an N-type connector at the IF port of the harmonic generator-mixer.

Figures 35 thru 41 show curves of the data obtained for second and third harmonic generation conversion loss as a function of input power. These curves are for the most part self-explanatory but there are several facts that should be noted.

The gallium arsenide material, $\rho = 1.3 \times 10^{-3} \Omega$cm (Figure 35), and the silicon material (Figure 36) exhibit similar functional dependence of P_2 (the harmonic power) to P_1 (the fundamental power). For both of these materials, $P_2 \propto P_1^2$ at lower levels of input power, and $P_2 \propto P_1$ for higher input power. This functional dependence

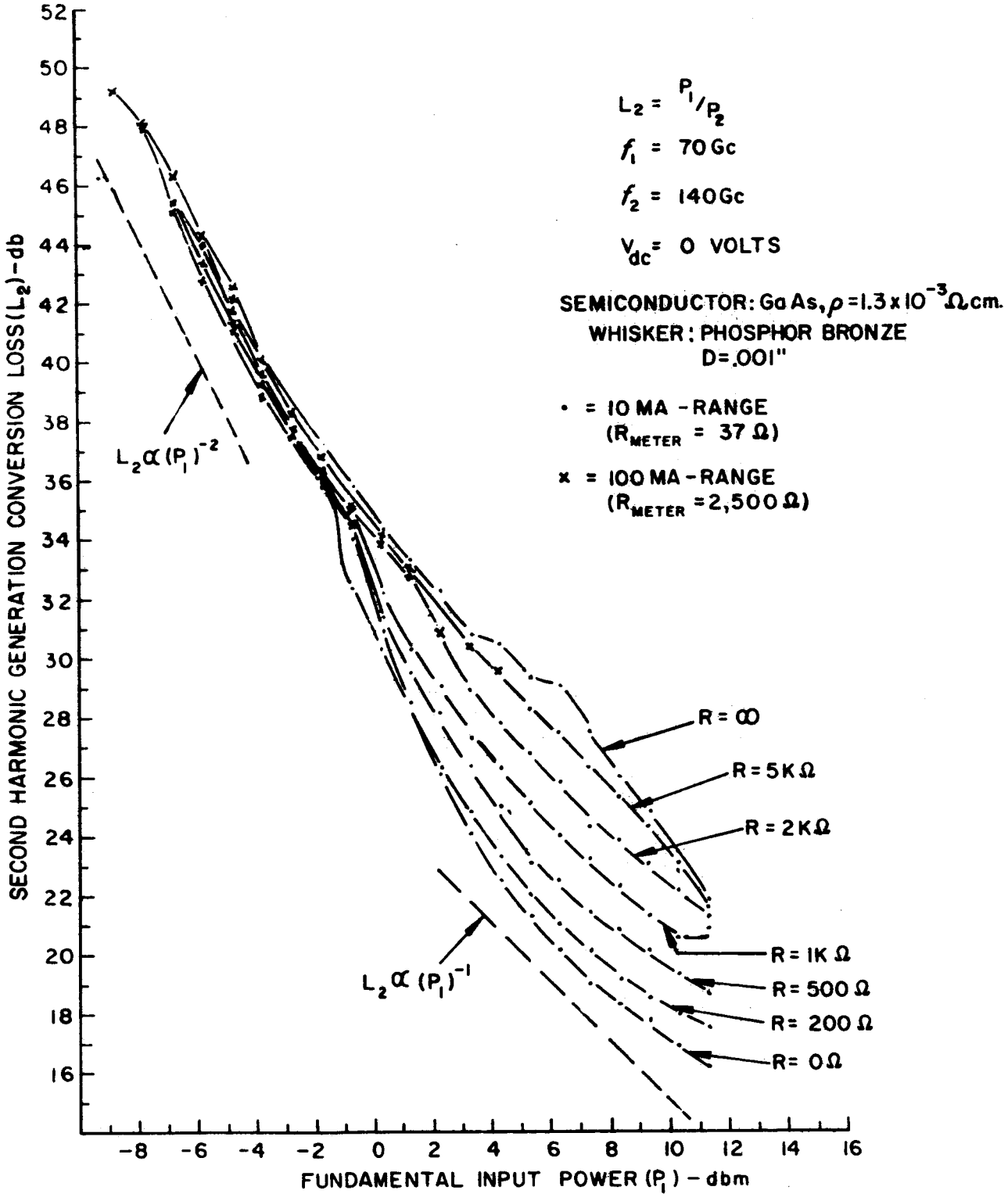

FIG. 35 - MEASURED SECOND HARMONIC GENERATION CONVERSION LOSS

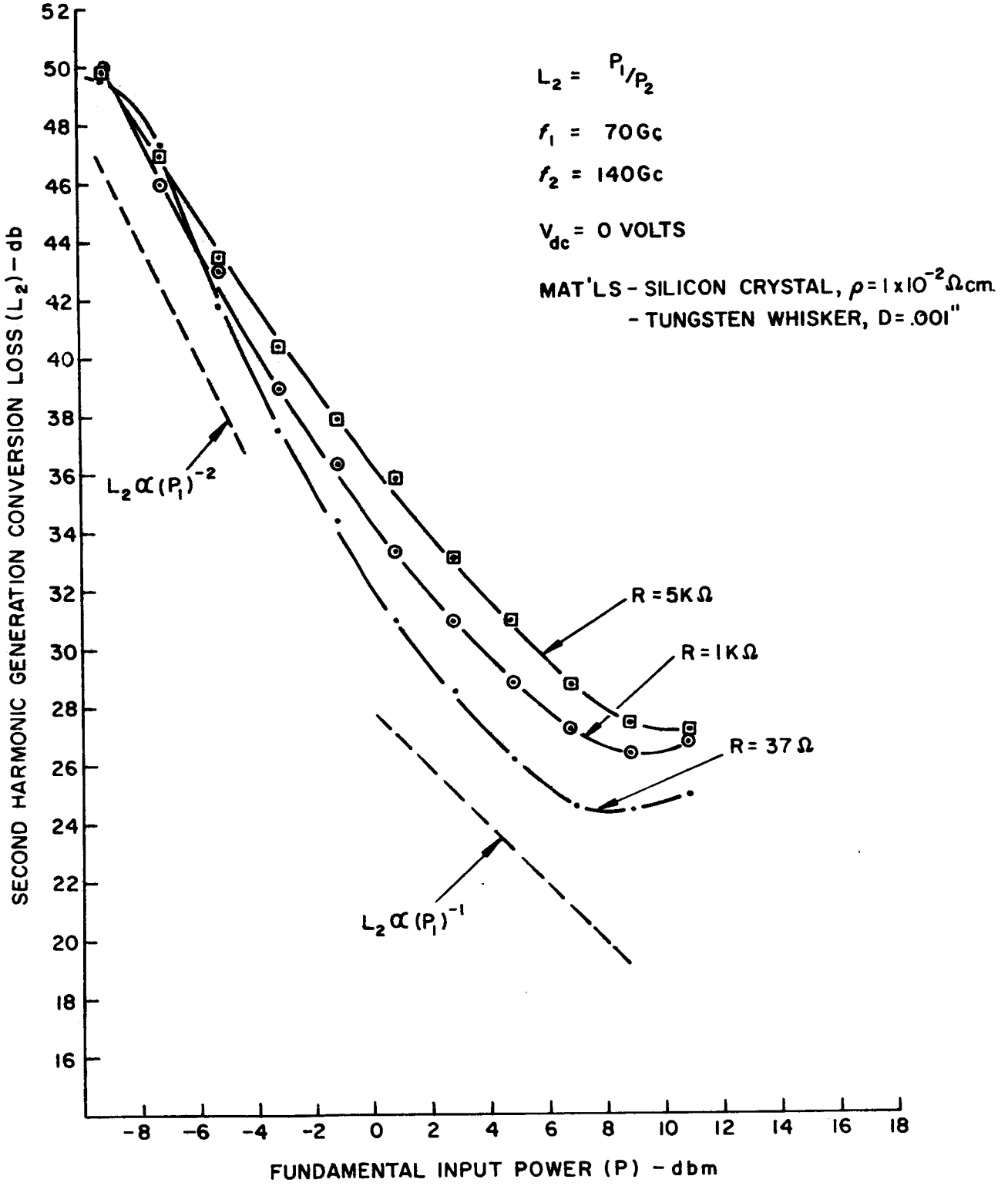

FIG. 36 - MEASURED SECOND HARMONIC GENERATION CONVERSION LOSS.

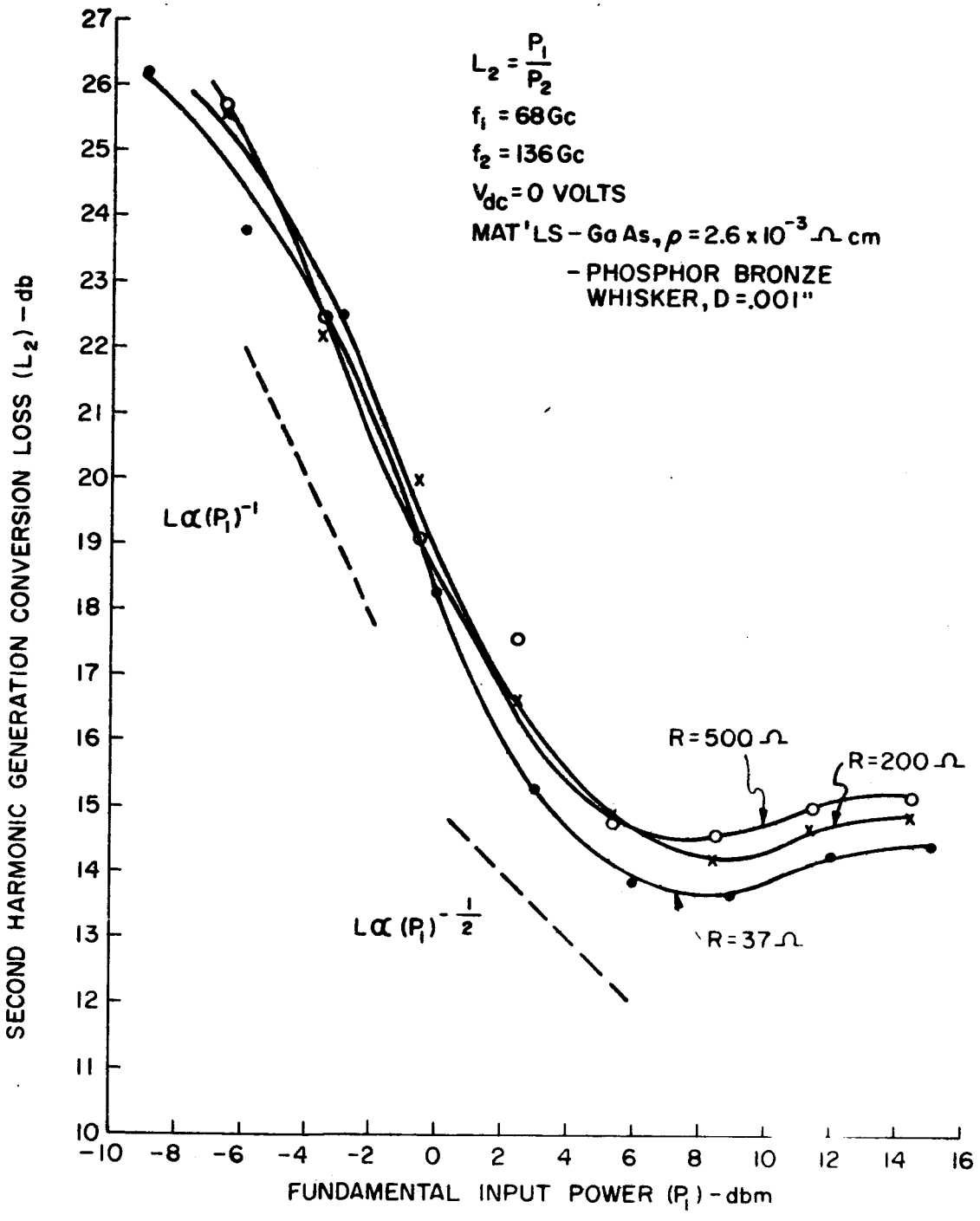

FIG. 37 - MEASURED SECOND HARMONIC GENERATION CONVERSION LOSS.

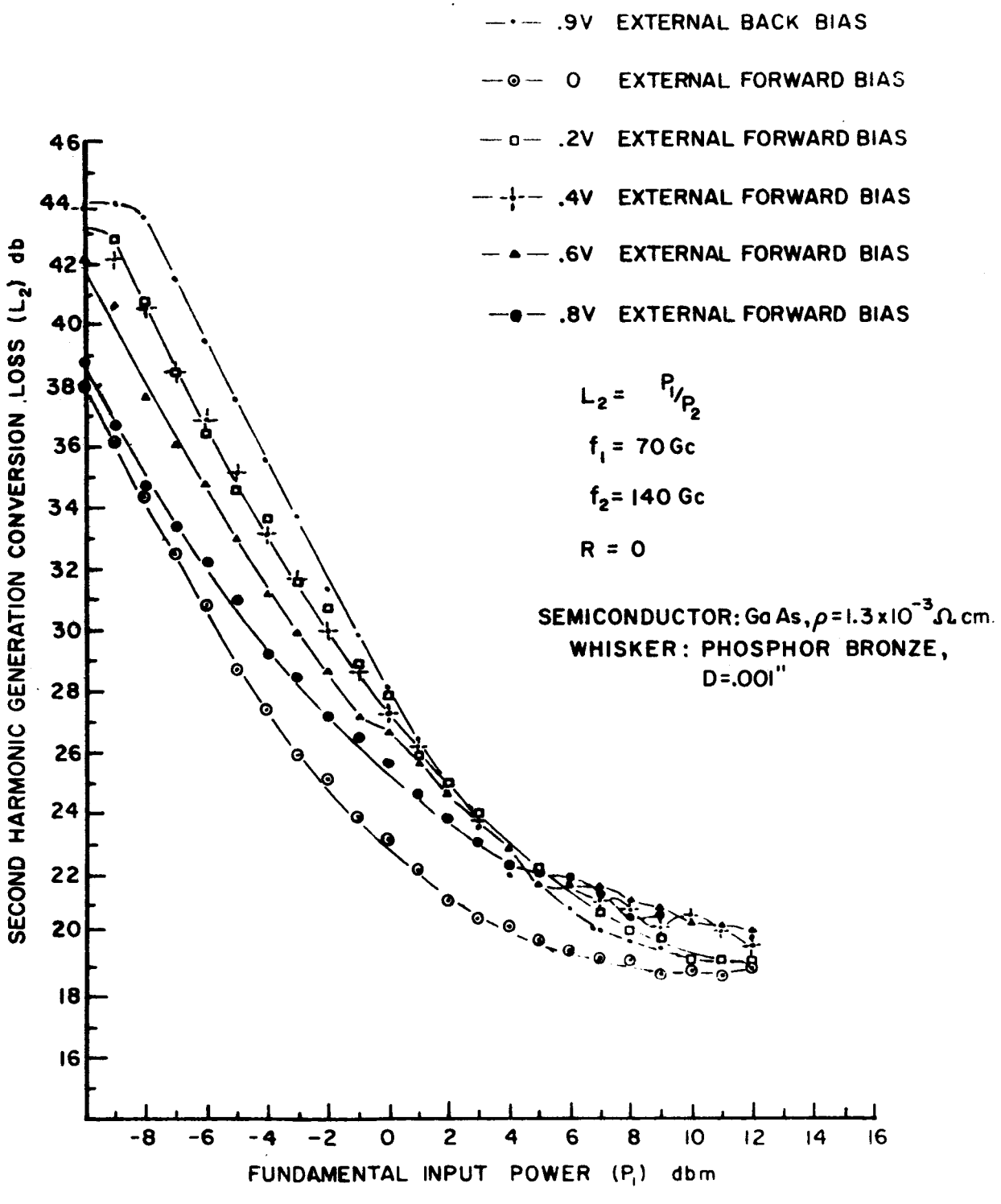

FIG. 38 - MEASURED SECOND HARMONIC GENERATION CONVERSION LOSS.

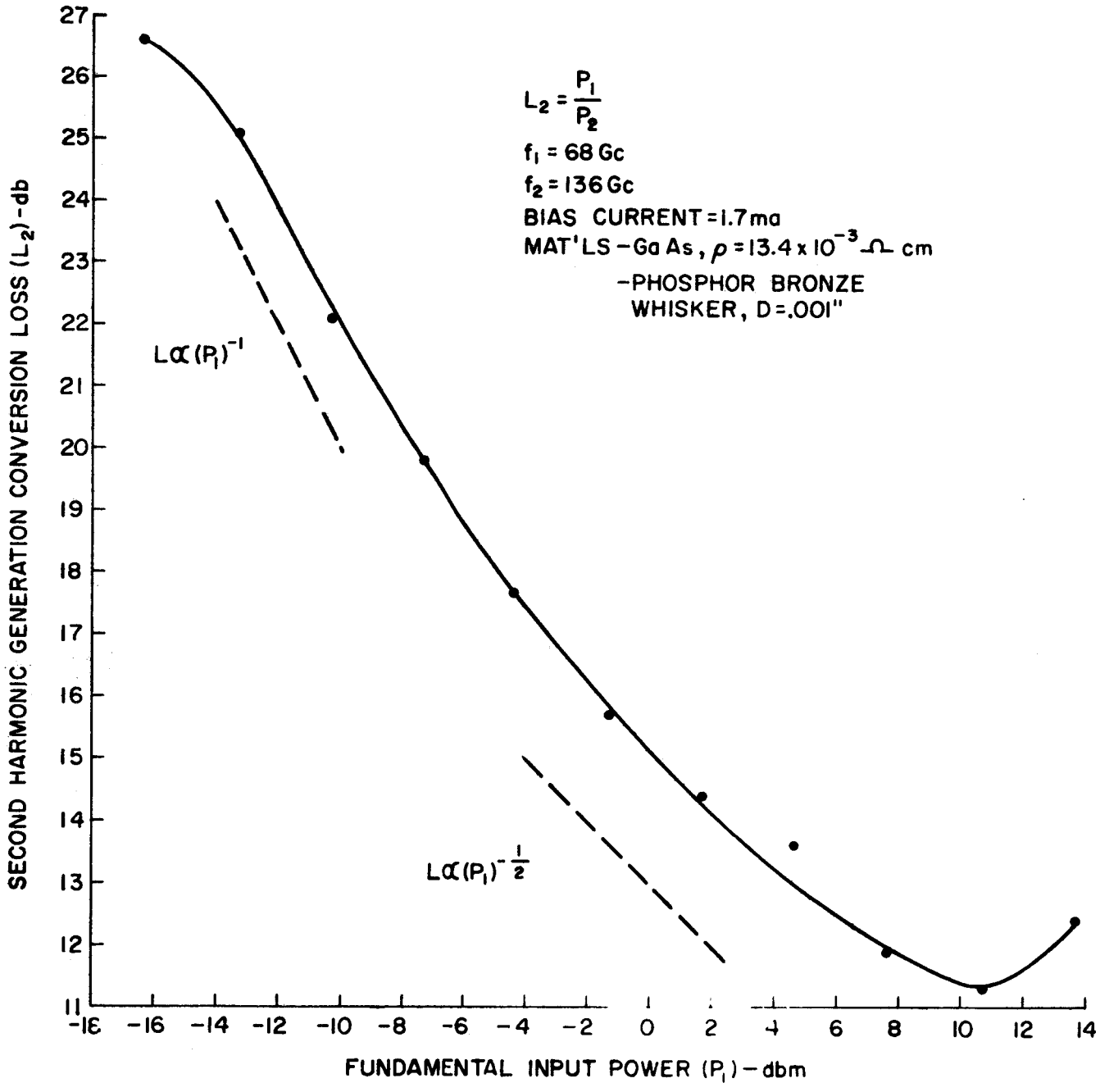

FIG. 39 – MEASURED SECOND HARMONIC GENERATION CONVERSION LOSS.

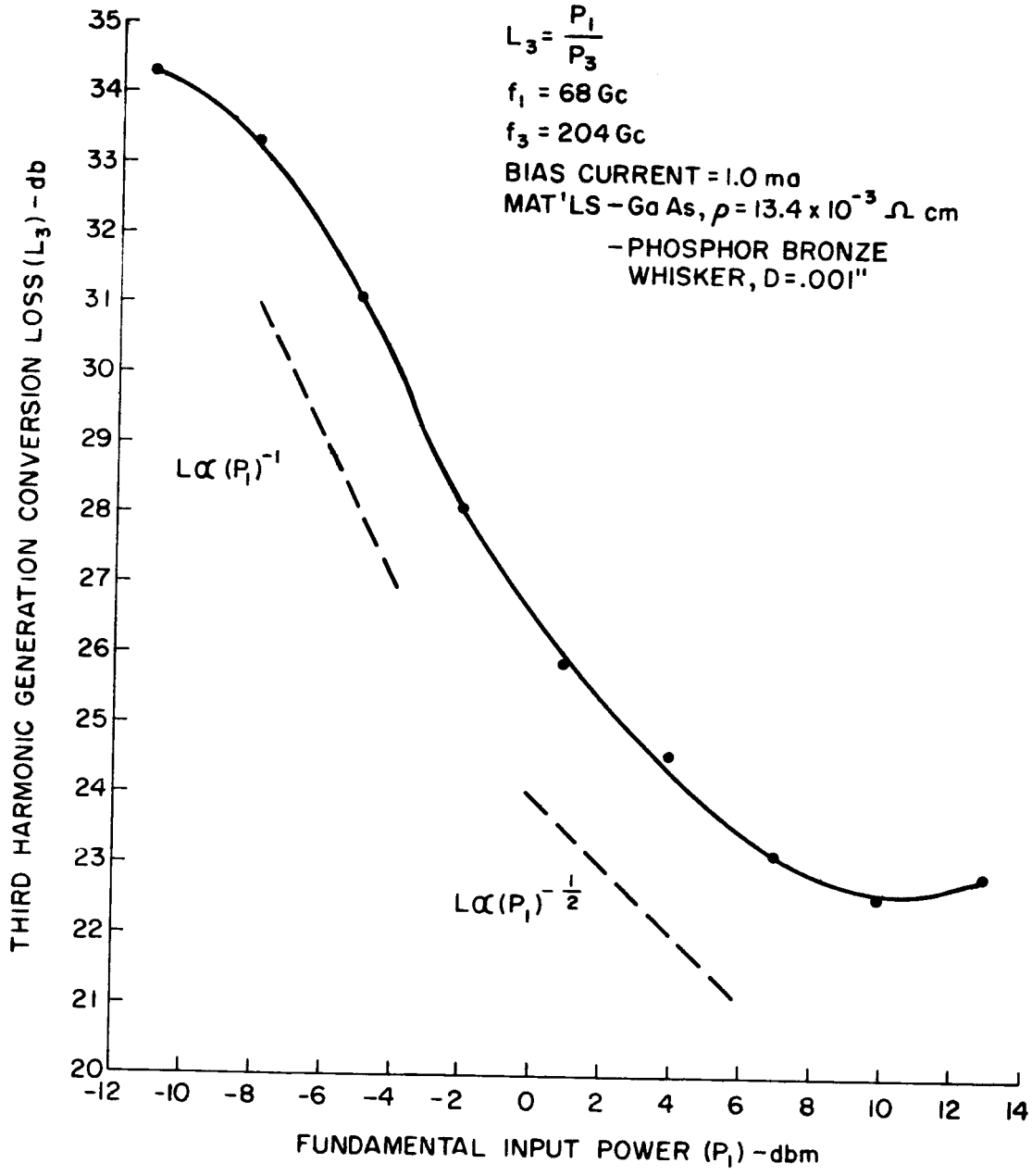

FIG. 40 – MEASURED THIRD HARMONIC GENERATION CONVERSION LOSS.

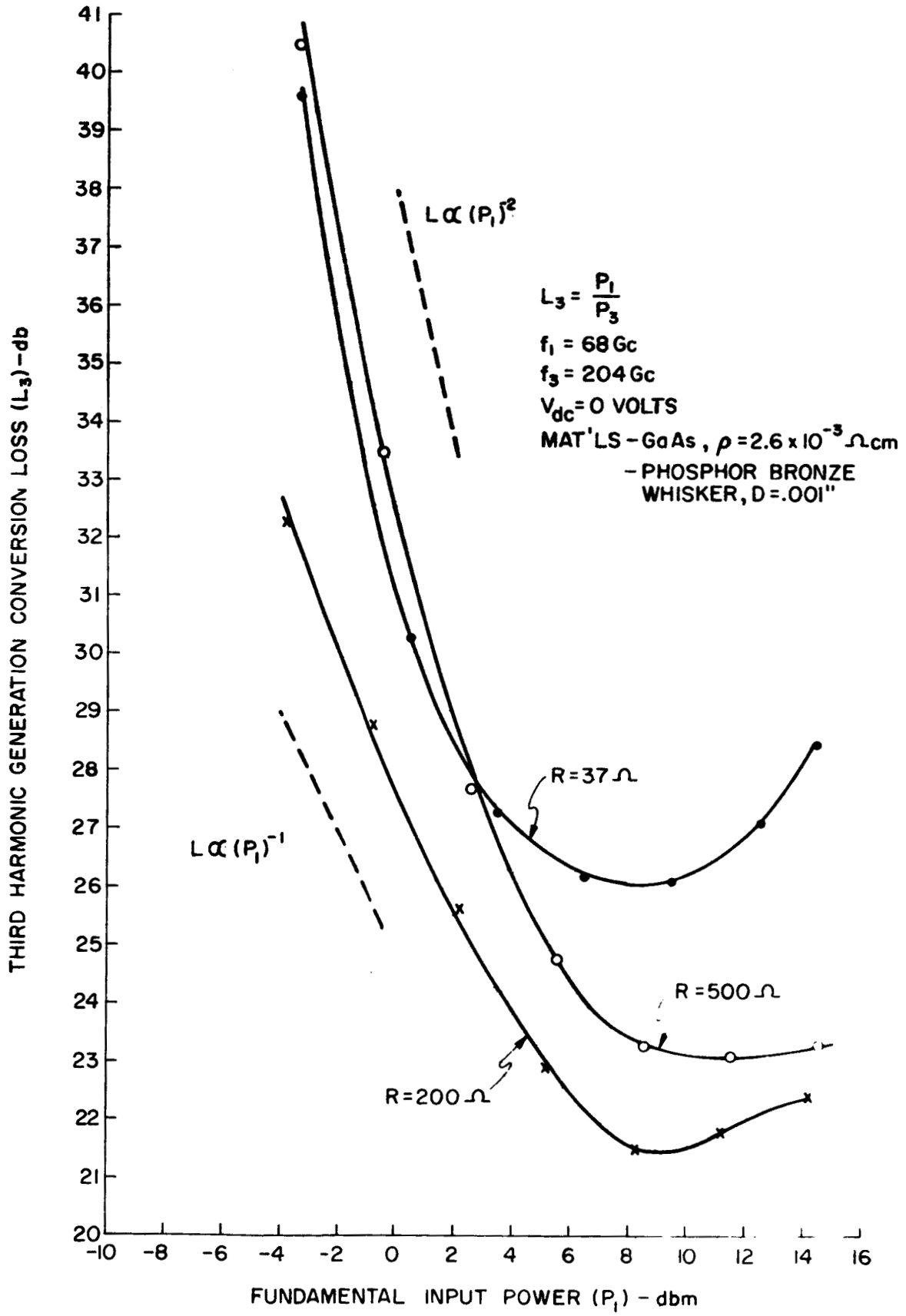

FIG. 41 -MEASURED THIRD HARMONIC GENERATION CONVERSION LOSS.

of P_2 on P_1 is similar to that found previously for silicon point contact harmonic generators.[4] For the other two gallium arsenide materials (Figures 37 and 39), $\rho = 2.6 \times 10^{-3}\ \Omega$-cm and $\rho = 13.4 \times 10^{-3}\ \Omega$-cm, $P_2 \propto P_1$ for lower power levels and $P_2 \propto P_1^{1/2}$ for higher power levels.

The data for Figures 39 and 40 were taken with an external forward bias voltage applied and adjusted to maximize the harmonic output. The total bias current, as stated on the curves, is the sum of the external bias plus self-bias due to the RF power. The measurements for Figures 39 and 40 were made on the same diode and show the difference between second and third harmonic conversion loss. The shape of the two curves is very similar and shows an increase in loss of approximately 11.5 db from second to third harmonic.

Third harmonic generation efficiency measurements were made on the silicon material but exhibited a very high conversion loss. The minimum loss obtained was 31.6 db with 20 mw of input power. With 1 mw input, the loss was 48.5 db.

In general, the harmonic generation conversion loss is somewhat better than that previously obtained for doublers starting at a lower frequency. This improvement is believed to be due to better semiconductor materials and improved waveguide structures obtained with the electroforming process. The data presented in the curves is typical of what has been observed. On occasion, second harmonic conversion loss as low as 10 db was measured with the gallium arsenide $\rho = 1.3 \times 10^{-3}\ \Omega$cm material, but unfortunately the junctions would not last for any length of time. The problem of junction deterioration was not nearly as severe with the other two gallium arsenide materials. Diodes with minimum conversion losses on the order of 10 to 14 db were repeatedly made with these materials and, in most cases, these diodes would last for two weeks or more. One of the major differences in the

---

4. C.M. Johnson, D.M. Slager, and D.D. King, "Millimeter Waves From Harmonic Generators," Review of Scientific Instruments, Vol. 25, pp. 213-217; March 1954.

materials is that the material with $\rho = 1.3 \times 10^{-3} \Omega cm$ is tellurium doped whereas the other two gallium arsenide materials contain no third doping element. It is not felt that any definite conclusions can be drawn since data are available on only these three gallium arsenide materials, but the evidence certainly warrants further investigations.

6. Mixers

Over the past few years, the state of the art in millimeter wave mixers, both harmonic and conventional, has been greatly improved. The improvements have been made possible by the better semiconductor materials, waveguide structures, IF amplifiers, and associated superheterodyne receiver components. This laboratory has conducted numerous programs to increase the sensitivity of the millimeter wave mixer and, at present, is conducting experiments on mixers for frequencies from 94 Gc to 600 Gc. Some of the data reported here is the result of efforts on these programs. Much of the information gained is of a general nature and can be used advantageously at all millimeter wave frequencies.

a. Crystal Noise Ratio

The noise figures of millimeter wavelength superheterodyne receivers are usually substantially higher than those of corresponding centimeter wavelength receivers. A major contributing factor to these high noise figures is local oscillator noise. The magnitude and frequency distribution of the noise emanating from a klystron local oscillator are functions of the operating voltages and currents, klystron mode, and the Q of the klystron cavity. It is well established that the magnitude of the LO noise is much greater for higher frequency klystrons than for lower frequency ones. The frequency distribution of this noise is such that it is greatest at the frequency of the coherent local oscillator signal and decreases with increasing separation from the coherent output. The frequency distribution is primarily determined by the Q of the klystron cavity; hence the actual frequency spread of the noise would be greater for a high frequency klystron even if its cavity

had the same Q as that of a lower frequency klystron. Since the cavity Q's are generally lower at the higher frequencies, the noise spectrum of the high frequency klystrons is wider yet. Similar effects exist for voltage tunable LO sources such as carcinotrons and backward wave oscillators. In these cases the electronic tuning of the periodic structure again causes the noise sidebands to be clustered near the frequency of the coherent output. A portion of these relatively strong noise sidebands beat with the LO's coherent output to produce a substantial noise input to the IF amplifier.

The usual method of suppression of the LO noise is through the use of a balanced mixer. The problems inherent in developing a balanced mixing system using harmonic mixers are particularly formidable. Construction of the hybrid junction required for a balanced mixer becomes more difficult as the frequency is increased. Since the above statement is applicable to almost all millimeter wavelength components, it is not the principal hurdle to be overcome. The major difficulty is the fabrication of pairs of crystals whose electrical properties at RF and IF are matched. It has been our experience in fabricating our own mixer diodes, that the best performance is consistently obtained when each individual diode is assembled to optimize its performance in its own mount. The observed performance of these diodes is substantially better than could be hoped for by adjusting pairs of crystals to match each others characteristics. It should be noted that if the individual crystals of a balanced mixer are sufficiently mismatched signal rather than LO noise will be suppressed. In that case the performance of the "balanced mixer" will be poorer than that which could be provided by either mixer crystal operating alone. In the case of a frequency sweeping radiometer, employing a voltage tunable LO, the balanced mixer solution to the LO noise problem is even less satisfactory. It is a characteristic of BWO's and other voltage tuned oscillators, that their power output varies considerably over their tuning range. As a result, the matched pair of crystals (if they could

be built) would have to have closely matched RF and IF characteristics which track each other as a function of LO power level as well as frequency, a very unlikely result.

The above discussion shows that local oscillator noise suppression is most difficult to achieve where it is needed most, i.e., in the millimeter wavelength bands. In addition to the noise originating in the local oscillator, excess IF noise is generated in the crystal due to the high level excitation by the LO. A portion of this noise follows the familiar 1/F frequency dependence. It has long been recognized that an alternate method of avoiding the reduction of receiver sensitivity due to LO noise is to operate the receiver at higher intermediate frequencies[5, 6] using a single ended mixer. In this way, advantage can be taken of the frequency of the noise from both the crystal and the local oscillator. In the case of a radiometer, an additional advantage of a high intermediate frequency is that it then becomes easier to obtain a large IF bandwidth, which in turn results in an improved capability for detecting small temperature differences.

Measurements have been performed with both harmonic and conventional mixers and the evidence supports the principle of using a high IF.[7, 8, 9]

---

5. R.V. Pound, Microwave Mixers, MIT Radiation Lab. Series, Vol. 16, pp. 239-249, McGraw-Hill, New York; 1948.
6. M. Cohn and J.B. Newman, "Microwave Mixer Performance at Higher Intermediate Frequencies," 1959 IRE National Convention Record, Part 3, pp. 169-176; March 1959.
7. M. Cohn, F.L. Wentworth, and J.C. Wiltse, "High Sensitivity 100 to 300 Gc Radiometers," Proc. IEEE, Vol. 51, No. 9, pp. 1227-1232; September 1963.
8. J.M. Cotton, M. Cohn, F. Sobel, J.C. Wiltse, "Millimeter Wave Research," Electronic Communications, Inc., Final Report on Contract No. AF 30(602)-2457; December 1962.
9. Contract No. DA 36-039 AMC-02347(E), Diode Millimeter Wave Type Mixer (3.2mm), U.S. Army Electronics Research and Development Laboratory, Fort Monmouth, N.J.

These measurements were performed to determine the optimum IF frequency for a low noise figure mixer. The measured excess noise ratio at various frequencies is as follows: 50 at 90 Mc, 37 at 120 Mc, 15 at 150 Mc, 8 at 180 Mc, 6 at 750 Mc, and less than 2 in the interval from 2 to 4 Gc. The crystal noise ratio is calculated from:

$$t = F_{IF}\left(\frac{N_X}{N_L} - 1\right) + 1 \qquad (12)$$

where: N_X = Output noise power with mixer at input of first IF amplifier

N_L = Output noise power with reference load at input

F_{IF} = IF noise figure

t = Crystal noise ratio

The crystal noise ratio of a mixer, either harmonic or conventional, is not a function of local oscillator frequency. The fact that the problem is more significant at the higher RF is due only (as was explained) to increased noise from the local oscillator source. Therefore, the fact that these measurements were performed with a LO of 70 and 94 Gc does not mean that they do not hold true for LO frequencies greater than 100 Gc. There are, however, other factors which are frequency dependent and therefore cannot be directly extrapolated from one frequency to another. It has been found though that improvements made in mixers operating at 70 or 94 Gc can, in general, be applied to higher frequency mixers with good results.

b. Conversion Loss

The conversion loss of a mixer is a factor which is frequency dependent. In a point contact mixer, the minimum achievable conversion loss is determined by the action of the local oscillator on the barrier resistance of the diode. The frequency dependence of the actual conversion loss can be approximated by the following equation:

$$L_c = L_b(1 + 4\pi f C_b R_s) \qquad (13)$$

where L_b = Minimum conversion loss

C_b = Barrier capacity

R_s = Spreading resistance

L_c = Actual conversion loss

As the frequency is increased, the actual conversion loss increases due to the degrading effects of the barrier capacity and the spreading resistance. However, the barrier capacity is not a predictable quantity since it is dependent on the semiconductor material and procedures used in forming the junction.

The conversion loss of a diode is not affected by the intermediate frequency of the system, but, as lower conversion losses are obtained, noise from the LO source is more efficiently heterodyned into the IF band and hence becomes more significant. Therefore, diodes with poor conversion loss normally have the lowest noise ratio.

Extensive measurements have been performed on conventional mixers operating at 94 Gc.[9] Typical conversion losses for diodes operating at this frequency have been about 8.0 db. Conversion loss as low as 4.5 db was obtained for one diode but that was an exceptional diode and such results are not readily repeatable. These tests were performed at an intermediate frequency of 2 - 4 Gc. The achievment of forming a good mixer diode is normally accomplished only after several contacts are made while observing the I-V characteristics on a curve tracer.

The problems involved in making harmonic mixing conversion loss measurements are much greater than conventional mixing measurements. This is due mainly to a lack of accurate power measuring equipment at 140 Gc. It is most regretable that a number of weeks were lost in tracking down sources of error and then recalibrating such pieces of equipment as rotary vane attenuators which were thought to be accurate beyond doubt.

After discovering and correcting the sources of error, diode junctions were formed which had conversion losses on the order of 10 db. These measurements were made with 70.0 Gc fundamental LO power of +11 dbm and 137.2 Gc signal power of -50 dbm. The 140 Gc signal was obtained from a harmonic generator. The crystal material used in all of the mixer measurements was the tellurium doped gallium arsenide, $\rho = 1.3 \times 10^{-3} \Omega cm$.

It is significant to note that the above value of conversion loss achieved with second harmonic mixing, is only slightly greater than would be expected for fundamental mixing at 140 Gc. Like the improved performance recently observed with conventional mixers and harmonic generators, the improved harmonic mixing performance is believed to be due to, 1) the use of electroformed waveguide structures, and 2) better diode forming techniques as achieved through the use of the dual I-V characteristics. The excellent performance obtained with harmonic mixing confirms the approximate analysis presented by Meredith and Warner.[10]

---

10. R. Meredith and F.L. Warner, "Superheterodyne Radiometers for Use at 70 Gc and 140 Gc," IEEE Trans, Vol. MTT-11, pp. 397-411; September 1963.

IV. FERRITE MODULATOR (TASK III)

One of the requirements for a ferrite rotator which is to be used as part of a modulator for a Dicke-type radiometer is that its bandwidth be large enough for the receiver passbands on each side of the LO frequency. It has been shown[11] that a Faraday rotator device can be built such that the rotation of the plane of polarization is independent of frequency. This is made possible by using the ferromagnetic medium as a dielectric waveguide. When the diameter to free space wavelength ratio of the ferrite rod is of such magnitude as to give a constant phase velocity to free space velocity ratio, the wave is essentially propagated in an infinite medium. The rotation per unit length will then depend only on the M_s of the ferrite and its dielectric constant.

The ferrite modulator development began with the construction of a dielectric waveguide structure such as shown in Figure 42. The frequency band chosen for this initial design was in the 70 Gc region rather than the 140 Gc region in order that certain modifications of the dielectric waveguide could be made easier. Once the design parameters were fixed at 70 Gc, the device could be scaled for operation at 140 Gc. Figures 43 and 44 show the results obtained with the 70 Gc rotator for 90° and 45° of rotation respectively. It should be pointed out that the waveguide input and output ports were aligned at 90° or 45° with respect to each other. This can be seen by noting that there was zero coil current for the isolation curves. The isolation curve shown in Figure 44 is of no interest since there was no provision made to absorb the reflected energy. This data was taken to observe only the insertion loss values as a result of reducing the length of the ferrite rod.

A scaled version of the 70 Gc rotator design was constructed for operation at 140 Gc. It soon became apparent that a simple scaling

---

11. C.E. Barnes, "Broadband Isolators and Variable Attenuators for Millimeter Wavelengths," IRE Trans. on Microwave Theory and Techniques, Vol. MTT-9, pp. 519-523; November, 1961.

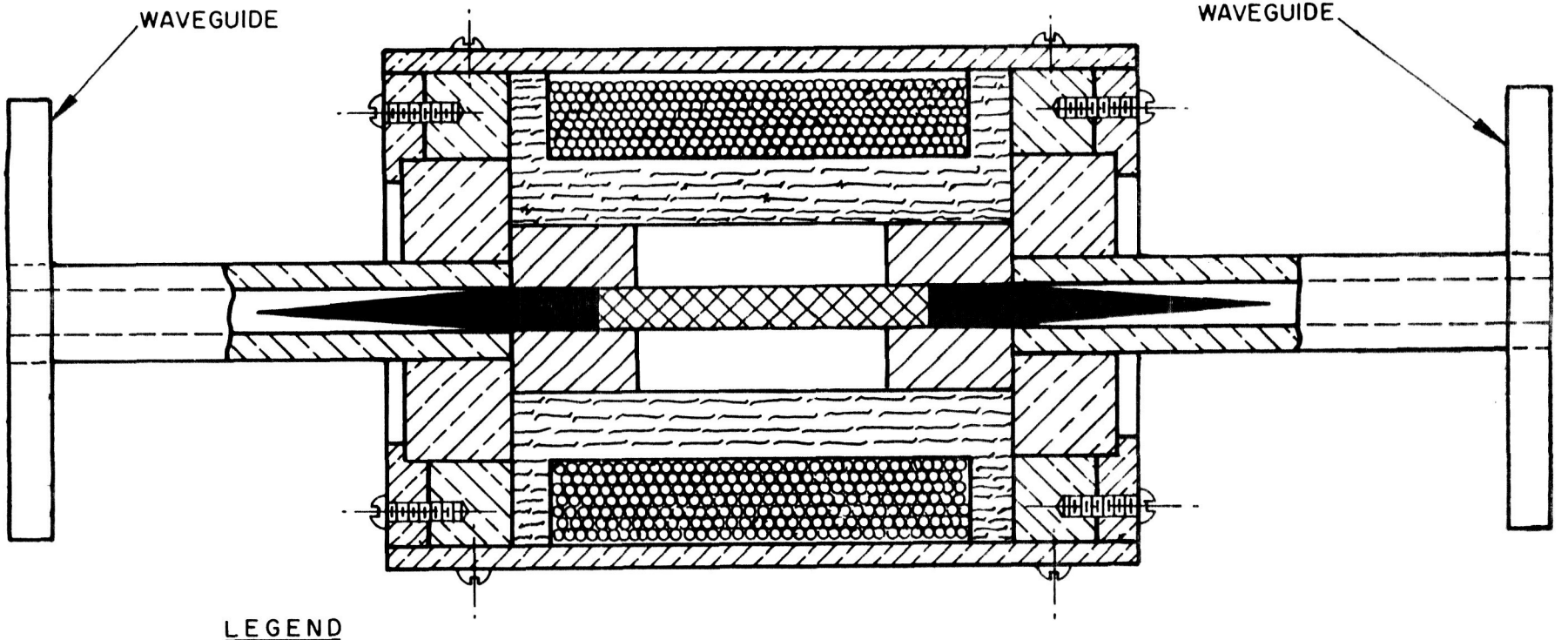

FIG.42- ROTATOR STRUCTURE

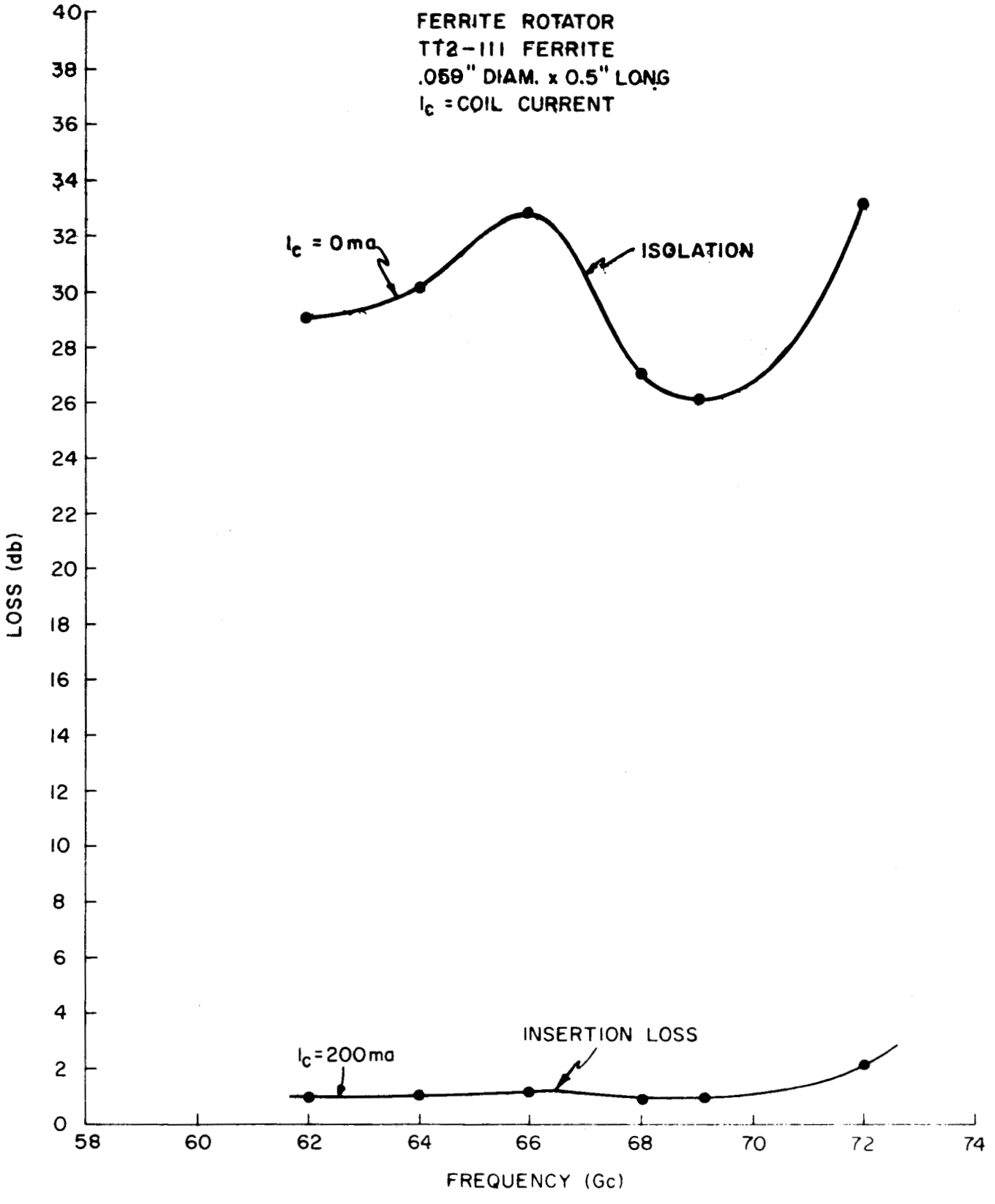

FIG.43 - MATCHED FERRITE ROTATOR CHARACTERISTICS

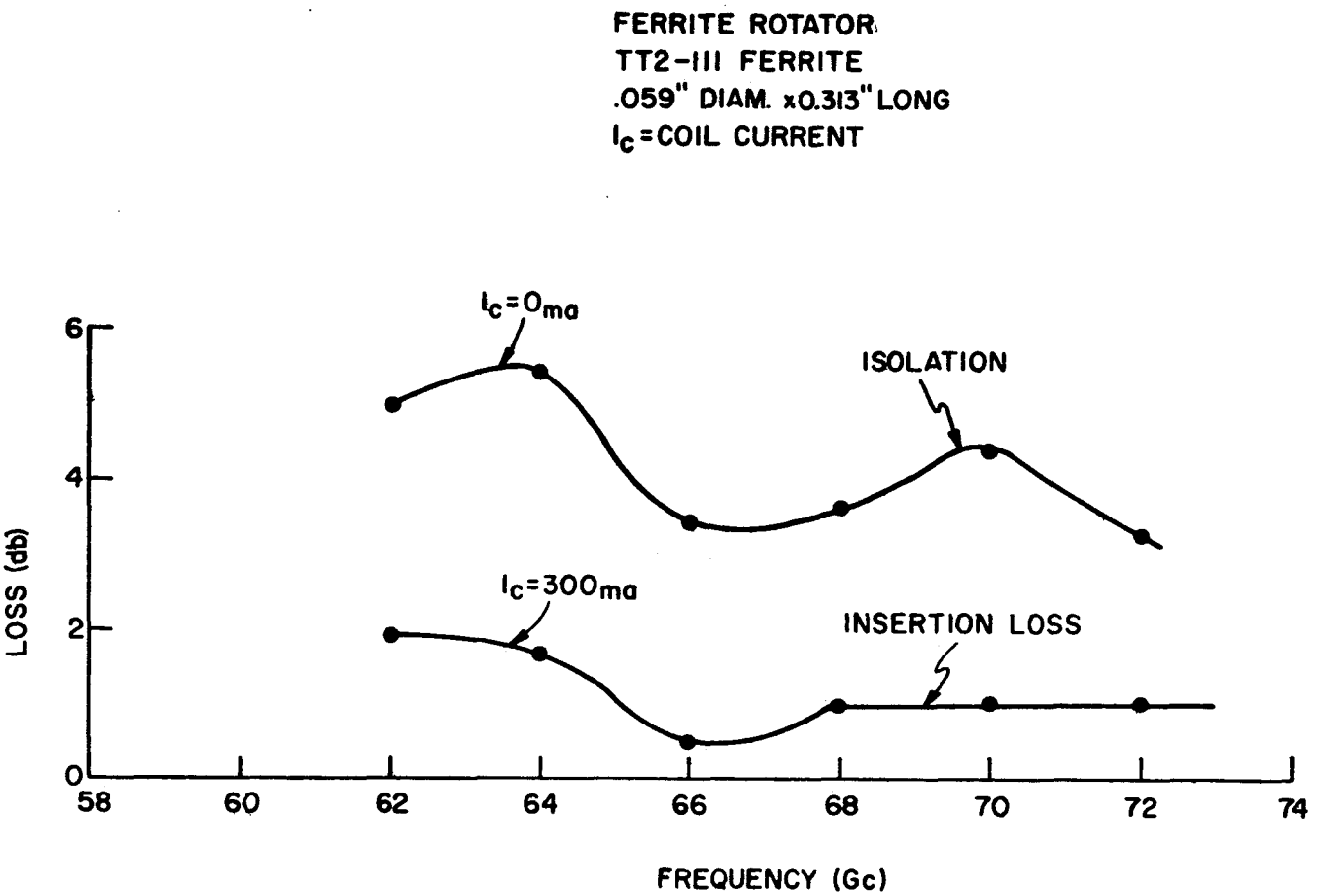

FIG.44- FERRITE ROTATOR CHARACTERISTICS

design would not give the desired results at these higher frequencies. The adaption of this design for the 2mm wavelength region presented many problems in the way of fabrication and repeatability of measurements. The matching tapers were again of "lucalox,"[12] as was the case for the 70 Gc design, and consequently very difficult to machine to small dimensions without material casualties resulting. Anomalies in the insertion loss measurements were found to be caused by the random positioning of the alumina matching tapers with respect to the ferrite. Small air gaps at this interface would cause radiation losses. Several attempts were made to prevent this. A thin film of low loss epoxy adhesive was used to cement the alumina to the ferrite. This resulted in an insertion loss of 5.0 db at 140 Gc. Measurements were not taken over the entire band of frequencies at this point because it was felt certain that high loss would also exist at frequencies above and below 140 Gc. Another adhesive such as "Eastman 90" was used; however, this also resulted in an increase in insertion loss. It became apparent that a suitable adhesive would be difficult to find, if at all. One other alternative was to encapsulate the three pieces such that the potting material would form the holder for the ferrite and alumina. Case A of Figure 45 shows this loading configuration except that instead of a teflon holder there was now a potting compound holder. The material used for this encapsulation was "Scotchcast".[13] An insertion loss of 3.5 db at 140 Gc resulted from this arrangement. This was better than the adhesive, but still not as good as needed. At this point it was decided to do away with the interface problem by machining a piece of ferrite which included the matching tapers. This construction is shown in Case B of Figure 45. The overall length of the dielectric waveguide in this Case was the same as in Case A; the teflon holder

---

12. A high purity alumina product of the General Electric Co.

13. An epoxy resin manufactured by the 3M Company.

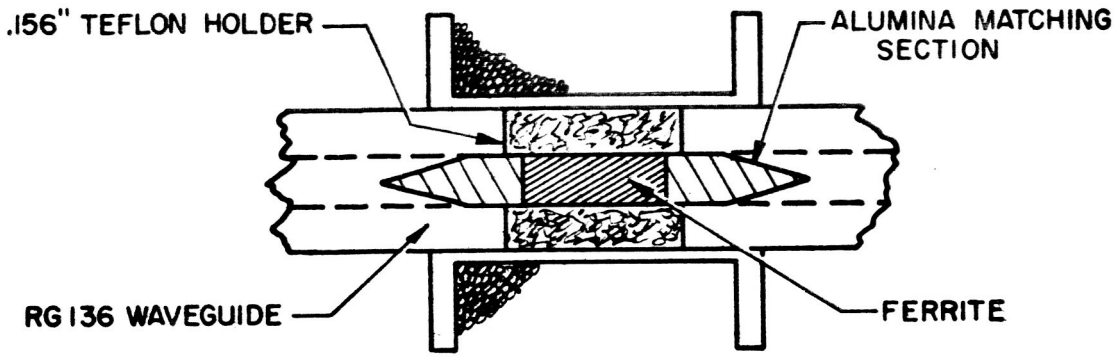

CASE A

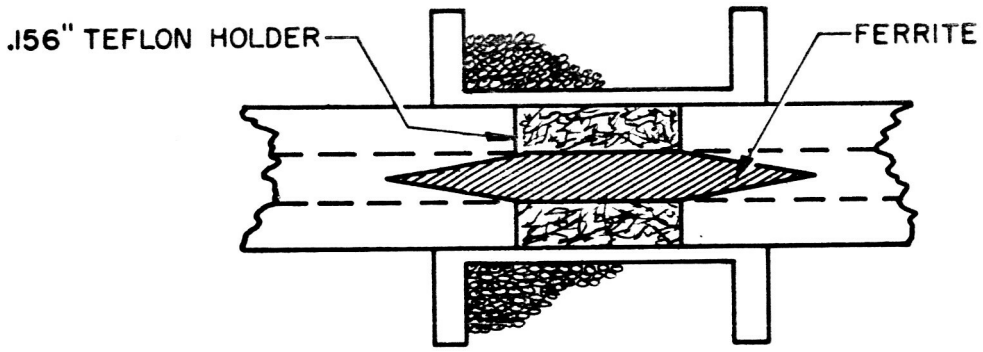

CASE B

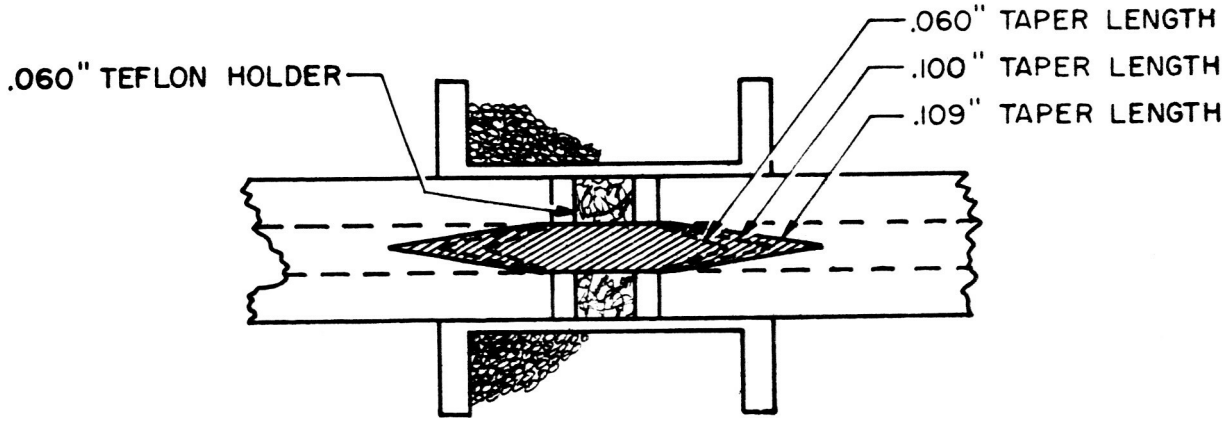

CASE C

FIG.45-BASIC ROTATOR LOADING

was the same size as that in Case A. The taper angle of the one piece ferrite rod was made smaller resulting in a longer taper than that of the alumina matching sections. This was done to absolutely insure good launching efficiency. Insertion loss measurements made on this assembly are shown by curve 1 of Figure 46. These losses were much higher than expected; and they could not be accounted for by a mismatched structure since the maximum VSWR was only 1.55 over the entire bandwidth. Other than the losses due to the ferrite itself only one other possible cause existed for the high insertion loss. This was the teflon holder supporting the ferrite rod. The length of this holder was .156". Comparing this with the .338" overall length of the ferrite, it can be seen that nearly half of the rod was covered by the holder. A surface wave propagating along the ferrite rod would encounter the dissipative effects of teflon at these high frequencies, and consequently increase the insertion loss. The holder length was decreased to .060" and the insertion loss measurements repeated. The results of these tests are shown in curve 2 of Figure 46. A substantial reduction in insertion loss can be seen from this data. Case C of Figure 45 shows this new rotator loading configuration.

A decision was now made to shorten the length of the ferrite rod in order to further reduce the insertion loss. The cylindrical portion of the rod was held constant and the taper length reduced. This meant that the taper angle would get larger making the tips more blunt. The length of taper was cut back from .109" to .100" as a first try. This produced the results shown in curve 3 of Figure 46. The insertion loss was thereby further decreased. The taper length was then reduced to .060" but the insertion loss increased to a value of 7.5 db at 137 Gc. The coil current needed for 45° of rotation increased from the 25 ma needed in the former cases to 150 ma in the latter case. This was a good indication that the launching efficiency decreased due to the shorter and more blunt taper matching section. The final ferrite rod configuration

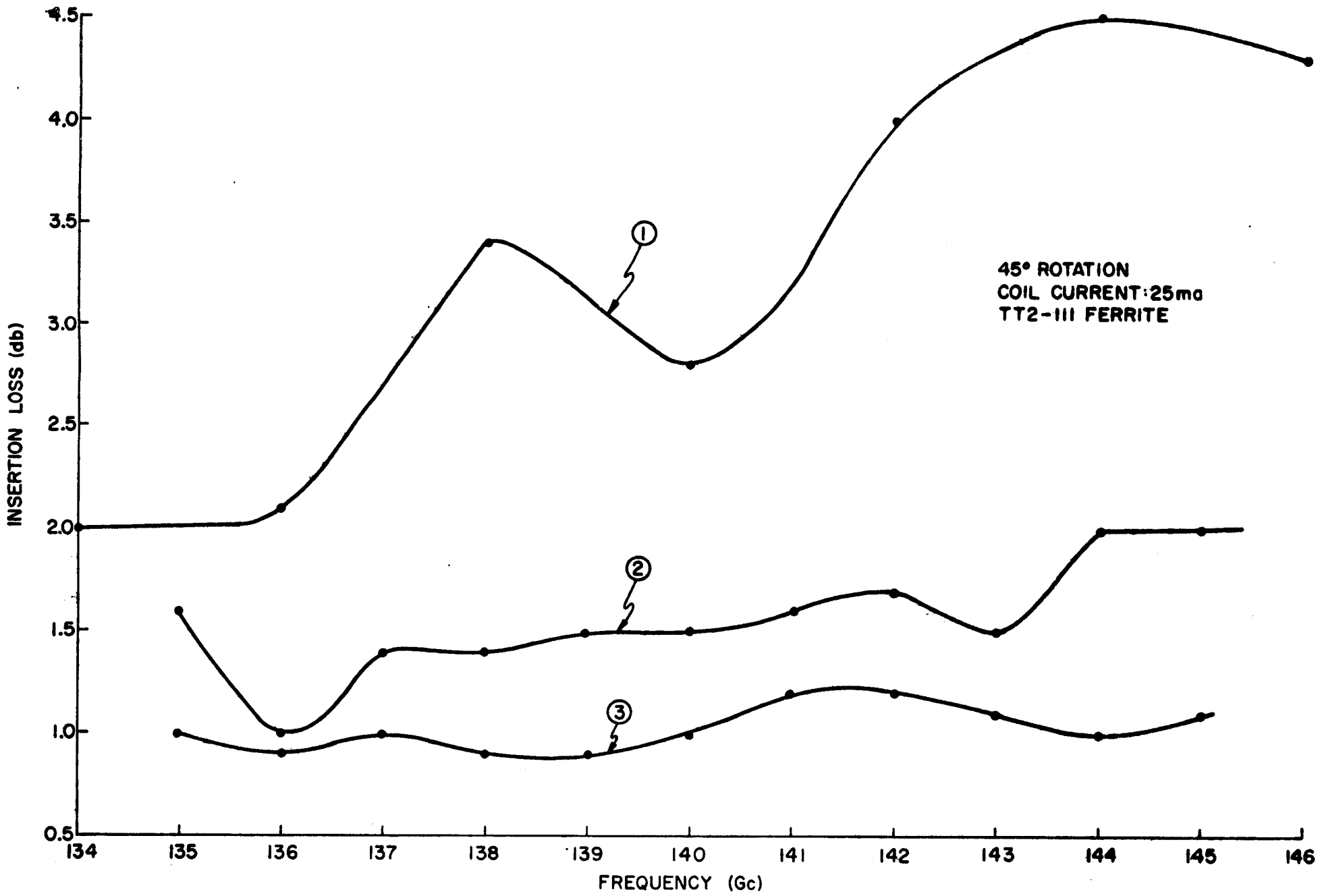

FIG. 46-FERRITE ROTATOR CHARACTERISTICS-INSERTION LOSS vs FREQUENCY

for the best results as shown by curve 3 of Figure 45 is one consisting of tapers that are .100" in length with a cylindrical section .065" long. The teflon holder remains .060" long, although a slight decrease in insertion loss might result if this length were further reduced.

A waveguide junction (See Figure 48) was fabricated for use with the ferrite rotator. This structure had to exhibit a high degree of symmetry between the rectangular waveguid ports which would be used for the thermal reference source and the radiometer antenna. An assymetrical structure would not give a one to one comparison of the two inputs. In order to obtain this symmetry with as much accuracy as possible, the entire junction was electroformed. This technique provides an internal waveguide surface which is far superior to that of extruded waveguide. A reduction in surface roughness in turn results in reduced wall losses and better fitting movable short circuits.

Separate measurements were made on the waveguide junction. Figure 47 shows the results of these measurements. The insertion loss ranged from 0.7 to 1.4 db over the band for a fixed position of the tuning short. Tuning was done at 140 Gc. Isolation values varied from a low of 11.6 db to a high of 27 db.

Combining the ferrite rotator with the waveguide junction such as shown in Figure 48 gives the results shown in Figure 49. (A photograph if this combined structure is shown in Figure 50.) This data shows that for a fixed amount of rotation the insertion loss of each component does not add up to give the total insertion loss measured at each frequency. It also shows that the minimum isolation of 11.6 db, which was measured with the junction only, has decreased to 7.0 db when the junction is mated with the rotator.

Closer examination of Figure 49 shows that the insertion loss increases at the frequencies where the isolation is low. This indicates

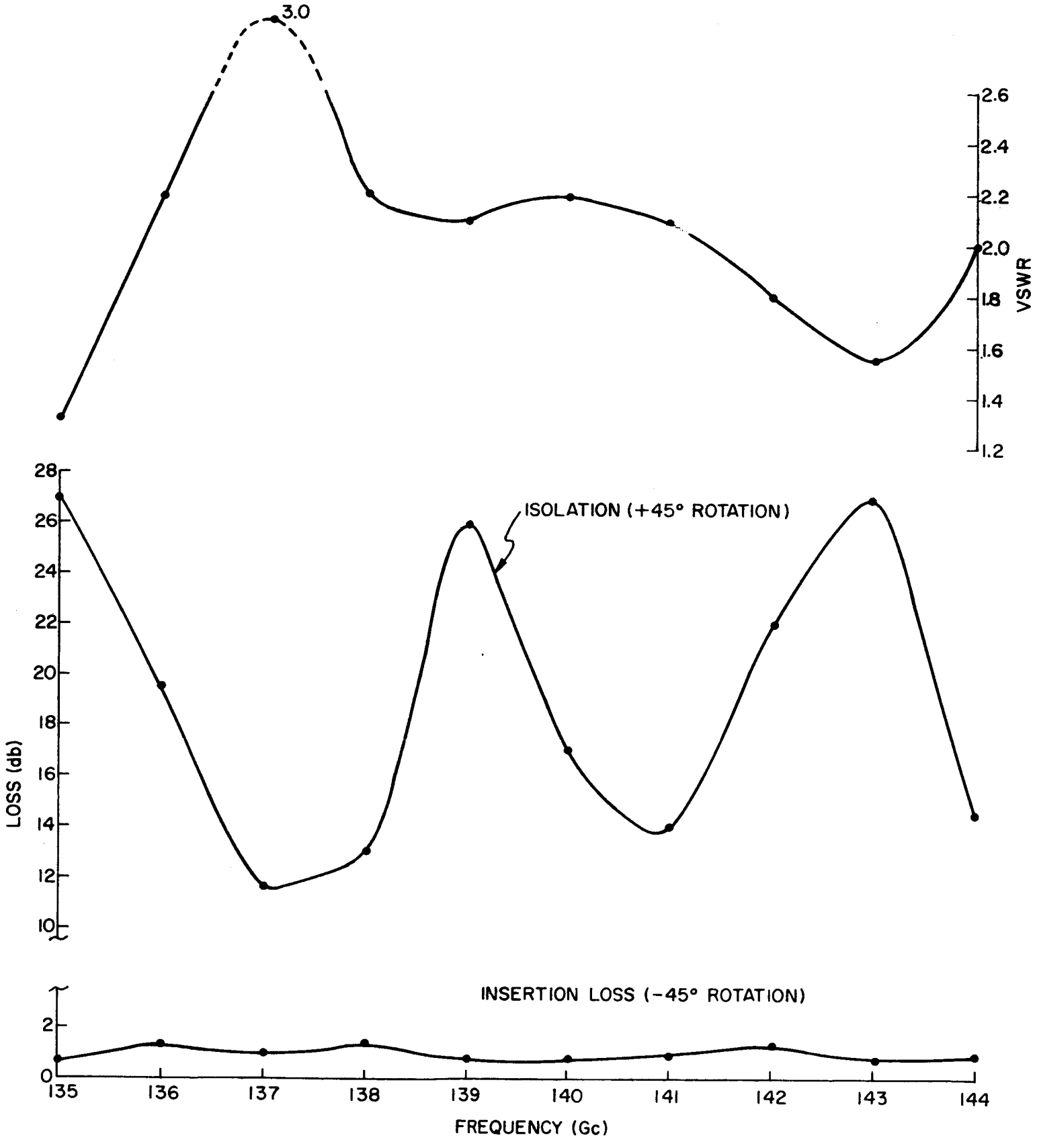

FIG.47 - ROTATOR JUNCTION CHARACTERISTICS-SHORT TUNED AT 140 Gc

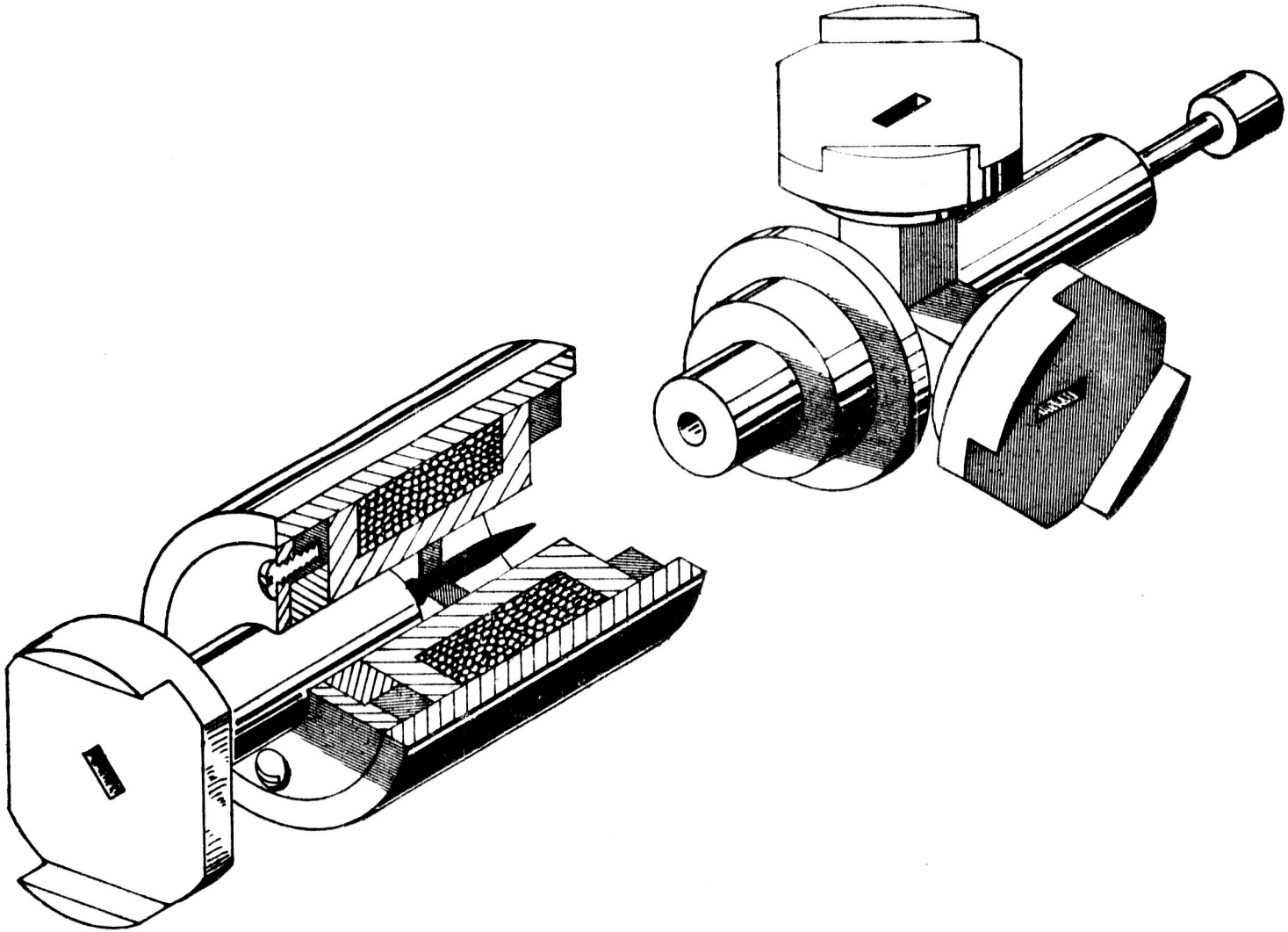

FIG. 48 - COMBINED ROTATOR AND JUNCTION ASSEMBLY

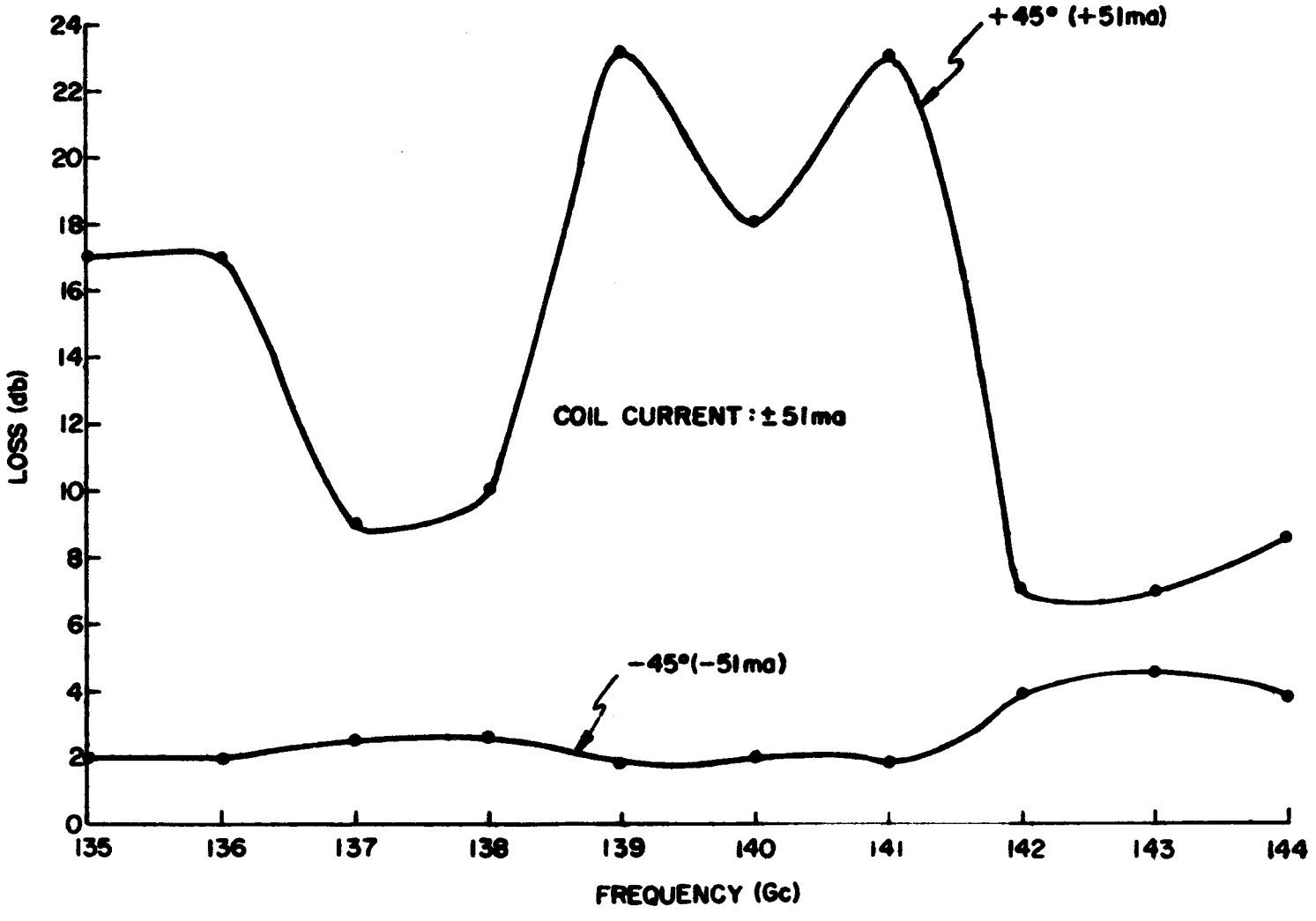

FIG. 49-COMBINED CHARACTERISTICS OF ROTATOR AND JUNCTION TUNED AT 140 Gc

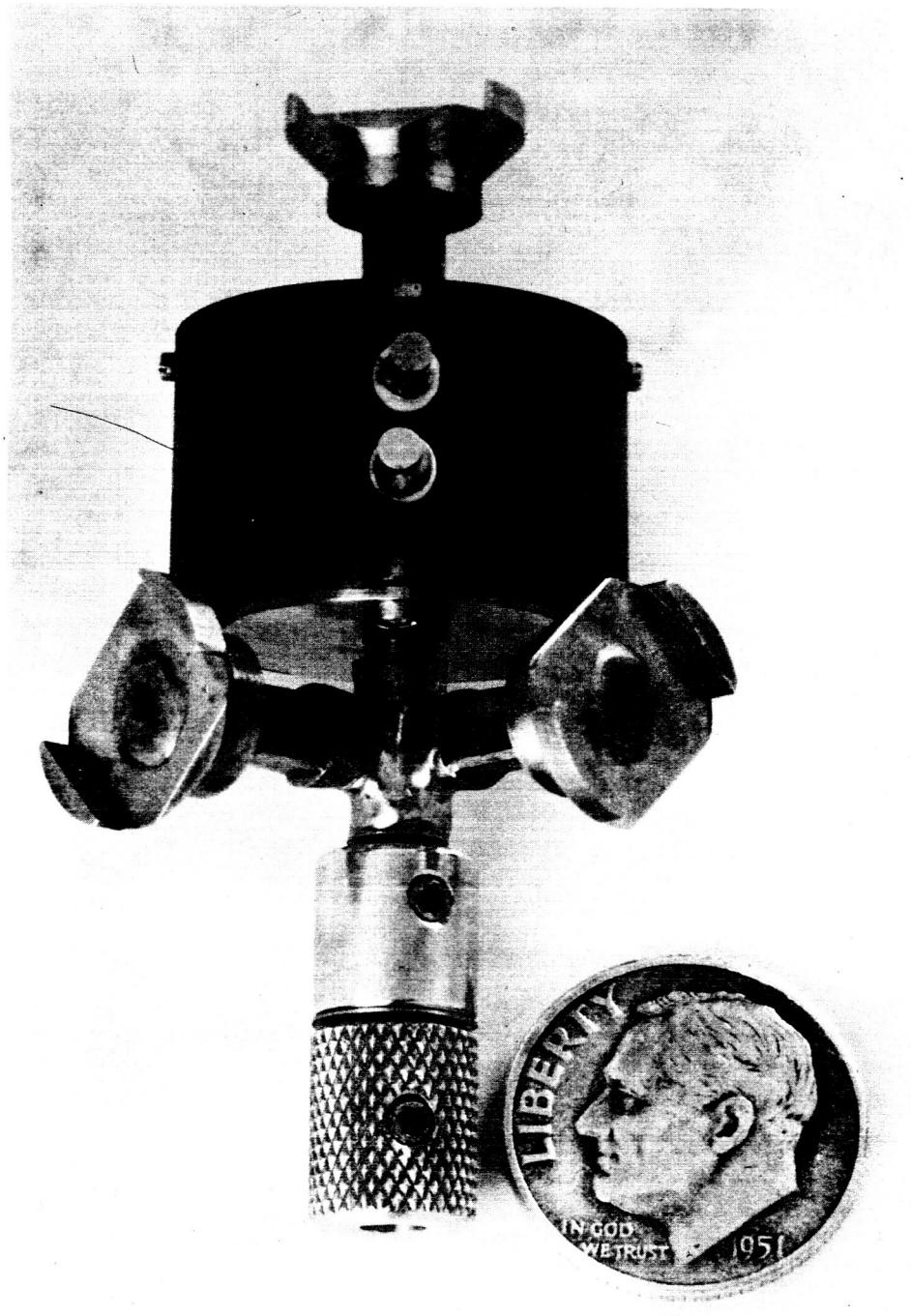

Figure 50 - Photograph of Combined Rotator and Junction Assembly

that part of the total energy presented to the junction is going to the wrong port. This can happen if for some reason the rotation of the plane of polarization does not remain independent of frequency. It was found that the rotator alone exhibited no evidence of frequency dependent rotation over the band measured. However, the input and output ports of the rotator in this case were rectangular waveguide. When the junction replaces one of these ports, a section of tapered ferrite is now within a circular waveguide instead of a rectangular one. It is apparent then that the polarization must have been restrained in the regions where the ferrite protruded into the rectangular waveguide, as it would be in a Reggia-Spencer[14] configuration. In the case of the circular waveguide there are no parallel guide walls to restrain the rotation of the plane of polarization. One can hence expect frequency dependent rotation on the conically tapered ferrite rod within the guide walls. One way to eliminate this phenomenon is to somehow remove the magnetic field in this area alone. A possible expedient could be that of placing a section of mu-metal in the area of the taper to divert the magnetic lines of force of the coil. Although there was not enough time to complete these investigations, it is felt that once this problem is solved a more useful component could result. The curves of Figure 49 show that over a 3 Gc band centered at 140 Gc, a useful component already exists.

---

14. F. Reggia and E.G. Spencer, "A New Technique in Ferrite Phase Shifting for Beam Scanning of Microwave Antennas," Proc. IRE, Vol. 45, pp. 1510-1517; November 1957.

V. CONCLUSIONS

During the course of this program, components and techniques have been developed which substantially increase the frequency range over which superheterodyne receivers are practical.

One of the developed items, a ferroelectric bolometer, is not a receiver component but an instrument to measure low level absolute power levels. Such an instrument is needed to evaluate the performmance of conventional mixers, harmonic mixers, and harmonic generators. Its performance has been evaluated in the frequency interval from 70 to 308 Gc. In the frequency interval where alternate power measuring instruments are available, its performance has been shown to be frequency independent. At the higher frequencies, the waveguide mount containing the ferroelectric bolometer as well as the mounts for the other power measuring instruments were very oversize and hence possibly overmoded. The ferroelectric bolometer mount can be redesigned so as to eliminate higher order modes even at submillimeter wavelengths. Through the use of a temperature compensating bridge, the effects of ambient temperature fluctuations have been minimized. Power levels down to four microwatts have been measured. Such a power measuring capability is sufficient to determine the power output of millimeter and submillimeter wavelength harmonic generators.

Significant improvements have been made in the performance of semiconductor diode devices. Through the use of precision electroformed waveguide structures, smoother waveguide surfaces and more uniform waveguide dimensions have been achieved resulting respectively in reduced waveguide wall losses and better fitting and hence higher reflectivity movable short circuits. The improved performance is also due to the new diode forming techniques as observed by the dual I-V characteristic method described in this report. Excellent correlation between curve separation and millimeter wave device

operation has provided a much higher yield of devices with excellent performance.

Conventional mixers (fundamental mixing) fabricated and formed by the new techniques operating at about 3 millimeters wavelength have typically had crystal conversion losses of about 7 or 8 db and crystal noise ratios (including LO noise) of less than 1.5 at intermediate frequencies of 2 to 4 Gc. The above performance is comparable to that achieved with commercially available cartridge crystals at wavelengths of about one cm. Second harmonic mixing at a wavelength of about two mm has yielded conversion losses of about 10 db and demonstrates that harmonic mixing is only slightly less sensitive than conventional mixing. In many applications the slight performance degradation can be tolerated for the benefits of using lower frequency local oscillator sources which may be all solid state.

Crystal harmonic generator improvements have resulted in second and third harmonic generation efficiencies from a 70 Gc source of 11.5 and 21.5 db respectively. These results are nearly an order of magnitude improvement over previously achieved performance.

The above cited improvements in harmonic mixing and harmonic generation significantly increase the sensitivity and extend the frequency range where superheterodyne receivers and radiometers are feasible. In addition they offer the possibility of achieving an all solid state unit at mm wavelengths. Further work is needed to improve the reliability and lifetime of these delicate diode devices.

The performance achieved with the two mm Faraday rotation type ferrite modulator indicates that a useful device has been achieved. Additional work is needed to further extend the bandwidth if the modulator is to be used with radiometers having a 2 to 4 Gc IF and capable of accepting both RF passbands. The bandwidth achieved is nearly sufficient for a double passband system having 1 to 2 Gc IF amplifiers. It is more than sufficient for systems employing solid state 500 to 1000 Mc

amplifiers. Low noise, low power drain, 500 to 1000 Mc, tunnel diode and transistor amplifiers suitable for use as IF preamplifiers and amplifiers in a space borne radiometer are currently available. Due to the small size of the ferrite rod used in the 2 mm ferrite modulator, it is doubtful if this type of structure can be scaled for operation at even shorter wavelengths. The development of ferrite modulators at shorter wavelengths will probably require the investigation of quasi-optical or oversize and hence overmoded guided structures.